QUARTERLY OF APPLIED MATHEMATICS

Vol. V JULY, 1947 No. 2

THE INFLUENCE OF THE WIDTH OF THE GAP UPON THE THEORY OF ANTENNAS*

BY

L. INFELD

University of Toronto

1. Introduction. The modern theories of antennas differ from the older sinusoidal theory in one essential point: they take into consideration the existence of the gap as the region from which the energy radiates, whereas the sinusoidal theory[1] spreads the sources over the whole length of the antenna.

The gap, in all these modern theories, is characterized by a *given* difference of potential $(-V)$ and by this difference only. The dimensions of the gap and the electric field in the gap do not enter the picture. If we denote by d the dimensions of the gap, and by E_z the tangential component of the electric field along the short line representing the length of the gap, then the *physical* quantity which enters the theory is:

$$-V = \int_{-d/2}^{d/2} E_z dz, \tag{1.1}$$

and the knowledge of E_z and d is not assumed. Neither E_z nor d appears in the theories of antennas, because the gap is represented by what I shall call a *δ-gap*. Its model is obtained by the following limiting process: let us assume that the dimensions of the gap (d) tend to zero. Let us assume further that at the same time E_z increases, but in such a way that the integral (1.1) remains constant. In other words, E_z becomes proportional to a Dirac function:

$$E_z = -V\delta(z), \tag{1.2}$$

where $\delta(z)$ is defined by

$$\delta(z) = 0 \quad \text{for} \quad z \neq 0 \tag{1.3}$$

$$\int_{-\infty}^{\infty} \delta(z)dz = 1. \tag{1.4}$$

This δ-gap model is the basis of nearly all recent investigations on the theory of antennas. In the final solution neither d or E_z appears. They were wiped out by the limiting process $d \to 0$.

Most of the investigations based on this δ-gap model employ an approximation procedure which is so complicated that it becomes practically impossible to carry it

* Received Aug. 9, 1946. This paper was written in 1942 and issued as a classified report by the National Research Council of Canada.

[1] J. Labus, Hochfrequenz Technik und Elektroakustik **41**, 17–23 (1933).

beyond the first few steps. Even the first approximation gives a good agreement with experiment. But the question of convergence is hardly investigated. There is a danger that pushing the approximation further would spoil rather than improve such an agreement.

From the theoretical point of view this is an essential point to which little attention has been paid.

All the existing theories of antennas can, so far as the author knows, be classified as follows:

1. The sinusoidal theory which assumes a sinusoidal distribution of the current and ignores the gap and the boundary conditions on the surface of the antenna.[1]

2. The theories based upon the model of a δ-gap, leading to an integral equation and its approximate[2] solution. In connection with these theories, that of King[3] may be mentioned, which though taking into account the boundary conditions on the surface, ignores the role and the structure of the gap.

3. The theory of Stratton and Chu[4] based upon the model of a δ-gap and upon a rigorous solution of Maxwell's equations. This theory is, however, restricted to an infinite cylinder, sphere and spheroid. The last case is the only one of any practical value for the construction of antennas. The advantage of the method of Stratton and Chu is that it avoids approximate solutions and therefore most easily allows investigation of the convergence of expressions which appear in it.

4. The theory of Schelkunoff[5] which represents the antenna as consisting of two thin cones, and the gap as a singularity of the field at the point where the two tips meet. This is the only theory which takes into account the gap and does not represent it by a δ-model. The drawback of this theory is its great complexity and also the fact that it ignores the boundary conditions on the spherical ends of the cones.

The present paper, which tries to clear up the problem of convergence and that of the structure of the gap, is based exclusively on Stratton and Chu's papers, especially those referring to the sphere and spheroid. I shall quote them as SC II and SC III respectively. The solutions given in SC II and III are not based upon approximation methods and they satisfy the boundary conditions rigorously. The restriction of the shape to a sphere or spheroid matters little in an investigation such as this which does not pretend to be of immediate practical value. It is obvious that the general results obtained here for the spheroid will hold also for (say) a cylindrical antenna, a problem much more difficult mathematically because of the boundary conditions at its ends.

Any theory of an antenna leads to the calculation of

$$I(0)/V = \text{driving-point admittance}, \tag{1.5}$$

where $I(0)$ is the current at the center of the gap, if the dimensions of the gap tend to zero. In calculating (1.5) for a sphere or spheroid, SC are led to a series

---

[2] E. Hallen, Nova Acta Reg. Soc. Sci. Upsaliensis **11**, No. 4 (1939).

[3] L. V. King, Phil. Trans. Roy. Soc. (A) **236**, 381–422 (1937).

[4] Stratton and Chu, J. of Appl. Phys. **12**, 230 (1941); 236–240 quoted here as SC II; 241–248 quoted here as SC III.

[5] S. A. Schelkunoff, Proc. I.R.E. **29**, 493–521 (1941).

$$I(0)/V = Y(0) = \sum_{n=1}^{\infty} Y_n, \tag{1.6}$$

by which the driving-point admittance is represented. The grave difficulty encountered here is that the series (1.6), or rather its imaginary part, *diverges*. The authors dismiss this difficulty by a remark that this divergence is due to the δ-model of the gap. They write[6] "this difficulty is no fault of the mathematical formulation of the problem but results from our assumption that the voltage is applied across a segment of vanishing length, implying in turn an infinite field intensity and infinite current density at the point of application." The authors claim further that a finite gap will not change the first few modes in (1.6) but will make (1.6) quickly convergent. Thus, according to the authors, we ought to take the first few modes for a finite gap, and neglect others. This sounds very vague. On the one hand if we do this, we take into account the fact that the gap is finite; otherwise (1.6) is meaningless. On the other hand, however, this finite gap will not play any role in the result. Instead of introducing its dimensions we cross out all the modes for which n is greater than a certain M. But how many expressions must we keep and how many must we cross out? How will this procedure depend on the dimensions of the gap? These are the questions which we shall try to clarify later.

The same difficulty appearing in the theories of SC appears also in the theories listed before under 2. The difference is, so far as I know, that the difficulty which came out so clearly in SC, was not even discussed in the theories based on the solutions of the integral equations. But if the driving-point admittance (or rather its imaginary part) becomes infinite for a sphere and a spheroid, then it will also become infinite for a cylinder; this can be deduced from the integral equations of one of the theories[2] and was shown by Prof. Stevenson.[7] But infinite $Y(0)$ means zero impedance, that is zero resistance and zero reactance. Therefore the matching problem cannot be solved for a δ-gap.

The theory gives results agreeing with experiment only because the approximate procedure, owing to the technical difficulties, cannot be pushed too far. It will be obvious from the content of this paper that any procedure which does not introduce the finite dimensions of the gap must lead to infinites; therefore any satisfactory theory must introduce these dimensions from the beginning, or, at least say in what stage of approximation and how they should be introduced.[8]

It is the purpose of this paper to analyze the influence of a finite gap upon the theory of antennas. The case in which this analysis is comparatively simple is that of a sphere. The essential features of the difficulties just discussed come out especially clearly in this case. For this reason most of the paper is devoted to the spherical antenna and only at its end is the spheroidal antenna discussed and then less fully.

This paper is in great part a result of discussions in a research group concerned with the problems of antennas and wave guides. In the group were Professors V. G. Smith, A. F. Stevenson, J. L. Synge and myself. The discussions which we have had

---

[6] SC III, p. 247.

[7] Privately communicated at our research group.

[8] A general theory (due to J. L. Synge), which takes into account both the dimensions of the gap and the electric field in the gap, will appear shortly.

have been extremely helpful in clearing up many difficulties and a great part of what is written down here is due to my colleagues.

To concentrate only on the logical part of the argument and not to interrupt it by calculations, most of them have been shifted to the Appendices.

2. The admittance of a sphere. A metallic sphere has a radius a. A field E_θ' is applied at the surface of the sphere; we assume that E_θ' is a function of the colatitude θ and of the time t through the factor $e^{i\omega t}$. We write

$$E_\theta' = -\frac{V}{a} f(\theta), \tag{2.1}$$

where

$$\int_0^\pi f(\theta) d\theta = 1, \tag{2.2}$$

and where

$$V = -a \int_0^\pi E_\theta' \, d\theta \tag{2.3}$$

is the applied voltage. Our assumptions here are more general than in SC II in which a special $f(\theta)$ was assumed. In SC II we have:

$$f(\theta) = \delta\left(\frac{\pi}{2} - \theta\right), \tag{2.4}$$

the voltage being applied across a narrow strip along the equator. The admittance for any θ (between 0 and π) is:

$$Y(\theta) = \frac{I(\theta)}{V} = 2\pi \sin\theta \sum_{n=1}^{\infty} \frac{\int_0^\pi f(\theta) P_n'(\cos\theta) \sin\theta d\theta}{Z_n \left[\int_0^\pi (P_n')^2 \sin\theta d\theta\right]} P_n'(\cos\theta). \tag{2.5}$$

This formula, which is basic for our further considerations is not in SC II. It is a generalization of SC II (19) in which $f(\theta) = \delta(\theta)$ and $\theta = \pi/2$ is assumed. However there is no difficulty in deriving (2.5) for anyone who has studied SC II. A few remarks about it are added in Appendix A.

About the notation in (2.5): P_n' are the associated spherical harmonics:

$$P_n' = -d P_n/d\theta. \tag{2.6}$$

The Z_n are certain complex factors depending on

$$ak = 2\pi a/\lambda \qquad (\lambda = \text{wave length}, \ a = \text{radius})$$

and the index n. We shall say more about them later, but for the moment it is sufficient to know that for very great n we have* in m.k.s. units

$$Z_n = -120\pi i n/ak. \tag{2.7}$$

---

* Comp. (SC II), equation (11), putting $2\pi\omega\epsilon_2 = 2\pi(\epsilon_2/\mu_2)^{1/2}\omega(\epsilon_2\mu_2)^{1/2} = k/60$ and $k = \omega(\epsilon_2\mu_2)^{1/2}$.

We are interested firstly in the simple case of a gap, resembling the δ-gap, but finite. We assume that $f(\theta)$ is a regular function, such that

$$f\left(\frac{\pi}{2}-\theta\right)=f\left(\frac{\pi}{2}+\theta\right), \tag{2.8}$$

i.e. symmetric with respect to the equatorial plane. In this case only the odd n's give contributions to (2.5). Puttihg $n=2m+1$, we can write instead of (2.5):

$$Y(\theta)=2\pi\sin\theta\sum_{m=0}^{\infty}\frac{\int_0^{\pi}f(\theta)\sin\theta P'_{2m+1}d\theta}{Z_{2m+1}\left[\int_0^{\pi}(P'_{2m+1})^2\sin\theta d\theta\right]}\cdot P'_{2m+1}(\cos\theta). \tag{2.9}$$

Furthermore we assume that $f(\theta)$ has its maximum for $\theta=\pi/2$, is always positive and goes to zero for $\theta=0$ and π. For example, we could choose for $f(\theta)$ the following function:

$$f(\theta)=2^{-2s-1}\frac{(2s+1)!}{(s!)^2}\sin^{2s+1}\theta, \tag{2.10}$$

where s is an integer. Indeed for great s such a function represents a steep field, concentrated symmetrically around the equatorial plane and is normalized according to (2.2). Though it is only a special case of $f(\theta)$, it will provide us with a convenient example and will allow us to see what happens if $s\to\infty$, that is, if our finite gap becomes a δ-gap. It is, at least, doubtful whether we are allowed to introduce immediately into (2.5) the δ-function and to make use of its properties. With these assumptions we shall calculate the input admittance for an arbitrary θ (in the interval 0, π). This generalization will allow us to study the character of the divergence if $s\to\infty$, $\theta\to\pi/2$.

The calculation of $\int_0^{\pi}f(\theta)\sin\theta\cdot P'_{2m+1}d\theta$ is done in Appendix B. The result is:

$$\int_0^{\pi}f(\theta)\sin\theta\cdot P'_{2m+1}\cdot d\theta=4(-1)^m(s+1)\frac{(2s+1)!(s+m+1)!(2m+1)!}{(2s+2m+3)!(s-m)!(m!)^2} \tag{2.11}$$

if $m\leqq s$, and

$$\int_0^{\pi}f(\theta)\sin\theta\cdot P'_{2m+1}\cdot d\theta=0, \tag{2.12}$$

if $m>s$.

Furthermore, because

$$\left[\int_0^{\pi}P'_{2m+1}\sin\theta d\theta\right]^{-1}=\frac{4m+3}{4(m+1)(2m+1)}, \tag{2.13}$$

we have for the admittance (2.9) as function of θ:

$$Y=2\pi\sin\theta\sum_{m=0}^{s}(-1)^m(s+1)\frac{(2s+1)!(s+m+1)!2m!(4m+3)}{Z_{2m+1}(2s+2m+3)!(s-m)!m!(m+1)!}P'_{2m+1}(\cos\theta) \tag{2.14}$$

For a finite s, the sum is finite, and therefore the problem of convergence does not appear. Our example, as expressed by the choice of (2.10), is only one of the possible examples. We could have taken a properly normalized step function instead, as we

shall do in Appendix E. Our choice (2.10), however, has the advantage that the series by which Y is represented is finite.

Let us write

$$Y = Y(\theta, s), \tag{2.15}$$

indicating the explicit dependence of Y on θ and s. First we wish to calculate:

$$Y(\theta) = \lim_{s\to\infty} Y(\theta, s). \tag{2.16}$$

To do this, we split $Y(\theta, s)$ into two parts:

$$Y(\theta, s) = Y_{0,M}(\theta, s) + Y_{M,s}(\theta, s), \tag{2.17}$$

where:

$$Y_{0,M}(\theta, s) = 2\pi \sin\theta \sum_{m=0}^{M} (-1)^m (s+1) \frac{(2s+1)!(s+m+1)!2m!(4m+3)P'_{2m+1}(\cos\theta)}{Z_{2m+1}(2s+2m+3)!(s-m)!m!(m+1)!} \tag{2.18}$$

$$Y_{M,s}(\theta, s) = 2\pi \sin\theta \sum_{m=M+1}^{s} \text{ as above.} \tag{2.19}$$

Here M is assumed to be an arbitrary but great number, later kept *constant*, while $s\to\infty$ The $Y_{M,s}(\theta, s)$ is calculated approximately by the use of Stirling's formula for $m!$, and by replacing summation by integration. The calculations are performed in Appendix C and the result is

$$Y_{M,s}(\theta, s) = \frac{iak\sqrt{\sin\theta}}{60\pi} \sum_{m=M+1}^{s} (-1)^{m+1} m^{-1} \cos\left[\frac{\pi}{4} + \left(2m + \frac{3}{2}\right)\theta\right] \cdot \exp\left[-s\int_0^{m/s} \log\frac{1+\zeta}{1-\zeta}\, d\zeta\right]. \tag{2.20}$$

Now if $s\to\infty$, we have (App. C),

$$Y_{M,\infty}(\theta) = \frac{iak\sqrt{\sin\theta}}{60\pi} \sum_{m=M+1}^{\infty} (-1)^{m+1} m^{-1} \cos\left[\frac{\pi}{4} + \left(2m + \frac{3}{2}\right)\theta\right]. \tag{2.21}$$

Let us now investigate this expression near the equatorial plane by putting

$$\theta = \frac{\pi}{2} - \frac{d}{2a} \quad \text{or} \quad \theta = \frac{\pi}{2} + \frac{d}{2a}, \tag{2.22}$$

where d is small compared to a. Then we have:

$$Y_{M,\infty}\left(\frac{d}{2a}\right) = \frac{iak}{60\pi}\int_M^{\infty} m^{-1} \cos\left[\left(2m + \frac{3}{2}\right)\frac{d}{2a}\right] dm, \tag{2.23}$$

and, for small d, we finally obtain the leading term:

$$Y_{M,\infty}\left(\frac{d}{2a}\right) = -\frac{iak}{60\pi} Ci\left(\frac{Md}{a}\right). \tag{2.24}$$

We see the character of the divergence of our series if $s\to\infty$, $d\to 0$: $Y_{M,\infty}(\to 0)$ increases to infinity like $\log d/a$:

$$|Y_{s\to\infty}| \sim |\log(d/a)|. \tag{2.25}$$

Therefore we cannot define the driving-point admittance by a δ-gap with $\theta=\pi/2$. Such a driving-point admittance does not exist. There are three possible ways of saving this situation, which we can represent schematically in the following way:

1. $f(\theta)\neq\delta$; $d\neq 0$.
2. $f(\theta)\neq\delta$; $d=0$.
3. $f(\theta)=\delta$; $d\neq 0$.

In the first case we take a continuous field distribution and Y at the distance $d/2$ from the equatorial plane. The difficulty in accepting this view is that we must know $f(\theta)$ and connect d with $f(\theta)$ in some way. The most obvious way would be to assume that $f(\theta)$ is a step function, and to identify d with the width of this step function on the one hand, and with the dimensions of the gap on the other. This special choice of $f(\theta)$ is discussed in Appendix E. Generally, however, we must introduce three arbitrary factors: (a) the function $f(\theta)$, (b) the dimension of the gap, (c) some connection between d and $f(\theta)$. As long as there is no experimental evidence to guide us in determining all these factors, this view seems to be too arbitrary for a satisfactory theory.

In the second case the driving-point admittance is given by (2.9) for $\theta=\pi/2$. Here only the function $f(\theta)$ is arbitrary and on its choice Y will depend.

In the third case we go back to the δ-function but calculate Y, not in the equatorial plane but at the distance d from it. In this case the definition of the driving-point admittance will be simplest if we can identify d with the physical dimensions of the gap. We shall accept here this point of view, assuming that d—the only new parameter entering the theory—represents the ***known*** dimension of the gap.

It is possible that one of the other views will turn out to be more convenient and the present discussion tends to show how the frame of the theory of the antenna must be broadened to include the size of the gap.

At present however, we shall accept the simplest view: *δ electric field and finite gap*, corresponding to our ***third*** case.

For this case $Y_{M,\infty}(d/2a)$ is expressed in (2.24) and the remaining task is to calculate

$$\lim_{s\to\infty} Y_{0,M}\left(s, \frac{d}{2a}\right) = Y_{0,M}\left(\frac{d}{2a}\right). \tag{2.26}$$

This is done in Appendix C. According to (C.2), (C.3) and (C.9), we have:

$$\lim_{s\to\infty} \frac{(s+1)(s+m+1)!(2s+1)!}{(s-m)!(2s+2m+3)!} = \frac{1}{2^{2m+2}}. \tag{2.27}$$

Therefore

$$Y\left(\frac{d}{2a}\right) = 2\pi\cos\left(\frac{d}{2a}\right)\sum_{m=0}^{M}(-1)^m \frac{2m!(4m+3)}{2^{2m+2}(m+1)!Z_{2m+1}} P'_{2m+1}\left(\sin\frac{d}{2a}\right) - \frac{iak}{60\pi} Ci\left(\frac{Md}{a}\right), \tag{2.28}$$

which we interpret as the final result representing the input admittance at the end of a small but finite gap in the center of a conducting sphere, when the field in the gap is represented by a δ-function.

For $d \to 0$ we have, because

$$P'_{2m+1}(0) = (-1)^m \frac{(2m+1)!}{(m!)^2 2^{2m}}, \tag{2.29}$$

the following formula for $Y_{0,M}(d \to 0)$

$$Y_{0,M}(0) = \frac{\pi}{2} \sum_{m=0}^{M} \frac{[P'_{2m+1}(0)]^2(4m+3)}{Z_{2m+1}(m+1)(2m+3)}. \tag{2.30}$$

This is exactly the formula for the driving-point admittance obtained by SC II, (19), if we there replace n by $2m+1$. Though our discussion shows that $Y_{M,\infty}(0)$ and therefore $Y(0)$ becomes infinite at the driving-point, one could argue, as SC does:

In $Y_{0,M}(d/2a)$ the gap d will play a small role and therefore we may assume $d=0$. On the other hand, if d is finite the integral representing $Y_{M,\infty}(d/2a)$ can be neglected and thus we arrive at a formula (2.30) which is convergent and does not contain the dimensions of the gap. But the argument could just as well be reversed. We could say: For small d the end of the series represented by the *Ci* function becomes essential, whereas a large d will modify even the first few expressions of our series. In a satisfactory theory we must be able to answer the following question: how can we choose M for a given ak, d, $\epsilon > 0$ so that

$$|Y_{M,\infty}| < \epsilon. \tag{2.31}$$

Our discussions provide an answer to this question which was not supplied by SC. Let us take as an example:

$$ka = \sqrt{2}; \qquad d/a = 0.1; \qquad M = 15.$$

Then the absolute value of the first term in the sum in (2.28) is approximately

$$\frac{3\pi}{2} |Z_1^{-1}|.$$

But, as will be seen from equations (3.5) and (3.16),

$$|Z_1^{-1}| = \frac{\sqrt{2}}{2\pi \times 60};$$

therefore the first expression is $3\sqrt{2}/4 \times 60$. On the other hand the absolute value of the integral expression is $(\sqrt{2}/60\pi)Ci(1.5) \sim (\sqrt{2}/2\pi \times 60)$, which is of the same order as the first expression in the series (2.28).

The result as expressed by (2.28) could have been found much more quickly by the use of Dirac's δ-function. Indeed, putting $f(\theta) = \delta[(\pi/2) - \theta]$ in (2.9), we find

$$Y\left(\frac{d}{2a}\right) = 2\pi \cos\left(\frac{d}{2a}\right) \sum_{m=1}^{\infty} \frac{P'_{2m+1}(0) P'_{2m+1}(\sin d/2a)}{Z_{2m+1}\left[\int_0^{\pi} (P'_{2m+1})^2 \sin\theta d\theta\right]}. \tag{2.32}$$

By splitting this into two parts and using the asymptotic formula for P'_{2m+1}, we

again obtain (2.28). But in obtaining (2.28) by the transition $s \to \infty$, we avoided the use of Dirac's δ-function and at the same time gave an example of the input admittance with a given field distribution in the gap. Though the choice of M is arbitrary, as long as we can apply Stirling's formula, our equation (2.28) will be the more exact the greater is the chosen M.

3. The coefficients Z_{2m+1}. The coefficients Z_n are defined in SC II, (8), (6). Assuming σ (conductivity) $\to \infty$, we have, in m.k.s. units,

$$Z_n = i \cdot 2\pi \cdot 60 \left[\frac{H^{(2)}_{n-1/2}(ka)}{H^{(2)}_{n+1/2}(ka)} - \frac{n}{ka} \right]. \tag{3.1}$$

We shall now show how these expressions can be calculated without the knowledge of Hankel's functions. The reason for doing it is that we intend to apply a similar method later when dealing with the problem of a spheroidal antenna.

Because of the recurrence formula:

$$H^{(2)}_{2m+1/2} - \frac{2m+1}{ka} H^{(2)}_{2m+3/2} = H^{(2)}_{2m+3/2}, + \frac{1}{2ak} H^{(2)}_{2m+3/2}, \tag{3.2}$$

we can write (3.1)

$$Z_{2m+1} = i \cdot 2\pi \cdot 60 \left[\frac{(x^{1/2} H^{(2)}_{2m+3/2})'}{x^{1/2} H^{(2)}_{m+3/2}} \right], \tag{3.3}$$

where we put

$$x = ka. \tag{3.4}$$

But the $x^{1/2} H^{(2)}_{2m+3/2}$ are "densities" corresponding to Hankel's functions of the second kind. We write

$$x^{1/2} H^{(2)}_{2m+3/2} = h_{2m+3/2} = h, \tag{3.5}$$

where $h_{2m+3/2}$ satisfies the equation:

$$h'' + \frac{4m^2 + 6m + 2}{x^2} h + h = 0. \tag{3.6}$$

It is more convenient to calculate Z_{2m+1} directly, and not by means of the h's. Indeed we can easily find the differential equation which Z must satisfy. We write:

$$\zeta_{2m+1} = \frac{h_{2m+3/2}}{h'_{2m+3/2}} \tag{3.7}$$

$$Z_{2m+1} = i \frac{2\pi \times 60}{\zeta_{2m+1}}. \tag{3.8}$$

Then (omitting the indices)

$$\zeta' = 1 - \left(\frac{h}{h'} \right)^2 \frac{h''}{h}, \tag{3.9}$$

which, because of (3.6) and (3.7), becomes

$$\zeta' + \zeta^2\left(\frac{\nu^2}{x^2} - 1\right) = 1, \tag{3.10}$$

where

$$\nu^2 = 4m^2 + 6m + 1. \tag{3.11}$$

Riccati's equation (3.10) can be solved by a recurrence formula. Its derivation is given in Appendix D. This formula is:

$$\zeta_{2m+1} = \frac{\zeta_{2m-1} \times [x^2/(4m+1) - 2m] + x^2}{\zeta_{2m-1}[2m(2m+1) - x^2] + x\{[x^2/(4m+1)] - (2m+1)\}}, \tag{3.12}$$

and it is a purely algebraical formula which does contain derivatives. We start by finding ζ_{-1}. For $m = -1$, equation (3.10) takes the form:

$$\zeta_{-1}' - \zeta_{-1}^2 = 1. \tag{3.13}$$

As a solution of (3.13) we choose

$$\zeta_{-1} = i. \tag{3.14}$$

In justifying (3.14) we must go back to (3.5) and (3.7). If

$$\frac{h'}{h} \sim -i \quad \text{for} \quad x \to \infty,$$

then

$$x^{1/2}H^{(2)} \sim h \sim e^{-ix} \quad \text{for} \quad x \to \infty.$$

We can now calculate the first ζ in our series corresponding to $m = 0$. We have, from (3.12) and (3.14),

$$\zeta_1 = -\frac{x}{1 - x^2 + x^4} + \frac{ix^4}{1 - x^2 + x^4}, \tag{3.15}$$

or, because of (3.8):

$$\frac{1}{Z_1} = \frac{1}{2\pi \times 60}\left[\frac{x^4}{1 - x^2 + x^4} + \frac{ix}{1 - x^2 + x^4}\right]. \tag{3.16}$$

We see: for $x \to 0$, the real part of ζ_1 goes to zero as x and the imaginary part as x^4. For $x \to \infty$, the real part of ζ_1 goes to zero as $1/x^3$ and the imaginary part goes to i. From the recurrence formula it follows that for *all* m and small $x (x \ll 2m)$ the real part of ζ goes to zero as x, and is negative, whereas the imaginary part goes to zero at least as x^4.

For very great m and very small x, $(x \ll 2m)$ we find the leading term by writing (3.10):

$$\zeta' + \zeta^2 \frac{4m}{x^2} = 1. \tag{3.17}$$

The leading term is:

$$\xi_{2m+1} = -x/2m, \tag{3.18}$$

in agreement with (2.7), if we take into account (3.8).

4. The spheroidal antenna. We shall now generalize our arguments for the case of a spheroid.

We characterize the points in space by the spheroidal coordinates ξ, η, Φ with:

$$\xi \geqq 1; \qquad -1 \leqq \eta \leqq 1; \qquad 0 \leqq \Phi \leqq 2\pi, \tag{4.1}$$

where ξ, η, Φ are defined in terms of cylindrical coordinates by

$$r^2 = f^2(\xi^2 - 1)(1 - \eta^2); \qquad z = f\xi\eta; \qquad \Phi = \Phi, \tag{4.2}$$

and in terms of polar coordinates by

$$R^2 = f^2(\xi^2 + \eta^2 - 1); \qquad \cos\theta = \frac{\xi\eta}{(\xi^2 + \eta^2 - 1)^{1/2}}, \qquad \Phi = \Phi. \tag{4.3}$$

Here $2f$ is the distance between the foci.* A spheroid is characterized by a *constant* coordinate $\xi = \xi_0$. Knowing ξ_0 and f we can find the half-axes a, b:

$$a = f\xi_0; \qquad b = f\sqrt{\xi_0^2 - 1}. \tag{4.4}$$

In CS III, the input admittance of such a spheroidal antenna is calculated. Again, as in the case of a spheroidal antenna, the δ-model of the gap is assumed and the imaginary part of the input admittance is infinite.

We start by generalizing CS III in two respects: *first*, we do not take the δ-model of a gap but an arbitrary field; *secondly* we write down the admittance not for $\eta = 0$, but for any η ($|\eta| \leqq 1$). The argument is very similar to that in the case of a sphere and hardly worth repeating. The result of these generalizations leads us to the following formula corresponding to (2.5) in the case of a sphere:

$$Y = 2\pi(1 - \eta^2) \sum_{l=0}^{\infty} \frac{\int_{-1}^{+1}(1 - \eta^2) f(\eta) Se_l^1(\eta)\, d\eta}{Z_l \int_{-1}^{+1}(1 - \eta^2)\left[Se_l^1(\eta)\right]^2 d\eta} Se_l^1(\eta). \tag{4.5}$$

It is written in such a way as to expose an analogy with (2.5) and, at the same time, to use the notation in SC III. To establish a connection with SC III one must substitute in (4.5)

$$\frac{2\pi}{Z_l} = -\frac{ikf}{60} \frac{(\xi_0^2 - 1) Re_l^4(\xi_0)}{d/d\xi_0\left[(\xi_0^2 - 1) Re_l^4(\xi_0)\right]}. \tag{4.6}$$

Equations (4.5) and (4.6) are, for $\eta = 0$ and $f(\eta) = \delta(\eta)$, identical with SC III (2.8).

For the sake of completeness we shall explain the notation in (4.5) and (4.6):

The function $f(\eta)$ satisfies the condition

$$\int_{-1}^{+1} f(\eta)\, d\eta = 1, \tag{4.7}$$

* This f will hardly be confused with $f(\eta)$ characterizing the electric field and always written with its argument η.

and in the case of a symmetrical field:

$$f(\eta) = f(-\eta). \tag{4.8}$$

The functions Se_l^1 and Re_l^4 are solutions of the equation:

$$(1 - z^2)W'' - 4zW' + (\lambda - f^2k^2z^2)W = 0 \tag{4.9}$$

for $z = \eta$ and $z = \xi$ respectively. The eigenvalues of λ_l are determined by the condition that Se_l^1 remains finite at the poles $\eta = \pm 1$. The function Re_l^4 for given eigenvalues of λ_l is so chosen that the field at large distances from the center reduces to a wave travelling radially outward. The functions Se_l^1 and Re_l^4 are related to the spherical harmonics and Hankel's functions through coefficients which must be determined numerically. However, for our argument the knowledge of these relations is not essential.

The prolate spheroid has a gap across the equator $\eta = 0$. By a method similar to that of Section 2, we shall now calculate the input admittance at the points

$$z = \pm d/2, \tag{4.10}$$

which, because of the second equation in (4.2) means:

$$\eta = \pm d/2f\xi_0, \tag{4.11}$$

or, finally, because of (4.4):

$$\eta = \pm d/2a, \tag{4.12}$$

where a is here half the long axis. For $f(\eta)$ we shall take the δ-function:

$$f(\eta) = \delta(\eta), \tag{4.13}$$

and our problem will be to find what happens to (4.5) if $d \to 0$. It would have been more rigorous to take, say:

$$f(\eta) \sim (1 - \eta^2)^s \tag{4.14}$$

and then go to the limit $s \to \infty$, as we did in Section 2. However it will be much quicker to use the δ-functions instead and we have seen in Section 2 that the result is the same, which is also true in the case of a spheroid.

We now rewrite (4.5), introducing $f(\eta) = \delta$ and $\eta = d/2a$. Because $Se_l^1 = 0$ if l is odd, we have:

$$Y\left(\frac{d}{2a}\right) = 2\pi[1 - (d/2a)^2]\sum_{m=0}^{\infty} \frac{Se_{2m}^1(0)Se_{2m}^1(d/2a)}{Z_{2m}\int_{-1}^{+1}(1 - \eta^2)(Se_{2m}^1)^2 d\eta}. \tag{4.15}$$

Now again we write (4.15) in the form

$$Y = Y_{0,M} + Y_{M,\infty}, \tag{4.16}$$

and shall proceed to calculate $Y_{M,\infty}$ approximately for sufficiently great M. For the moment we shall ignore Z_{2m} and shall calculate all other expressions appearing in (4.15).

The functions Se_{2m}^1 must be finite and satisfy (4.9) for $z = \eta$. But if λ_{2m} is very great, which we assume, $f^2k^2\eta$ can be neglected in (4.9), because $|\eta| \leq 1$. Therefore, for great λ_{2m} we can write (4.9):

$$(1-\eta^2)Se_{2m}^{1\prime\prime} - 4\eta Se_{2m}^{1\prime} + \lambda_{2m} Se_{2m}^{1} = 0. \tag{4.17}$$

Therefore, Se_{2m}^{1} will not depend on f for large λ_{2m}. Substituting in (4.17):

$$Se_{2m}^{1} = (1-\eta^2)^{-1/2} P, \tag{4.18}$$

we can write instead of (4.17):

$$P'' + 2\eta P' - \frac{\eta^2}{1-\eta^2} P + \lambda_{2m} P = 0. \tag{4.19}$$

But this is exactly the equation for P'_{2m+1} for which an everywhere finite solution exists if

$$\lambda_{2m} = 2m(2m+3) \sim 4m^2, \tag{4.20}$$

and m is very large. The approximate expression for P'_{2m+1} with large m is:

$$P'_{2m+1}\left(\frac{d}{2a}\right) = 2(-1)^m \sqrt{\frac{m}{\pi \cos\left(d/2a\right)}} \cos\left[\left(2m+\frac{3}{2}\right)\frac{d}{2a}\right], \tag{4.21}$$

therefore, because of (4.18),

$$Se_{2m}^{1}(0) Se_{2m}^{1}\left(\frac{d}{2a}\right)\left[1-\left(\frac{d}{2a}\right)^2\right] = \frac{4m}{\pi}\left[1-\left(\frac{d}{2a}\right)^2\right]^{1/2} \cos\left[\left(2m+\frac{3}{2}\right)\frac{d}{2a}\right]. \tag{4.22}$$

The next step is to calculate the integral in the denominator of (4.15). Again because of (4.18), we have:

$$\int_{-1}^{+1} (1-\eta^2)(Se_{2m}^{1})^2 d\eta = \int_{-1}^{+1} (P'_{2m+1})^2 d\eta = \frac{4(m+1)(2m+1)}{4m+3} \sim 2m. \tag{4.23}$$

We can, therefore, write for small d and sufficiently great M:

$$Y_{M,\infty} = 2\pi\left[\frac{2}{\pi} \sum_{m=M+1}^{\infty} \frac{\cos\left[(2m+\frac{3}{2})(d/2a)\right]}{Z_{2m}}\right]. \tag{4.24}$$

The last step will be to find Z_{2m}.

5. The coefficients Z_{2m} for a spheroid. It will be a little more convenient to introduce, instead of Re_{2m}^{4}, the corresponding density-functions, as we did in Section 3. The equation which Re_{2m}^{4} satisfies is:

$$(\xi^2-1)Re_{2m}^{4\prime\prime} + 4\xi Re_{2m}^{4\prime} - (\lambda_{2m} - f^2k^2\xi^2) Re_{2m}^{4} = 0. \tag{5.1}$$

We now introduce

$$(\xi^2-1)Re_{2m}^{4} = \mathrm{P}, \tag{5.2}$$

and (5.1) becomes, because of (4.20),

$$(\xi^2-1)\mathrm{P}'' - [(4m^2+6m+2) - f^2k^2\xi^2]\mathrm{P} = 0. \tag{5.3}$$

Because of (4.6) we have:

$$\frac{2\pi}{Z_{2m}} = -\frac{ikf}{60}\,\mathrm{P}/\mathrm{P}' = -\frac{ikf}{60}\,\zeta_{2m}, \tag{5.4}$$

where

$$\mathrm{P}/\mathrm{P}' = \zeta_{2m} = \zeta.$$

We have:

$$\zeta' = 1 - \zeta^2 \mathrm{P}''/\mathrm{P}. \tag{5.5}$$

Putting

$$4m^2 + 6m + 2 = \nu^2; \qquad f^2k^2 = c^2, \tag{5.6}$$

we get from (5.5) because of (5.3)

$$\zeta' + \zeta^2\left(\frac{\nu^2}{\xi^2 - 1} - \frac{c^2\xi^2}{\xi^2 - 1}\right) = 1, \tag{5.7}$$

which is Riccati's equation for ζ. Introducing now:

$$\bar{\nu}^2 = \nu^2 - c^2, \tag{5.8}$$

we can write (5.7):

$$\zeta' + \zeta^2\left(\frac{\bar{\nu}^2}{\xi^2 - 1} - c^2\right) = 1. \tag{5.9}$$

The leading term of the solution for every great $\bar{\nu}$ and small ξ (so that $\bar{\nu}^2/\xi^2 - 1 \gg c^2$) is

$$\frac{\mathrm{P}}{\mathrm{P}'} = \zeta_{2m} \sim \pm\frac{1}{\bar{\nu}}\sqrt{\xi^2 - 1} \sim \pm\frac{1}{2m}\sqrt{\xi^2 - 1}. \tag{5.10}$$

The proper sign will be selected by the condition that for $\xi \to 0$ and $f \to 0$, our solution goes over into that of a spherical antenna.

Introducing (5.10) into (5.4) and into (4.24) we have:

$$Y_{M,\infty}\left(\frac{d}{2a}\right) = \mp\frac{2ikf}{60\pi}\sum_{m=M+1}^{\infty}\frac{\sqrt{\xi_0^2 - 1}}{2m}\cos\left[\left(2m + \frac{3}{2}\right)\frac{d}{2a}\right]. \tag{5.11}$$

Changing the summation into an integration we have, because of (4.4)

$$Y_{M,\infty}\left(\frac{d}{2a}\right) = \mp\frac{ikb}{60\pi}\int_M^{\infty}\frac{\cos\left[(2m + \frac{3}{2})(d/2a)\right]}{m}\,dm. \tag{5.12}$$

But for $b = a$ this is *exactly* (2.23) if we take the *lower* sign in (5.10). Therefore finally:

$$Y_{M,\infty}\left(\frac{d}{2a}\right) = -\frac{ibk}{60\pi}\,Ci\left(\frac{Md}{a}\right), \tag{5.13}$$

and because of (4.15):

$$Y\left(\frac{d}{2a}\right) = 2\pi\left[1 - \left(\frac{d}{2a}\right)^2\right]\sum_{m=0}^{M} \frac{Se_{2m}^{1}(0)Se_{2m}^{1}(d/2a)}{Z_{2m}\int_{-1}^{+1}(1-\eta^2)(Se_{2m}^{1})^2 d\eta} - \frac{ibk}{60\pi} Ci\left(\frac{Md}{a}\right). \tag{5.14}$$

As we see, the only difference between (5.13) and (2.24) is that in the case of the spheroid we have as a factor the *small* axis. Thus $Y_{M,\infty}(d\to 0)$ tends to infinity like

$$b \log (d/a) \tag{5.15}$$

and can be made to be always finite if $b \log d/a$ is finite.

For thin antennas and finite d, $Y_{M,\infty}$ is much smaller than in the case of a sphere with radius a; therefore the neglect of $Y_{M,\infty}$ is much more justified. This is however not true for thick antennas. But the essential result is the same as in the case of a spherical antenna: the dimensions of the gap must be involved in the theory of the antenna, otherwise the input admittance becomes infinite. But infinite driving-point admittance means zero driving-point impedance. In view of this result it is difficult to see what the curves 3 and 4 in SC III mean. They seem to represent the resistance and reactance of a spheroidal antenna and a current distribution which does not become infinite for $\eta = 0$. They may refer to a finite gap and to an electric field in the gap, but in that case we would like to know to what field and to what gap they refer. It is plausible that neither the field nor the size of the gap matters much if the antenna is thin and if the size of the gap is greater than the thickness of the antenna and much smaller than its length. But such a statement ought to be deduced from the theory or at least formulated explicitly as an assumption.

APPENDIX A. ON THE DERIVATION OF (2.5)

Equations (6) and (8) in SC II give

$$H_{\Phi|R=a} = -\sum_{n=1}^{\infty} \frac{A_n}{Z_n} e^{i\omega t} P_n'(\cos\theta), \tag{A.1}$$

where A_n is here used instead of $(\omega\mu_1/i\sigma_1)^{1/2}C_n$ in SC's notation. On the other hand SC II (7) is:

$$-\frac{V}{a} f(\theta) = E_\theta' = e^{i\omega t}\sum_{n=1}^{\infty} A_n P_n'(\cos\theta). \tag{A.2}$$

From (A.2) it follows because of the orthogonal properties of P_n', that:

$$A_n = -\frac{2n+1}{2n(n+1)}\left[\int_0^\pi f(\theta)(P_n')\sin\theta d\theta\right] e^{-i\omega t}\frac{V}{a}. \tag{A.3}$$

Putting (A.3) into (A.1) we have:

$$\begin{aligned} H_{\Phi|R=a} &= \sum_{n=1}^{\infty} \frac{V}{a}\frac{2n+1}{2n(n+1)}\left[\int_0^\pi f(\theta)(P_n')\sin\theta d\theta\right]\frac{P_n'}{Z_n} \\ &= \frac{V}{a}\sum_{n=1}^{\infty}\frac{\int_0^\pi f(\theta)(P_n')\sin\theta d\theta}{Z_n\int_0^\pi (P_n')^2\sin\theta d\theta} P_n'(\cos\theta). \end{aligned} \tag{A.4}$$

Finally from SC II (13) we see:

$$I = 2\pi a \sin\theta H_{\Phi|R=a};$$

therefore

$$Y = \frac{I}{V} = 2\pi \sin\theta \sum_{n=1}^{\infty} \frac{\int_0^\pi f(\theta)(P_n')\sin\theta d\theta}{Z_n \int_0^\pi (P_n')^2 \sin\theta d\theta} P_n'(\cos\theta) \tag{A.5}$$

which is exactly (2.5).

APPENDIX B. THE CALCULATION OF

$$B = 2^{-2s-1}\frac{(2s+1)!}{(s!)^2}\int_0^\pi \sin^{2s+2}\theta P'_{2m+1}d\theta. \tag{B.1}$$

Because of

$$P'_{2m+1} = -dP_{2m+1}/d\theta \tag{B.2}$$

and the recursion formula

$$\cos\theta P_{2m+1} = \frac{2(m+1)}{4m+3}P_{2(m+1)} + \frac{2m+1}{4m+3}P_{2m}, \tag{B.3}$$

we have, introducing $\mu = \cos\theta$:

$$\begin{aligned}\int_0^\pi P'_{2m+1}\sin^{2s+2}\theta d\theta &= 2(s+1)\int_1^{+1} P_{2m+1}(1-\mu^2)^s \mu d\mu \\ &= \frac{2(s+1)}{4m+3}\left\{2(m+1)\int_{-1}^{+1}(1-\mu^2)^s P_{2(m+1)}d\mu\right. \\ &\quad \left. + (2m+1)\int_{-1}^{+1}(1-\mu^2)^s P_{2m}d\mu\right\}.\end{aligned} \tag{B.4}$$

Therefore, the problem is reduced to finding an integral of the type

$$T_n^s = \int_{-1}^{+1}(1-\mu^2)^s P_{2n}d\mu. \tag{B.5}$$

To find T_n we must combine the results of Examples 1 and 6 on pp. 310, 311, in Whittaker and Watson's *Modern Analysis*, Fourth Edition, 1940. The result is:

$$\begin{aligned}T_n^s &= (-1)^n 2^{2s+1}\left(\frac{s!}{n!}\right)^2 \frac{(2n)!(s+n)!}{(s-n)!(2s+2n+1)!} \quad \text{if} \quad s \geqq n, \\ T_n^s &= 0 \quad \text{if} \quad s < n.\end{aligned} \tag{B.6}$$

The combination of (B.1) and (B.4), (B.5), (B.6) gives:

$$B = 2^{-2s}\frac{(s+1)(2s+1)!}{(4m+3)(s!)^2}\left[2(m+1)T_{m+1}^s + (2m+1)T_m^s\right], \tag{B.7}$$

which, because of (B.6) and some simple algebra, gives the results as expressed in (2.11) and (2.12).

APPENDIX C. CALCULATION OF $Y_{M,s}(\theta, s)$

Because of (2.7) we can write (2.19)

$$\sum_{m=M+1}^{s} C_m^s = \frac{Y \cdot 60}{iak \sin\theta}$$

$$= \sum_{m=M+1}^{s} (-1)^m (s+1) \frac{(2s+1)!(s+m+1)!2m!(4m+3)}{(2s+2m+3)!(s-m)!m!(m+1)!(2m+1)} P'_{2m+1}(\cos\theta). \quad (C.1)$$

First, we calculate the expressions in which s appears. These are:

$$\frac{(s+1)[1\cdot 2\cdot 3\cdots(s+m+1)][1\cdot 2\cdots(2s+1)]}{[1\cdot 2\cdots(s-m)][1\cdot 2\cdots(2s+1)(2s+2)\cdots(2s+2m+3)]}$$

$$= \frac{[(s+1-m)\cdots(s+1+m-m)][(s+1)(s+2)\cdots(s+m+1)]}{2^{2m+2}(s+1)(s+1+\frac{1}{2})(s+2)(s+2+\frac{1}{2})\cdots(s+m+1)(s+m+1+\frac{1}{2})}$$

$$= \frac{1}{2^{2m+2}} \prod_{\alpha=0}^{m} \frac{[1-\alpha/(s+1)]}{[1+(\alpha+\frac{1}{2})/(s+1)]}. \quad (C.2)$$

Assuming that s is great, taking log of the above expression and changing the summation into integration, we have:

$$\frac{1}{2^{2m+2}} \prod_{\alpha=0}^{m} \frac{[1-\alpha/(s+1)]}{[1+(\alpha+\frac{1}{2})/(s+1)]} \sim \frac{1}{2^{2m+2}} \exp\left[-s\int_0^x \log\frac{1+\xi}{1-\xi}\,d\xi\right], \quad (C.3)$$

where

$$x = m/s. \quad (C.4)$$

If for the expressions depending on m, we use Stirling's formula, we obtain:

$$C_m^s = \frac{1}{2m\sqrt{\pi m}}(-1)^m \exp\left[-s\int_0^x \log\frac{1+\xi}{1-\xi}\,d\xi\right] P'_{2m+1}(\cos\theta). \quad (C.5)$$

Now for P'_{2m+1} with great m we have approximately:

$$P'_{2m+1} = -2\sqrt{\frac{m}{\pi\sin\theta}} \cos\left(\frac{\pi}{4} + \left(2m+\frac{3}{2}\right)\theta\right), \quad (C.6)$$

therefore

$$C_m^s = \frac{(-1)^{m+1}}{m\pi\sqrt{\sin\theta}} \exp\left[-s\int_0^{m/s} \log\frac{1+\xi}{1-\xi}\,d\xi\right] \cos\left[\frac{\pi}{4} + \left(2m+\frac{3}{2}\right)\theta\right], \quad (C.7)$$

and because of (C.1) we have (2.20):

$$Y_{M,S} = \frac{iak\sqrt{\sin\theta}}{60\pi} \sum_{m=M+1}^{s} (-1)^{m+1} \frac{1}{m} \exp\left[-s\int_0^{m/s} \log\frac{1+\xi}{1-\xi}\,d\xi\right] \cos\left[\frac{\pi}{4} + \left(2m + \frac{3}{2}\right)\theta\right]. \quad (C.8)$$

If $s \to \infty$ the expression in the exponent is:

$$\lim_{s\to\infty}\left[-s\int_0^{m/s} \log\frac{1+\xi}{1-\xi}\,d\xi\right] = -\lim_{\alpha\to 0}\left[\frac{1}{\alpha}\int_0^{m\alpha} \log\frac{1+\xi}{1-\xi}\,d\xi\right] = 0. \quad (C.9)$$

Therefore (2.21) follows from (C.8) and (C.9).

APPENDIX D. THE RECURSION FORMULA (3.12)

We can deduce the recursion formula (3.12) for any cylindrical function density z_p satisfying the equation:

$$z_p'' - \frac{p^2 - \frac{1}{4}}{x^2} z_p + z_p = 0. \quad (D.1)$$

The known recursion formula for z_p is:

$$\frac{p - \frac{1}{2}}{x} z_{p-1} - z'_{p-1} = z_p. \quad (D.2)$$

On the other hand we have, because of (D.2),

$$\frac{z_p'}{z_p} = \frac{-(p-\frac{1}{2})x^{-2}z_{p-1} + (p-\frac{1}{2})x^{-1}z'_{p-1} - z''_{p-1}}{(p-\frac{1}{2})x^{-1}z_{p-1} - z'_{p-1}}. \quad (D.3)$$

This gives, because of (D.1):

$$\frac{z_p'}{z_p} = \frac{-(p-\frac{1}{2})x^{-2}z_{p-1} + (p-\frac{1}{2})x^{-1}z'_{p-1} - \left\{\left[(p-1)^2 - \frac{1}{4}\right]x^{-2} - 1\right\}z_{p-1}}{(p-\frac{1}{2})x^{-1}z_{p-1} - z'_{p-1}}. \quad (D.4)$$

Putting

$$z_p'/z_p = y_p, \quad (D.5)$$

we have

$$y_p = \frac{1 + (p-\frac{1}{2})x^{-1}y_{p-1} - (p-\frac{1}{2})^2x^{-2}}{(p-\frac{1}{2})x^{-1} - y_{p-1}}. \quad (D.6)$$

Now, by employing this formula twice, we have:

$$y_p = \frac{y_{p-2}\,x(x^2/(2p-2) - (p-\frac{1}{2})) + (p-3/2)(p-\frac{1}{2}) - x^2}{y_{p-2}x^2 + x(x^2/(2p-2) - (p-3/2))}.$$

Let us now introduce

$$p = 2m + 3/2, \quad (D.7)$$

as dedicated by the comparison of z_p'/z_p with (3.4). Thus we have:

$$y_{2m+3/2} = \frac{x\,(x^2/(4m+1) - (2m+1))\,y_{2m-1/2} + 2m(2m+1) - x^2}{x^2 y_{2m-1/2} + x(x^2/(4m+1) - 2m)}. \tag{D.8}$$

Finally, introducing:

$$\zeta_{2m+1} = \frac{1}{y_{2m+3/2}}, \tag{D.9}$$

we have our recursion formula (3.12).

APPENDIX E. THE DRIVING-POINT ADMITTANCE IF $f(\theta)$ IS A STEP FUNCTION

We shall calculate the driving-point admittance for a spherical antenna, assuming for $f(\theta)$ a step function defined by:

$$\begin{aligned} f(\theta) &= \frac{a}{d} \quad \text{for} \quad \frac{\pi}{2} + \frac{d}{2a} \geqq \theta \geqq \frac{\pi}{2} - \frac{d}{2a}, \\ f(\theta) &= 0 \quad \text{for} \quad \theta > \frac{\pi}{2} + \frac{d}{2a} \quad \text{and} \quad \theta < \frac{\pi}{2} - \frac{d}{2a}. \end{aligned} \tag{E.1}$$

We assume that d is small and we shall calculate the admittance for

$$\cos\theta_0 = \frac{d}{2a}, \quad \text{that is} \quad \theta_0 = \frac{\pi}{2} - \frac{d}{2a}. \tag{E.2}$$

We introduce (E.1) into (2.9). We have, because of (2.6) and because d is small:

$$\int_0^\pi f(\theta) P_{2m+1}' \sin\theta d\theta = 2P_{2m+1}\left(\frac{d}{2a}\right)\frac{a}{d}. \tag{E.3}$$

Therefore (2.9) can be written for our choice of $f(\theta)$:

$$Y\left(\frac{d}{2a}\right) = \frac{4\pi a}{d}\sum_{m=0}^{\infty} \frac{P_{2m+1}(d/2a)P_{2m+1}'(d/2a)}{\left[\int_0^\pi (P_{2m+1}')^2 \sin\theta d\theta\right] Z_{2m+1}}. \tag{E.4}$$

We are interested in calculating $Y_{M,\infty}(d/2a)$ defined by:

$$Y_{M,\infty}\left(\frac{d}{2a}\right) = \frac{4\pi a}{d}\sum_{m=M+1}^{\infty} \frac{P_{2m+1}(d/2a)P_{2m+1}'(d/2a)}{Z_{2m+1}\left[\int_0^\pi (P_{2m+1}')^2 \sin\theta d\theta\right]}. \tag{E.5}$$

For great m we have:

$$\begin{aligned} P_{2m+1}\left(\frac{d}{2a}\right) &= (-1)^m\sqrt{\frac{1}{\pi m}}\sin\left[\left(2m+\frac{3}{2}\right)\frac{d}{2a}\right] \\ P_{2m+1}'\left(\frac{d}{2a}\right) &= (-1)^m 2\sqrt{\frac{m}{\pi}}\cos\left[\left(2m+\frac{3}{2}\right)\frac{d}{2a}\right] \\ \left[\int_0^\pi (P_{2m+1}')^2 \sin\theta d\theta\right]^{-1} &= \frac{1}{2m} \end{aligned} \tag{E.6}$$

$$\frac{1}{Z_{2m+1}} = \frac{iak}{4\pi \times 60m}.$$

Therefore

$$Y_{M,\infty}\left(\frac{d}{2a}\right) = \frac{iak}{60 \times \pi} \sum_{M+1}^{\infty} \frac{\sin\left[(2m+\frac{1}{2})d/a\right]}{2m^2 d/a}. \tag{E.7}$$

Changing summation into integration we have:

$$Y_{M,\infty}\left(\frac{d}{2a}\right) = \frac{iak}{\pi \times 60} \int_{\pi M(d/a)}^{\infty} \frac{\sin x}{x^2}\, dx, \tag{E.8}$$

and the leading part of (E.8) is for sufficiently small d:

$$Y_{M,\infty}\left(\frac{d}{2a}\right) = -\frac{iak}{\pi \times 60} Ci\left(\frac{2Md}{a}\right). \tag{E.9}$$

It is interesting to compare this result with (2.24). The only difference is in the argument of the Ci function, which matters very little, if the argument is small.

One would be tempted to calculate the driving-point admittance by taking $\theta = \pi/2$ and not, as we did, $\theta = \pi/2 - d/2a$. This means that in (E.4) and (E.5) we would have to substitute zero instead of $d/2a$ as an argument in P'_{2m+1}. Then for $Y_{M,\infty}(0)$ we easily find:

$$Y_{M,\infty}(0) = \frac{iak}{\pi \times 60} \sum_{M+1}^{\infty} \frac{\sin\left[(2m+3/2)d/2a\right]}{m^2 d/a}, \tag{E.10}$$

and changing summation into integration we have

$$Y_{M,\infty}(0) = -\frac{iak}{\pi \times 60} Ci\left(\frac{Md}{a}\right),$$

that is the same result as in (2.24).

The argument will be very similar in the case of a spheroid. Thus we can collect all the results concerning $Y_{M,\infty}$ in the following two tables:

Sphere			Spheroid		
$f(\theta)$	θ	$Y_{M,\infty}$	$f(\eta)$	η	$Y_{M,\infty}$
Dirac's function	$\frac{\pi}{2}$	∞	Dirac's function	0	∞
	$\frac{\pi}{2} \pm \frac{d}{2a}$	$-\frac{iak}{60\pi} Ci\left(\frac{Md}{a}\right)$		$\pm\frac{d}{2a}$	$-\frac{ibk}{60\pi} Ci\left(\frac{Md}{a}\right)$
Step function	$\frac{\pi}{2}$		Step function	0	
	$\frac{\pi}{2} \pm \frac{d}{2a}$	$-\frac{iak}{60\pi} Ci\left(\frac{2Md}{a}\right)$		$\pm\frac{d}{2a}$	$-\frac{ibk}{60\pi} Ci\left(\frac{2Md}{a}\right)$

MULTIPLE REFLECTIONS BY PLANE MIRRORS*

BY

L. B. TUCKERMAN

National Bureau of Standards

The article by Synge[1] called to my mind a more general treatment of reflections by plane mirrors which I saw when, in 1898, as a sophomore in college, I was studying quaternions. I cannot cite the reference because I took no particular note of it at the time. I never had occasion to use the theory until 1921 when I needed it to determine the errors in my optical lever system,[2] which consists of an autocollimated three-mirror combination.

My attention has since been called to a book by Silberstein[3] which treats the same problem with a modified Gibbs notation. Silberstein's Eq. (25) on p. 22 is identical in form with Synge's Eq. (4.1) but his later treatment is different and he does not note, a Synge does, that the formulae represent rotations.

The quaternion treatment of the problem is so simple that I had no trouble in reconstructing it, at least in its essential features. Comparing it with Synge's and Silberstein's treatments strengthens my feeling that Heaviside, Föppl, Gibbs and their followers did the world a disservice in rejecting Hamilton's simple, concise notation and algorithms for the cumbersome complexity of the vector notations currently taught. It therefore occurred to me that the readers of the Quarterly of Applied Mathematics might be interested in seeing an outline of the quaternion treatment.

When the first draft of this paper was submitted for publication, the reviewer called attention to a recent article by Coxeter.[4] He gives a very general quaternion treatment of reflection and rotation in three and four dimensions but does not discuss special cases in detail.

In his introduction Coxeter states: "Apparently none of these men thought of considering first the simpler operation of *reflection* and deducing a rotation as the product of two reflections."

The article which I read, presented a rotation as the simpler operation and considered a reflection as a rotatory inversion, compounded of a rotation and a central inversion. This is the order used in the following discussion.

The underlying basic theorem of reflection at plane mirrors is not confined to rays of light incident upon the mirror but applies to the whole image space. It may be stated as follows: *The image space formed by a plane mirror can be derived from the object space by rotating the object space 180° about any normal to the plane, followed by a central inversion about the foot of the normal.*

In the quaternion notation the square of a vector is negative instead of positive. This, as Hamilton showed, makes it possible to treat a "quaternion," the sum of a scalar and a vector, as a single quantity in addition, multiplication, division and

Received July 1, 1946; revised Dec. 20, 1946.

[1] J. L. Synge, *Reflection in a corner formed by three plane mirrors*, this Quarterly **4**, 166–176 (1946).

[2] L. B. Tuckerman, *Optical strain gages and extensometers*, Proc. A.S.T.M. **23**, Part II, 602–610 (1923).

[3] Ludwig Silberstein, *Simplified method of tracing rays through any optical system of lenses, prisms and mirrors*. London, Longmans, Green and Co., 1918.

[4] H. S. M. Coxeter, *Quaternions and reflections*, Amer. Math. Monthly **53**, 36–146 (1946).

differentiation instead of introducing the multiplicity of scalar and vector operations of the notations of Heaviside, Föppl and Gibbs.

Computations with quaternions are thus carried out with the simplicity of ordinary algebraic computations. The only complexity, if it may be called a complexity, is the necessity, common to all vector notations, of remembering that in general $\mathbf{ab} \neq \mathbf{ba}$. The separation of the quaternion results into their scalar and vector parts can be made at any desired stages in the process by the operators, S = scalar part and V = vector part.

The quaternion formula for rotation of a vector $\mathbf{i}$ through an angle ϑ about a unit vector $\mathbf{n}$ as axis is:

$$\mathbf{i}' = q\mathbf{i}q^{-1}, \tag{1}$$

where the quaternion

$$q = \cos \tfrac{1}{2}\vartheta + \mathbf{n} \sin \tfrac{1}{2}\vartheta \tag{2}$$

is the sum of $Sq = \cos \frac{1}{2}\vartheta$ and $Vq = \mathbf{n} \sin \frac{1}{2}\vartheta$.

If $\vartheta = 180°$, this reduces to:

$$\mathbf{i}' = \mathbf{nin}^{-1}. \tag{3}$$

The central inversion merely requires changing the sign of all vectors passing through the foot of the normal, giving for the effect of a single plane mirror

$$\mathbf{i}' = -\mathbf{nin}^{-1} = \mathbf{nin}. \tag{4}$$

Equations (1) and (2) are identical in form with Coxeter's (p. 139) Theorem 3.2 and Eq. (4) with his Theorem 3.1.

The equivalence of Eq. (4) with Synge's Eq. (4.1) may readily be verified by expressing it in quaternion notation. Writing $(\mathbf{n} \cdot \mathbf{i}) = S\mathbf{ni}$ and $\mathbf{n}^2 = -1$, gives:

$$\mathbf{i}' = \mathbf{i} - 2\mathbf{n}(\mathbf{n} \cdot \mathbf{i}) = \mathbf{i} + 2\mathbf{n}S\mathbf{ni} = \mathbf{i} + \mathbf{n}(\mathbf{ni} + \mathbf{in}) = (1 + \mathbf{n}^2)\mathbf{i} + \mathbf{nin} = \mathbf{nin}. \tag{5}$$

The effect of two mirrors is obtained by simple iteration:

$$\mathbf{i}'' = \mathbf{n}_2\mathbf{i}'\mathbf{n}_2 = \mathbf{n}_2\mathbf{n}_1\mathbf{i}\mathbf{n}_1\mathbf{n}_2 = q\mathbf{i}q^{-1}. \tag{6}$$

The second central inversion cancels the first, so the result is a pure rotation. The angle ϑ and the direction of the axis $\mathbf{a}$ are given by

$$\cos \tfrac{1}{2}\vartheta + \mathbf{a} \sin \tfrac{1}{2}\vartheta = q = \mathbf{n}_2\mathbf{n}_1 = S\mathbf{n}_2\mathbf{n}_1 + V\mathbf{n}_2\mathbf{n}_1. \tag{7}$$

Here $S\mathbf{n}_2\mathbf{n}_1 = -\cos(\mathbf{n}_2, \mathbf{n}_1)$, where $(\mathbf{n}_2, \mathbf{n}_1)$ represents the angle between the normals to the two mirrors, and $V\mathbf{n}_2\mathbf{n}_1$ is a vector with a length equal to $\sin(\mathbf{n}_2, \mathbf{n}_1)$ perpendicular to $\mathbf{n}_2$ and $\mathbf{n}_1$, and therefore parallel to the line of intersection of their planes.

Since in the reflection from one mirror we are free to choose *any normal* as the axis of rotation, it is convenient to choose some point on the line of intersection of the two planes as the common foot of the normals to the two planes. With this choice, the equations prove the familiar result: *The image space formed by successive reflections at two plane mirrors can be derived from the object space by rotating the object space through an angle ϑ given by* $\cos \frac{1}{2}\vartheta = -\cos(\mathbf{n}_2, \mathbf{n}_1)$ *about the line of intersection of the two planes.*

The effect of three mirrors is obtained by a further simple iteration:

$$\mathbf{i}''' = \mathbf{n}_3\mathbf{i}''\mathbf{n}_3 = \mathbf{n}_3\mathbf{n}_2\mathbf{i}'\mathbf{n}_2\mathbf{n}_3 = \mathbf{n}_3\mathbf{n}_2\mathbf{n}_1\mathbf{i}\mathbf{n}_1\mathbf{n}_2\mathbf{n}_3 = -qiq^{-1}. \tag{8}$$

The third mirror introduces another central inversion. The negative sign before the last term in Eq. (8) represents the resultant central inversion. In this case we are free to choose the common point of intersection of the three planes as the common foot of the normals to the three planes. We may then state: *The image space formed by successive reflections at three plane mirrors can be derived from the object space by rotating the object through an angle, ϑ about an axis,* **a** *passing through the common point of intersection of the three planes, followed by a central inversion about that point. The angle, ϑ and the direction of the axis,* **a** *of the resultant rotatory inversion are given by*:

$$\cos \tfrac{1}{2}\vartheta + \mathbf{a} \sin \tfrac{1}{2}\vartheta = q = \mathbf{n}_3\mathbf{n}_2\mathbf{n}_1 = S\mathbf{n}_3\mathbf{n}_2\mathbf{n}_1 + V\mathbf{n}_3\mathbf{n}_2\mathbf{n}_1. \tag{9}$$

Now

$$\begin{aligned}\cos \tfrac{1}{2}\vartheta = Sq = S\mathbf{n}_3\mathbf{n}_2\mathbf{n}_1 &= -S\mathbf{n}_1\mathbf{n}_2\mathbf{n}_3 = S\mathbf{n}_2\mathbf{n}_1\mathbf{n}_3 = -S\mathbf{n}_3\mathbf{n}_1\mathbf{n}_2 \\ &= S\mathbf{n}_1\mathbf{n}_3\mathbf{n}_2 = -S\mathbf{n}_2\mathbf{n}_3\mathbf{n}_1.\end{aligned} \tag{10}$$

If then, $\frac{1}{2}\vartheta$ is defined as a positive acute angle, one half the angle of rotation will have one of the four values, $\pm\frac{1}{2}\vartheta$ and $(180° \pm \frac{1}{2}\vartheta)$. The angle of rotation will therefore have one of the two values, $\pm\vartheta$. The magnitude of the angle of rotation is thus the same for all orders of incidence and its sign changes when the cyclic order is reversed.

Synge's convenient choice makes the subscript of each **a** correspond to the subscript of the **n** of the second mirror on which the ray falls. Then by an elementary expansion formula:

$$\mathbf{a}_1 \sin \tfrac{1}{2}\vartheta = V\mathbf{n}_2\mathbf{n}_1\mathbf{n}_3 = V\mathbf{n}_3\mathbf{n}_1\mathbf{n}_2 = -\mathbf{n}_1S\mathbf{n}_2\mathbf{n}_3 + \mathbf{n}_2S\mathbf{n}_3\mathbf{n}_1 + \mathbf{n}_3S\mathbf{n}_1\mathbf{n}_2. \tag{11}$$

Letting

$$\begin{aligned}M_1 = -S\mathbf{n}_2\mathbf{n}_3 = \cos(\mathbf{n}_2, \mathbf{n}_3), \qquad M_2 = -S\mathbf{n}_3\mathbf{n}_1 = \cos(\mathbf{n}_3, \mathbf{n}_1) \\ \text{and} \quad M_3 = -S\mathbf{n}_1\mathbf{n}_2 = \cos(\mathbf{n}_1, \mathbf{n}_2),\end{aligned} \tag{12}$$

we have

$$\begin{aligned}-\mathbf{a}_1 \sin \tfrac{1}{2}\vartheta &= -M_1\mathbf{n}_1 + M_2\mathbf{n}_2 + M_3\mathbf{n}_3, \\ -\mathbf{a}_2 \sin \tfrac{1}{2}\vartheta &= +M_1\mathbf{n}_1 - M_2\mathbf{n}_2 + M_3\mathbf{n}_3, \\ -\mathbf{a}_3 \sin \tfrac{1}{2}\vartheta &= +M_1\mathbf{n}_1 + M_2\mathbf{n}_2 - M_3\mathbf{n}_3.\end{aligned} \tag{13}$$

These are obviously equivalent to Synge's Eqs. (3.10) and show that in those equations

$$\pm 1/k = \sin \tfrac{1}{2}\vartheta. \tag{14}$$

Adding the second and third of Eqs. (13) gives

$$-(\mathbf{a}_1 + \mathbf{a}_3) \sin \tfrac{1}{2}\vartheta = 2M_1\mathbf{n}_1, \tag{15}$$

so that the three vectors $\mathbf{n}_1$, $\mathbf{a}_2$ and $\mathbf{a}_3$ are coplanar. Similarly, so are $\mathbf{n}_2$, $\mathbf{a}_3$ and $\mathbf{a}_1$ and $\mathbf{n}_3$, $\mathbf{a}_1$ and $\mathbf{a}_2$.

The angles which $\mathbf{n}_1$ makes with $\mathbf{a}_2$ and $\mathbf{a}_3$ are given by

$$\begin{aligned}\sin \tfrac{1}{2}\vartheta \cos(\mathbf{n}_1\mathbf{a}_2) &= -\sin \tfrac{1}{2}\vartheta S\mathbf{n}_1\mathbf{a}_2 = M_1 + M_2M_3 - M_2M_3 = M_1 \\ &= -\sin \tfrac{1}{2}\vartheta S\mathbf{n}_1\mathbf{a}_3 = \sin \tfrac{1}{2}\vartheta \cos(\mathbf{n}_1\mathbf{a}_3).\end{aligned} \tag{16}$$

Thus $\mathbf{a}_2$ and $\mathbf{a}_3$ are vectors coplanar with $\mathbf{n}_1$ making the same angle with it. Since they are not identical they must lie on opposite sides of $\mathbf{n}_1$. This proves that $\mathbf{n}_1$ bisects the side $\overline{\mathbf{a}_2\mathbf{a}_3}$ of the spherical triangle $\overline{\mathbf{a}_1\mathbf{a}_2\mathbf{a}_3}$, with similar results for $\mathbf{n}_2$ and $\mathbf{n}_3$.

Squaring the first of Eqs. (13) and remembering that $\mathbf{a}_1^2=\mathbf{n}_1^2=\mathbf{n}_2^2=\mathbf{n}_3^2=-1$, gives:

$$-\sin^2\tfrac{1}{2}\vartheta = -M_1^2 - M_2^2 - M_3^2 + 2M_2M_3S\mathbf{n}_2\mathbf{n}_3 - 2M_3M_1S\mathbf{n}_3\mathbf{n}_1 - 2M_1M_2S\mathbf{n}_1\mathbf{n}_2, \quad (17)$$

Substituting from Eqs. (12) gives:

$$\sin^2\tfrac{1}{2}\vartheta = M_1^2 + M_2^2 + M_3^2 - 2M_1M_2M_3, \quad (18)$$

which is equivalent to Synge's Eq. (3.9).

Since, except for sign, ϑ is known from Eq. (18), the directions of the axes $\mathbf{a}_1$, $\mathbf{a}_2$ and $\mathbf{a}_3$ are, except for sense, given by Eqs. (13). The sense of each may be arbitrarily chosen. When it is chosen, the sign of $\sin\frac{1}{2}\vartheta$ for each axis is given. Combined with the sign of $\cos\frac{1}{2}\vartheta$ determined from the order of incidence by Eqs. (10), this determines the sign of ϑ for each of the six orders.

These formulae give in essence all that is contained in Synge's three theorems, and the diagrams he gives can readily be constructed from them. Numerical computations using them are straightforward. They are especially simple when one or more of the angles between the mirror normals differ so little from 90° that small quantities of the second order may be neglected.

In collimated systems, in which a group of any number of plane mirrors lies wholly within a region of parallel rays, any parallel displacement of the image space of the mirrors with respect to their object space does not affect the relative relation of the final image to the original object. For such systems the effect of any number of plane mirrors may be regarded as a rotation or rotatory inversion in which merely the angle of rotation and the direction of the axis are significant. These can also be found by simple iteration of Equation (4):

$$\mathbf{i}^{(k)} = \mathbf{n}_k\mathbf{n}_{k-1}\cdots\mathbf{n}_2\mathbf{n}_1\mathbf{i}\mathbf{n}_1\mathbf{n}_2\cdots\mathbf{n}_{k-1}\mathbf{n}_k, \quad (19)$$

giving

$$(-1)^k q = (-1)^k(\cos\tfrac{1}{2}\vartheta + \mathbf{a}\sin\tfrac{1}{2}\vartheta) = S\mathbf{n}_k\mathbf{n}_{k-1}\cdots\mathbf{n}_2\mathbf{n}_1 + V\mathbf{n}_k\mathbf{n}_{k-1}\cdots\mathbf{n}_2\mathbf{n}_1, \quad (20)$$

to determine the angle ϑ and the direction of the axis of rotation, $\mathbf{a}$ of the rotation (k, even) or rotatory inversion (k, odd) of the object space into the image space after reflection from k mirrors. The computations are just as simple in form as those for three mirrors but of course the numerical work increases in proportion to the number of mirrors.

An important special case of an even number of mirrors is a nondeviating erecting system, one which turns the image formed by a lens system through 180° without deviating rays parallel to the axis of the lens system. Neglecting, for the time being, the axial and lateral displacement of the image, the condition for this is that $\vartheta=180°$ or

$$\cos\tfrac{1}{2}\vartheta = S\mathbf{n}_k\mathbf{n}_{k-1}\cdots\mathbf{n}_2\mathbf{n}_1 = 0. \quad (21)$$

This may be written:

$$S\mathbf{n}_k(S\mathbf{n}_{k-1}\cdots\mathbf{n}_2\mathbf{n}_1 + V\mathbf{n}_{k-1}\cdots\mathbf{n}_2\mathbf{n}_1) = S\cdot\mathbf{n}_kV\mathbf{n}_{k-1}\cdots\mathbf{n}_2\mathbf{n}_1 = 0. \quad (22)$$

Since $V\mathbf{n}_{k-1}\cdots\mathbf{n}_2\mathbf{n}_1$ is parallel to the axis of the rotatory inversion produced by the first $(k-1)$ mirrors, this merely requires that $\mathbf{n}_k$ shall be perpendicular to that axis. We may therefore state: *Any combination of an odd number of plane mirrors, with their normals arbitrarily oriented, may be converted to a nondeviating erecting system by adding another plane mirror whose normal is perpendicular to the axis of the rotatory inversion produced by the combination.*

An interesting, but impractical, special case is the combination of a cube corner with a fourth mirror in any orientation in which its normal makes an acute angle with the rays emerging from the cube corner. Since the quaternion product of three mutually perpendicular vectors is ± 1, it forms a nondeviating erecting system whose axis is parallel to the normal to the fourth mirror.

The scalar part of the product of any number of quaternions (including vectors) is the same, so long as the cyclic order is maintained. Consequently the angle of rotation produced by any number of mirrors is the same for the same cyclic order of incidence, but the axis will in general be different for different orders. This permits stating a sufficient, but not necessary, special condition:

$$\begin{aligned} 0 &= S\mathbf{n}_k\cdots\mathbf{n}_j\cdots\mathbf{n}_1 \\ &= S\mathbf{n}_1\mathbf{n}_kS\mathbf{n}_{k-1}\cdots\mathbf{n}_j\cdots\mathbf{n}_2 + S\cdot V\mathbf{n}_1\mathbf{n}_kV\mathbf{n}_{k-1}\cdots\mathbf{n}_j\cdots\mathbf{n}_2 \qquad (23) \\ &= S\mathbf{n}_j\mathbf{n}_{j-1}S\mathbf{n}_{j-2}\cdots\mathbf{n}_1\mathbf{n}_k\cdots\mathbf{n}_{j-1} + S\cdot V\mathbf{n}_j\mathbf{n}_{j-1}V\mathbf{n}_{j-2}\cdots\mathbf{n}_1\mathbf{n}_k\cdots\mathbf{n}_{j+1}. \end{aligned}$$

This is obviously satisfied if each term on the right hand side of either of these equations is equal to zero. We may therefore state: *If, in a combination of an even number of plane mirrors, the normals to the first and last or to any two consecutive mirrors are perpendicular to each other and the line of intersection of their planes is perpendicular to the resultant axis of the rotation which would be produced by the other mirrors alone, the combination will form a nondeviating erecting system.*

The condition will obviously be satisfied if all the lines of intersection of the planes of the other mirrors are perpendicular to the line of intersection of the two. This even more special condition is met by all nondeviating erecting systems which I have found described.

It is of course obvious that the mirrors must be so located as to permit unobstructed passage of the light through the combination. If a prism serves as a mirror combination it is further obvious that, to avoid refractive deviation, the exit face must be parallel to the image of the entrance face produced by the prism. This condition is of course never exactly met by any actual prism. One of the problems in prism design is to determine how large tolerances may be permitted in meeting such conditions without significant interference with the performance of an instrument.

The effect of small deviations may be treated as the effect of thin glass wedges cemented to the surface of perfect prisms. Such a wedge will produce a rotation of the image space on the object space represented by

$$q_w\mathbf{x}q_w^{-1} = (\cos\tfrac{1}{2}\vartheta_w + \mathbf{w}\sin\tfrac{1}{2}\vartheta_w)\mathbf{x}(\cos\tfrac{1}{2}\vartheta_w - \mathbf{w}\sin\tfrac{1}{2}\vartheta_w), \qquad (24)$$

where the vector $\mathbf{w}$ is parallel to the edge of the wedge and ϑ_w is the angular deviation produced by it. Since these deviations are small it is usually sufficient to write $q_w=(1+\frac{1}{2}\vartheta_w\mathbf{w})$. This quaternion is inserted between the proper pair of normals in Eq. (19). The difference between the two results for ϑ_w finite and $\vartheta_w=0$ gives the effect of the deviation.

Since, in general, four or more planes do not have a common point of intersection further computations are necessary if the relative position of image and object space is needed.

To compute this we choose arbitrarily an origin of coordinates at $\mathbf{d}_{j-1}=0$ and define object and image spaces by vectors $\mathbf{r}_h$ $(h=0, 1, 2, \cdots, j, \cdots, k-1, k)$ drawn from that origin. We represent by $\mathbf{d}_h$ a vector drawn from that origin to some arbitrary point on the h-th mirror. Equation (4) may then be written:

$$\mathbf{r}_h - \mathbf{d}_h = -\mathbf{n}_h(\mathbf{r}_{h-1} - \mathbf{d}_h)\mathbf{n}_h^{-1}. \tag{25}$$

Giving h in succession the values $j, j+1, \cdots, k-1, k$, $(j=1, \cdots, k)$ and substituting in succession the value of each $\mathbf{r}_{h-1}$ in Eq. (25) the effect of all or a part of the k mirrors is found.

In carrying out these substitutions, it is convenient to use an abbreviated notation due to Hamilton. We define:

$$\phi\mathbf{x} = q\mathbf{x}q^{-1} = (\cos\tfrac{1}{2}\vartheta + \mathbf{a}\sin\tfrac{1}{2}\vartheta)\mathbf{x}(\cos\tfrac{1}{2}\vartheta - \mathbf{a}\sin\tfrac{1}{2}\vartheta) \tag{26}$$

as an abbreviated form of Eqs. (1) and (2). Here ϕ is a "rotor," a special form of linear vector operator which rotates a vector through an angle ϑ about an axis parallel to the unit vector $\mathbf{a}$. Carrying out the operations indicated in Eq. (26) and remembering that

$$\mathbf{x} = -\mathbf{a}V\mathbf{a}\mathbf{x} - \mathbf{a}S\mathbf{a}\mathbf{x}, \tag{27}$$

where $-\mathbf{a}V\mathbf{a}\mathbf{x}$ is the component of $\mathbf{x}$ perpendicular and $-\mathbf{a}S\mathbf{a}\mathbf{x}$, the component parallel to $\mathbf{a}$, we find

$$\phi\mathbf{x} = (\cos\vartheta + \mathbf{a}\sin\vartheta)(-\mathbf{a}V\mathbf{a}\mathbf{x}) + (-\mathbf{a}S\mathbf{a}\mathbf{x}) \tag{28}$$

$$\mathbf{x} - \phi\mathbf{x} = (1-\phi)\mathbf{x} = (1 - \cos\vartheta - \mathbf{a}\sin\vartheta)(-\mathbf{a}V\mathbf{a}\mathbf{x}). \tag{29}$$

In the important special case when $\vartheta=0$, we have $q=1$, $\phi\mathbf{x}=\mathbf{x}$, and $(1-\phi)\mathbf{x}$ obviously reduces to zero. Again,

$$\mathbf{x} + \phi\mathbf{x} = (1+\phi)\mathbf{x} = (1 + \cos\vartheta + \mathbf{a}\sin\vartheta)(-\mathbf{a}V\mathbf{a}\mathbf{x}) + 2(-\mathbf{a}S\mathbf{a}\mathbf{x}). \tag{30}$$

In the important special case when $\vartheta=180°$, we have $q=-1$, and $(1+\phi)\mathbf{x}$ obviously reduces to $2(-\mathbf{a}S\mathbf{a}\mathbf{x})$. We will later find it necessary to solve equations of the form of Eqs. (29) and (30) for the components of an unknown vector $\mathbf{x}$. Since

$$(1 - \cos\vartheta + \mathbf{a}\sin\vartheta)(1 - \cos\vartheta - \mathbf{a}\sin\vartheta) = 2(1-\cos\vartheta), \tag{31}$$

Equation (29) is solved by:

$$-\mathbf{a}V\mathbf{a}\mathbf{x} = \frac{1}{2(1-\cos\vartheta)}(1 - \cos\vartheta + \mathbf{a}\sin\vartheta)(1-\phi)\mathbf{x}, \tag{32}$$

and the parallel component $-\mathbf{a}S\mathbf{a}\mathbf{x}$ is obviously arbitrary. If $\vartheta=0$, this takes on the indeterminate form 0/0. However, as noted above, in that case, the operator, $\phi=1$, is a pure scalar and represents a parallel displacement as a rotation through a zero angle about an infinitely distant axis. Every vector in the object space is imaged by a parallel vector in the image space. Then, not only the parallel, but the perpendicular component of $\mathbf{x}$ is arbitrary. In this case the solution of Eq. (29) is wholly indeterminate.

Equation (30) must first be solved for $-\mathbf{a}S\mathbf{a}\mathbf{x}$ as follows. Remembering that $SV\mathbf{a}\mathbf{x}=0$, $Sa V\mathbf{a}\mathbf{x}=0$ and $\mathbf{a}^2=-1$, we find

$$-Sa(1+\phi)\mathbf{x} = -Sa(1+\cos\vartheta+\mathbf{a}\sin\vartheta)(-\mathbf{a}V\mathbf{a}\mathbf{x}) - 2Sa(-\mathbf{a}S\mathbf{a}\mathbf{x}) = -2S\mathbf{a}\mathbf{x}. \quad (33)$$

Thus the component $\mathbf{x}$ parallel to $\mathbf{a}$ is one half the component of $(1+\phi)\mathbf{x}$ parallel to the same axis. Then, analogous to the solution of Equation (29) we have

$$-\mathbf{a}V\mathbf{a}\mathbf{x} = \frac{1}{2(1+\cos\vartheta)}(1+\cos\vartheta-\mathbf{a}\sin\vartheta)[(1+\phi)\mathbf{x}+\mathbf{a}S\mathbf{a}(1+\phi)\mathbf{x}]. \quad (34)$$

If $\vartheta=180°$ this takes on the indeterminate form 0/0. By returning to the original definition of ϕ in terms of q, it is easy to show that in this case the perpendicular component $-\mathbf{a}V\mathbf{a}\mathbf{x}$ is arbitrary and only the parallel component $-\mathbf{a}S\mathbf{a}\mathbf{x}$ is defined by Eq. (30). The reflection from a single mirror represents a special case of $\vartheta=180°$. In this case the vector $\mathbf{a}$ is normal to the mirror. Adding to $\mathbf{x}$ any vector in the plane of the mirror merely displaces the foot of the normal which, as noted at the beginning, is arbitrary. If $\vartheta\neq180°$, both components are determinate and their sum gives the vector $\mathbf{x}$. It is readily seen that:

$$\phi(\mathbf{x}+\mathbf{y}) = \phi\mathbf{x}+\phi\mathbf{y} \quad (35)$$

and

$$\phi_j\phi_k\mathbf{x} = q_j(q_k\mathbf{x}q_k^{-1})q_j^{-1} = q_jq_k\mathbf{x}q_k^{-1}q_j^{-1}. \quad (36)$$

The product of several such operations in sequence is thus evaluated by the multiplication in proper order of the quaternions in terms of which they are defined. We may then define:

$$\phi_{k,i}\mathbf{x} = q_{k,i}\mathbf{x}q_{k,i}^{-1} = \mathbf{n}_k\mathbf{n}_{k-1}\cdots\mathbf{n}_{i+1}\mathbf{n}_i\mathbf{x}\mathbf{n}_i^{-1}\mathbf{n}_{i+1}^{-1}\cdots\mathbf{n}_{k-1}^{-1}\mathbf{n}_k^{-1}. \quad (37)$$

It is frequently convenient to note:

$$\phi_{k,i}\phi_{(i-1),j} = \phi_{k,j}. \quad (38)$$

With this notation Eq. (25) may be written:

$$\mathbf{r}_k = -\phi_{k,k}\mathbf{r}_{k-1}+(1+\phi_{k,k})\mathbf{d}_k. \quad (39)$$

Starting with

$$\mathbf{r}_j = -\phi_{j,j}\mathbf{r}_{j-1}+(1+\phi_{j,j})\mathbf{d}_j, \quad (40)$$

and substituting successively the values of $\mathbf{r}_j, \mathbf{r}_{j+1}, \cdots, \mathbf{r}_{k-1}$ for $\mathbf{r}_{k-1}$ in Eq. (39), we find

$$\mathbf{r}_k = (-1)^{k-j+1}\phi_{k,j}\mathbf{r}_{j-1}+\sum_{h=j}^{h=k}[1+(-1)^{k-h}\phi_{k,h}](\mathbf{d}_h-\mathbf{d}_{h-1}). \quad (41)$$

If $j=1$ and all the $\mathbf{d}_h$'s are zero this obviously reduces to Eq. (19).

The process of computation consists in calculating in order

$$q_{k,k}=\mathbf{n}_k, \cdots, q_{k,h}=q_{k,h+1}\mathbf{n}_h, \cdots, q_{k,1}=q_{k,2}\mathbf{n}_1, \quad (42)$$

from which each of the $\vartheta_{k,h}$'s and $\mathbf{a}_{k,h}$'s are computed by:

$$Sq_{k,h} = \cos \tfrac{1}{2}\vartheta_{k,h}, \qquad \mathbf{a}_{k,h} = Vq_{k,h}/\sin \tfrac{1}{2}\vartheta_{k,h}. \tag{43}$$

The computations may frequently be shortened by using Eq. (38). The term $\phi_{k,j}\mathbf{r}_{j-1}$ is then computed either by Eq. (26) or by Eq. (28) whichever seems easier, and each of the terms in the summation in Eq. (41) by Eq. (29) or (30). They are then added.

Since the origin of coordinates and the points to which the vectors $\mathbf{d}_h$ are drawn are arbitrary, the computations can ordinarily be much simplified by suitably choosing them.

When two successive mirrors intersect, choosing a point on their common intersection makes $\mathbf{d}_h - \mathbf{d}_{h-1} = 0$ and the corresponding term in the summation vanishes. When three successive mirrors intersect, choosing their common point of intersection as the common foot of their normals makes $\mathbf{d}_{h-1} = \mathbf{d}_h = \mathbf{d}_{h+1}$ and two successive terms of the summation vanish. If they are the first three and we choose it as the origin of coordinates, we have $\mathbf{d}_{j-1} = \mathbf{d}_j = \mathbf{d}_{j+1} = \mathbf{d}_{j+2} = 0$ and three successive terms vanish. It was this choice which made the treatment of the three mirror problem so much simpler.

In numerical work it is convenient to express all the vectors in terms of a suitably chosen rectangular coordinate system represented by unit vectors, $\mathbf{i}$, $\mathbf{j}$, and $\mathbf{k}$. By substituting for $\mathbf{r}_{j-1}$, $\mathbf{i}$, $\mathbf{j}$, and $\mathbf{k}$ in turn and carrying through the computation, the position of the image of any point, $\mathbf{r}_{j-1} = x\mathbf{i} + y\mathbf{j} + z\mathbf{k}$, in the object space may be obtained by simple addition.

Equations (28), (29), (30), (38), (41), (42), and (43) are thus all that are needed to determine the relative position and orientation of object and image after reflection from any number of plane mirrors. It is, however, sometimes more convenient to calculate the parameters of the transformation of the object space into the image space.

The most general rigid displacement of a three dimensional Euclidean configuration is a twist about a screw. The relative position of image and object after reflection from an even number of plane mirrors will be known when the angle of the twist and the pitch and the position of the axis of the resultant screw are known.

A twist through an angle ϑ_k about a screw of pitch a_k/ϑ_k whose axis is parallel to the unit vector $\mathbf{a}_k$ is equivalent to a rotation about that axis followed by a parallel displacement $a_k\mathbf{a}_k$ along the axis. The effect of an even number of mirrors will therefore be given by an equation of the form:

$$\mathbf{r}_k = \phi_k\mathbf{r}_{j-1} + (1 - \phi_k)\mathbf{d}_{k,j} + a_k\mathbf{a}_k, \tag{44}$$

where the vector, $\mathbf{d}_{k,j}$ from the origin to the axis of the twist is given the double subscript to distinguish it from the vector $\mathbf{d}_k$ drawn to a point on the k-th mirror. Comparison with Eq. (41) shows that

$$\phi_k = \phi_{k,j}, \quad \vartheta_k = \vartheta_{k,j} \quad \text{and} \quad \mathbf{a}_k = \mathbf{a}_{k,j}. \tag{45}$$

These are computed by Eqs. (42) and (43) and a_k is given by

$$a_k = -S\mathbf{a}_k \sum_{h=j}^{h=k} [1 + (-1)^{k-h}\phi_{k,h}](\mathbf{d}_h - \mathbf{d}_{h-1}). \tag{46}$$

Then

$$(1 - \phi_k)\mathbf{d}_{k,j} = \sum_{h=j}^{h=k} [1 + (-1)^{k-h}\phi_{k,h}](\mathbf{d}_h - \mathbf{d}_{h-1}) - a_k\mathbf{a}_k. \tag{47}$$

These equations are solved for the perpendicular components of the $\mathbf{d}_{k,j}$'s, by Eq. (32). Their parallel components are arbitrary. The effect of all the even combinations of the k mirrors is then known in terms of the angle of the twist and the pitch and the position of the axis of the resultant screws.

If a twist upon a screw is combined with a central inversion, the result is a rotatory inversion. The relative position of image and object after reflection from an odd number of mirrors will be known when the position of the axis, the location of the center on that axis, and the angle of rotation of the resultant rotatory inversion are known.

A rotatory inversion through an angle ϑ_k about an axis parallel to a unit vector $\mathbf{a}_k$ is readily shown to be given by an equation of the form

$$\mathbf{r}_k = -\phi_k \mathbf{r}_{j-1} + (1 + \phi_k)\mathbf{d}_{k,j}, \tag{48}$$

where $\mathbf{d}_{k,j}$ is a vector drawn from the origin to the center of the resultant inversion. Comparison with Eq. (41) shows that, as in the case of an even number of mirrors.

$$\phi_k = \phi_{k,j}, \quad \vartheta_k = \vartheta_{k,j} \quad \text{and} \quad \mathbf{a}_k = \mathbf{a}_{k,j}. \tag{49}$$

These are computed by Eqs. (42) and (43). Then

$$(1 + \phi_k)\mathbf{d}_{k,j} = \sum_{h=j}^{h=k} [1 + (-1)^{k-h}\phi_{k,h}](\mathbf{d}_h - \mathbf{d}_{h-1}). \tag{50}$$

These equations are solved for the parallel and perpendicular components of the $\mathbf{d}_{k,j}$'s by Eqs. (33) and (34). The effect of all the odd combinations of the k mirrors

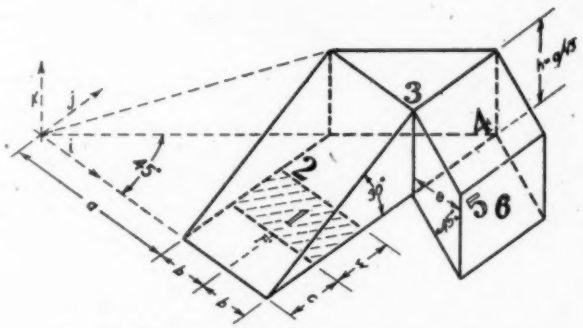

FIG. 1. Range finder five mirror prism combination.

is then known in terms of the position of the axis, the location of the center of inversion on that axis and the angle of rotation of their resultant rotatory inversions.

Although there are necessarily a considerable number of steps in such a computation, the steps are not complicated, consisting merely of simple multiplications and separation of quaternions into their scalar and vector parts.

As an illustration of the straightforwardness of these quaternion computations, suitable dimensions for the five-mirror combination shown in Fig. 1 are computed below. This is part of the prism system used in an Army range finder. The other part is a simple two-mirror system cemented below Face 1.

In use the axial ray from the right hand objective enters through Face 6, is re-

flected in turn from Faces 5, 4, 3 and 2 in succession and from the middle of the near edge of the silver strip on Face 1 at the point F in Fig. 1, and finally emerges through Face 2, which thus serves both as a mirror and an exit face. The image is focussed on that edge of the silver strip, where it is brought into coincidence with the image from the left hand objective, coming through the lower two-mirror system which is not shown.

We must assure ourselves that the image of the exit Face 2, in the space of the objective, is parallel to the entrance Face 6 and that light from the whole aperture of the objective has unobstructed passage to the edge of the silver strip where the coincidence is observed, and for a reasonable distance around it.

We therefore compute, in the space of the objective, the direction of the image of the normal to Face 2 and the position of the corners of the silver strip and of any prism faces which might obstruct the light. The plane of a mirror and its image in that plane coincide, so that we need only compute the relationship between the space of the objective and every other object space in which the prism faces lie.

Since the planes of Faces 1, 2 and 3 produced, intersect in a point, it is convenient to choose that point as the origin of co-ordinates. Choosing axes $\mathbf{i}$, $\mathbf{j}$, and $\mathbf{k}$ and dimensions as shown, and remembering that $\cos 60° = \sin 30° = \frac{1}{2}$, $\sin 60° = \cos 30° = \sqrt{3}/2$, and $\cos 45° = \sin 45° = 1/\sqrt{2}$, we have:

$$\mathbf{n}_1 = \mathbf{k}, \quad \mathbf{d}_1 = 0; \qquad \mathbf{n}_2 = \tfrac{1}{2}(\mathbf{j} - \sqrt{3}\,\mathbf{k}), \quad \mathbf{d}_2 = 0; \qquad \mathbf{n}_3 = \frac{1}{\sqrt{2}}(\mathbf{i} - \mathbf{j}), \quad \mathbf{d}_3 = 0;$$

$$\mathbf{n}_4 = -\frac{1}{\sqrt{2}}(\mathbf{i} + \mathbf{k}), \quad \mathbf{d}_4 = (a + 2b)\mathbf{i} + h\mathbf{k}; \qquad \mathbf{n}_5 = +\frac{1}{\sqrt{2}}(\mathbf{i} + \mathbf{k}), \quad \mathbf{d}_5 = (a + 2b)\mathbf{i},$$

where $h = a \tan 30° = a/\sqrt{3}$.

Then from Eq. (41),

$$\mathbf{r}_5 - \phi_{5,4}\mathbf{r}_3 = \mathbf{r}_5 + \phi_{5,3}\mathbf{r}_2 = \mathbf{r}_5 + \phi_{5,1}\mathbf{r}_0 = (1 + \phi_{5,5})(\mathbf{d}_5 - \mathbf{d}_4) + (1 - \phi_{5,4})(\mathbf{d}_4 - \mathbf{d}_3).$$

By Eqs. (42) and (43),

$$q_{5,5} = \mathbf{n}_5 = \frac{1}{\sqrt{2}}(\mathbf{i} + \mathbf{k}), \quad \cos \tfrac{1}{2}\vartheta_{5,5} = 0, \quad \vartheta_{5,5} = 180°, \quad \mathbf{a}_{5,5} = \mathbf{n}_5 = \frac{1}{\sqrt{2}}(\mathbf{i} + \mathbf{k}).$$

Since $\vartheta_{5,5} = 180°$, we have by Eq. (30).

$$(1 + \phi_{5,5})(\mathbf{d}_5 - \mathbf{d}_4) = 2[-\mathbf{a}_{5,5}S\mathbf{a}_{5,5}(\mathbf{d}_5 - \mathbf{d}_4)] = 2\left[-\frac{1}{\sqrt{2}}(\mathbf{i} + \mathbf{k})S\frac{1}{\sqrt{2}}(\mathbf{i} + \mathbf{k})(-h\mathbf{k})\right]$$

$$= -h(\mathbf{i} + \mathbf{k}).$$

It may be interesting to note again here that, since the position of the foot of the normal is arbitrary, $\mathbf{d}_4$ and $\mathbf{d}_5$ could have been written more generally as $\mathbf{d}_4 = (a+2b+h-z)\mathbf{i}+y\mathbf{j}+z\mathbf{k}$, $\mathbf{d}_5 = (a+2b-z')\mathbf{i}+y'\mathbf{j}+z'\mathbf{k}$, and $(1+\phi_{5,5})(\mathbf{d}_5-\mathbf{d}_4)$ would, as the result of more complicated computations, have come out the same.

$$q_{5,4} = q_{5,5}\mathbf{n}_4 = -\tfrac{1}{2}(\mathbf{i} + \mathbf{k})(\mathbf{i} + \mathbf{k}) = 1.$$

Then according to Eq. (29), $\phi_{5,4}\mathbf{r}_3=\mathbf{r}_3$ and $(1-\phi_{5,4})(\mathbf{d}_4-\mathbf{d}_3)=0$ and Eq. (41) reduces to

$$\mathbf{r}_5=\mathbf{r}_3-h(\mathbf{i}+\mathbf{k})=-\phi_{5,2}\mathbf{r}_2-h(\mathbf{i}+\mathbf{k})=-\phi_{5,1}\mathbf{r}_0-h(\mathbf{i}+\mathbf{k}).$$

$$q_{5,3}=q_{5,4}\mathbf{n}_3=\frac{1}{\sqrt{2}}(\mathbf{i}-\mathbf{j}).$$

By Eq. (26),

$$-\phi_{5,3}(x_2\mathbf{i}+y_2\mathbf{j}+z_2\mathbf{k})=\tfrac{1}{2}(\mathbf{i}+\mathbf{j})(x_2\mathbf{i}+y_2\mathbf{j}+z_2\mathbf{k})(\mathbf{i}-\mathbf{j})=y_2\mathbf{i}+x_2\mathbf{j}+z_2\mathbf{k}$$

$$q_{5,1}=q_{5,3}\mathbf{n}_2\mathbf{n}_1=\frac{1}{2\sqrt{2}}(\mathbf{i}-\mathbf{j})(\mathbf{j}-\sqrt{3}\,\mathbf{k})\mathbf{k}=\frac{1}{\sqrt{8}}(-1+\sqrt{3}\,\mathbf{i}-\sqrt{3}\,\mathbf{j}+\mathbf{k})$$

$$-\phi_{5,1}(x_0\mathbf{i}+y_0\mathbf{j}+z_0\mathbf{k})=-\tfrac{1}{8}(-1+\sqrt{3}\,\mathbf{i}-\sqrt{3}\,\mathbf{j}+\mathbf{k})(x_0\mathbf{i}+y_0\mathbf{j}+z_0\mathbf{k})\cdot(-1-\sqrt{3}\,\mathbf{i}+\sqrt{3}\,\mathbf{j}-\mathbf{k})$$

$$=\tfrac{1}{2}(y_0-\sqrt{3}\,z_0)\mathbf{i}+x_0\mathbf{j}+\tfrac{1}{2}(z_0+\sqrt{3}\,y_0)\mathbf{k}.$$

A unit vector normal to the exit Face 2 of the prism is $\mathbf{n}_2=\frac{1}{2}(\mathbf{j}-\sqrt{3}\mathbf{k})$ giving $x_0=0$, $y_0=\frac{1}{2}$ and $z_0=-\sqrt{3}/2$. Its image in the space of the objective is therefore

$$-\phi_{5,1}\mathbf{n}_2=\frac{1}{2}\left[\frac{1}{2}-\sqrt{3}\left(-\frac{\sqrt{3}}{2}\right)\right]\mathbf{i}+0\mathbf{j}+\frac{1}{2}\left[-\frac{\sqrt{3}}{2}+\frac{1}{2}\sqrt{3}\right]\mathbf{k}=\mathbf{i},$$

which is normal to the entrance Face 6 of the prism. If the angles of the prism combination are correct there will thus be no prismatic deviation.

The corners of the silver strip also lie in the space of $\mathbf{r}_0$. Their images are therefore given by

$$-\phi_{5,1}[a\mathbf{i}+(c+w)\mathbf{j}]-h(\mathbf{i}+\mathbf{k}),\qquad -\phi_{5,1}[(a+2b)\mathbf{i}+(c+w)\mathbf{j}]-h(\mathbf{i}+\mathbf{k}),$$

$$-\phi_{5,1}[a\mathbf{i}+c\mathbf{j}]-h(\mathbf{i}+\mathbf{k}),\qquad -\phi_{5,1}[(a+2b)\mathbf{i}+c\mathbf{j}]-h(\mathbf{i}+\mathbf{k}).$$

Carrying out the computations we find

$$\tfrac{1}{2}(c+w-2h)\mathbf{i}+a\mathbf{j}+\tfrac{1}{2}[\sqrt{3}\,(c+w)-2h]\mathbf{k},$$

$$\tfrac{1}{2}(c+w-2h)\mathbf{i}+(a+2b)\mathbf{j}+\tfrac{1}{2}[\sqrt{3}\,(c+w)-2h]\mathbf{k},$$

$$\tfrac{1}{2}(c-2h)\mathbf{i}+a\mathbf{j}+\tfrac{1}{2}[\sqrt{3}\,c-2h]\mathbf{k},$$

$$\tfrac{1}{2}(c-2h)\mathbf{i}+(a+2b)\mathbf{j}+\tfrac{1}{2}[\sqrt{3}\,c-2h]\mathbf{k}.$$

These give the location, in the space of the objective, of the "air image" of the silver strip, i.e., the location the image would have if the prism faces were front surface mirrors in air.

Face 5 lies in the space of the objective. Its corners and their "air images" are given by

$$(a+2b)\mathbf{i}+a\mathbf{j},\qquad (a+2b)\mathbf{i}+(a+2b)\mathbf{j},$$

$$(a+2b+e)\mathbf{i}+a\mathbf{j}-e\mathbf{k},\qquad (a+2b+e)\mathbf{i}+(a+2b)\mathbf{j}-e\mathbf{k}.$$

If the diameter d, of the objective is greater than $2b$, which is the case in all practical constructions, and light from the whole aperture of the objective is to reach all

parts of the silver strip, it is obvious, since the light is converging to a focus, that the **j** and **k** co-ordinates of the image of the silver strip must lie somewhat within the limits of the corresponding corners of Face 5. Since their **j** co-ordinates are equal it is obvious that there will necessarily be some vignetting of the image at the ends of the silver strip, the amount depending upon the aperture and focal length of the objective and the size of the prisms.

For the **k** co-ordinate of the back edge of this strip we have:

$$\tfrac{1}{2}[\sqrt{3}\,(c + w) - 2h] < 0$$

or

$$(c + w) < 2h/\sqrt{3} = 2a/3,$$

Allowing for some vignetting at the rear edge of the silver strip, which will do no harm, we may set $(c+w)=2a/3$. To allow an equal area for the matching image from the other objective we may set $c=a/3$.

For economy of glass it is obviously desirable to make the viewing aperture approximately square. The projection of $(c+w)=2a/3$ on Face 2 is $\sqrt{3}\cdot 2a/3=a/\sqrt{3}$. For economy of glass we should therefore make $b=a/2\sqrt{3}$.

The bottom edge of Face 5 coincides with the bottom edge of Face 6. The image is focussed on the bottom edge of the silver strip. The length of the path of the axial ray in the glass is therefore the difference of their **i** co-ordinates:

$$(a + 2b + e) - \tfrac{1}{2}(c - 2h) = (5 + 4\sqrt{3})a/6 + e.$$

Because of the index of refraction μ of the glass the image of the focal plane as seen from the lens in air will be displaced in the $+\mathbf{i}$ direction by $(\mu-1)/\mu$ times this length. The effective image of the focal plane, in the space of the objective, lies therefore at a distance

$$[1 - (\mu - 1)/\mu][(5 + 4\sqrt{3})a/6 + e] = [(5 + 4\sqrt{3})a/6 + e]/\mu$$

in the $-\mathbf{i}$ direction back of Face 6. The back principal plane of the objective must be placed a distance equal to its focal length f further in the $+\mathbf{i}$ direction.

At the front edge of the silver strip, where the images coincide, vignetting would be intolerable, so we must have

$$\tfrac{1}{2}[\sqrt{3}\,c - 2h] > -e$$

or

$$e > h - \sqrt{3}\,c/2 = h/2 = a/2\sqrt{3} = \sqrt{3}\,a/6,$$

The thickness e of the rhomb forming Faces 4 and 5 of the mirror combination must, therefore, be somewhat greater than one half the height of the rest of the combination.

The convergence of the rays in the glass is determined by the distance between the focal plane and the "glass image" of the lens, i.e., the distance the back principal plane would have if the light path to it lay wholly in glass. This distance is μf. If d is the diameter of the lens the theoretically necessary value is given by;

$$e = \sqrt{3}\,a/6 + [(5 + 4\sqrt{3})a/6 + e]d/2\mu f$$

or

$$e = [\sqrt{3} + (5 + 4\sqrt{3})d/2\mu f]a/6(1 - d/2\mu f).$$

In practice e is made slightly larger to provide against small misalignments.

In this prism combination, computation of the location of the images of the corners of the other prism faces is not necessary, because simple geometrical considerations show that Face 5 forms the limiting aperture. However, they could readily be computed if desired.

To complete the design it would, of course, be necessary to compute the dimensions and shape of the lower two-mirror prism so that the axial ray from the left hand objective lies in the same line,

$$x\mathbf{i} + (a + b)\mathbf{j} + (\sqrt{3}\,c/2 - h)\mathbf{k},$$

as the axial ray from the right hand objective, after two reflections in the prism has

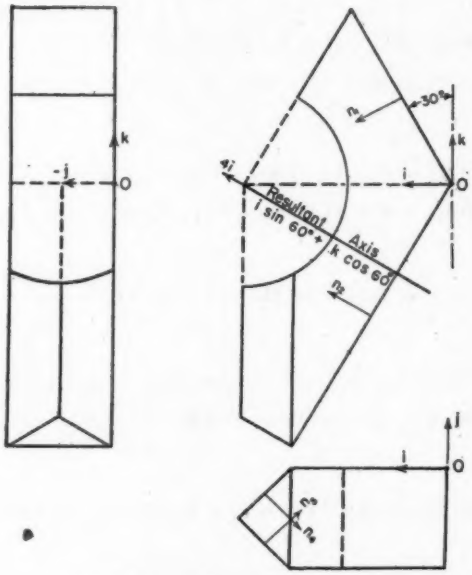

FIG. 2. Leman-Sprenger nondeviating erecting prism.

the direction, $-\mathbf{n}_2$ and is focussed on the same point F, giving $\mathbf{r}_2' = (a+b)\mathbf{i}+c\mathbf{j}$. These computations would obviously be much shorter than the previous ones.

For the purpose of establishing tolerances, computation of the effect of small deviations of the faces from their correct orientation is necessarily longer and more tedious, but is just as straightforward.

These computations of suitable dimensions of this prism combination could, of course, have been made by determining the parameters, the axis and angle of the rotatory inversion produced by Faces 1, 2 and 3, using Eqs. (10), (13) and (18), and combining their effect with the parallel displacement produced by Faces 4 and 5. The computations would, however, have been much longer.

As an illustration of the computation of the parameters of a transformation of an object space into an image space, the effect of a Leman-Sprenger nondeviating erecting prism is calculated below. Axes **i**, **j** and **k** and distances are chosen as shown in Fig. 2. Remembering that:

$$\cos 60° = \sin 30° = 1/2, \quad \sin 60° = \cos 30° = \sqrt{3}/2 \quad \text{and}$$
$$\sin 45° = \cos 45° = 1/\sqrt{2},$$

we have:

$$\mathbf{n}_1 = \tfrac{1}{2}(\sqrt{3}\,\mathbf{i} - \mathbf{k}), \quad \mathbf{d}_1 = 0; \qquad \mathbf{n}_3 = \frac{1}{\sqrt{2}}(-\mathbf{i} + \mathbf{j}), \quad \mathbf{d}_3 = 4\mathbf{i} - \mathbf{j},$$

$$\mathbf{n}_2 = \tfrac{1}{2}(\sqrt{3}\,\mathbf{i} + \mathbf{k}), \quad \mathbf{d}_2 = 0; \qquad \mathbf{n}_4 = \frac{1}{\sqrt{2}}(-\mathbf{i} - \mathbf{j}), \quad \mathbf{d}_4 = 4\mathbf{i} - \mathbf{j}.$$

The combination of Eqs. (41) and (44) reduces to:

$$\mathbf{r}_4 - \phi_4\mathbf{r}_0 = r_4 - \phi_{4,1}\mathbf{r}_0 = (1 - \phi_{4,3})(\mathbf{d}_3 - \mathbf{d}_2) = (1 - \phi_4)\mathbf{d}_{4,1} + a_4\mathbf{a}_4.$$

By Eq. (37),

$$q_{4,3} = \mathbf{n}_4\mathbf{n}_3 = \tfrac{1}{2}(-\mathbf{i} - \mathbf{j})(-\mathbf{i} + \mathbf{j}) = -\mathbf{k},$$
$$q_{2,1} = \mathbf{n}_2\mathbf{n}_1 = \tfrac{1}{4}(\sqrt{3}\,\mathbf{i} + \mathbf{k})(\sqrt{3}\,\mathbf{i} - \mathbf{k}) = \tfrac{1}{2}(-1 + \sqrt{3}\,\mathbf{j}).$$

By Eq. (38)

$$q_4 = q_{4,1} = q_{4,3}q_{2,1} = -\tfrac{1}{2}\mathbf{k}(-1 + \sqrt{3}\,\mathbf{j}) = \tfrac{1}{2}(\sqrt{3}\,\mathbf{i} + \mathbf{k}),$$

giving:

$$\cos \tfrac{1}{2}\vartheta_4 = -Sq_4 = 0, \qquad \cos \tfrac{1}{2}\vartheta_{4,3} = -Sq_{4,3} = 0,$$
$$\sin \tfrac{1}{2}\vartheta_4 = \sin \tfrac{1}{2}\vartheta_{4,3} = 1, \qquad \cos \vartheta_4 = \cos \vartheta_{4,3} = -1, \qquad \sin \vartheta_4 = \sin \vartheta_{4,3} = 0.$$

By Eq. (43),

$$\mathbf{a}_4 = Vq_4/\sin \tfrac{1}{2}\vartheta_4 = \tfrac{1}{2}(\sqrt{3}\,\mathbf{i} + \mathbf{k}), \qquad \mathbf{a}_{4,3} = Vq_{4,3}/\sin \tfrac{1}{2}\vartheta_{4,3} = -\mathbf{k}.$$

Then

$$-\mathbf{a}_{4,3}V\mathbf{a}_{4,3}(\mathbf{d}_3 - \mathbf{d}_2) = -(-\mathbf{k})V(-\mathbf{k})(4\mathbf{i} - \mathbf{j}) = \mathbf{k}(-4\mathbf{j} - \mathbf{i}) = (4\mathbf{i} - \mathbf{j}).$$

By Eq. (29),

$$(1 - \phi_{4,3})(\mathbf{d}_3 - \mathbf{d}_2) = (1 - \cos \vartheta_{4,3} + \mathbf{a}_{4,3} \sin \vartheta_{4,3})(4\mathbf{i} - \mathbf{j})$$
$$= 2(4\mathbf{i} - \mathbf{j}) = 8\mathbf{i} - 2\mathbf{j} = (1 - \phi_4)\mathbf{d}_{4,1} + a_4\mathbf{a}_4.$$

By Eq. (46),

$$a_4 = -S\mathbf{a}_4(1 - \phi_{4,3})(\mathbf{d}_3 - \mathbf{d}_2) = \tfrac{1}{2}S(\sqrt{3}\,\mathbf{i} + \mathbf{k})(8\mathbf{i} - 2\mathbf{j}) = 4\sqrt{3}.$$

By Eq. (47),

$$(1 - \phi_4)\mathbf{d}_{4,1} = (1 - \phi_{4,3})(\mathbf{d}_3 - \mathbf{d}_2) - a_4\mathbf{a}_4$$
$$= (8\mathbf{i} - 2\mathbf{j}) - 2\sqrt{3}\,(\sqrt{3}\,\mathbf{i} + \mathbf{k}) = 2(\mathbf{i} - \mathbf{j} - \sqrt{3}\,\mathbf{k}).$$

By Eq. (32),

$$-\mathbf{a}_4 V \mathbf{a}_4 \mathbf{d}_{4,1} = \frac{1}{2(1-\cos\vartheta_4)}(1-\cos\vartheta_4+\mathbf{a}_4\sin\vartheta_4)(1-\phi_4)\mathbf{d}_{4,1} = \mathbf{i}-\mathbf{j}-2\sqrt{3}\,\mathbf{k}.$$

Since the component of $\mathbf{d}_{4,1}$ parallel to the axis $\mathbf{a}_4$ is arbitrary it is convenient to add to this normal component a parallel component

$$2\sqrt{3}\,\mathbf{a}_4 = 3\mathbf{i}+2\sqrt{3}\,\mathbf{k},$$

giving for $\mathbf{d}_{4,1}$ the value

$$\mathbf{d}_{4,1} = 4\mathbf{i}-\mathbf{j}.$$

The resultant axis of rotation, shown in Fig. 2, thus intersects the prolongation of the roof angle formed by $\mathbf{n}_3$ and $\mathbf{n}_4$ at the point $\mathbf{r}=4\mathbf{i}-\mathbf{j}$ and is perpendicular to the entance face of the prism.

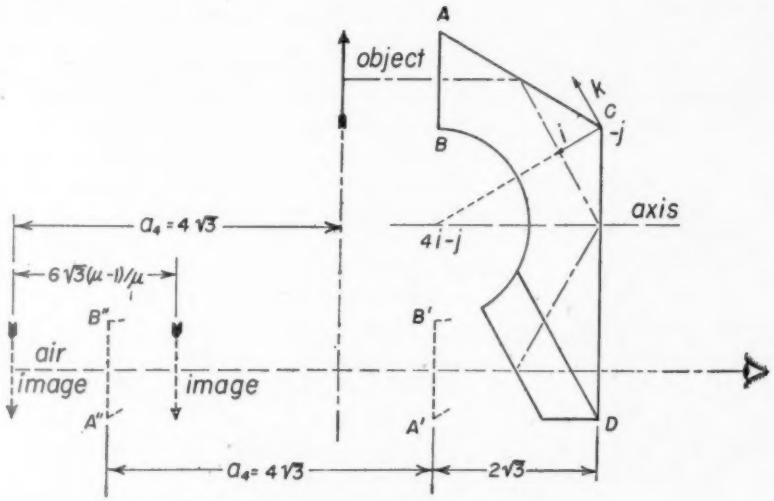

FIG. 3. Leman-Sprenger nondeviating erecting prism.

If the erecting system consisted of front surface mirrors, the image, besides being rotated through 180° about the axis would be displaced backward through the distance $a_4=4\sqrt{3}$. Since, however, the path through the prism is in glass, this backward displacement is partially compensated for by a forward displacement equal to $(\mu-1)/\mu$ times the length of the glass path, where μ is the index of refraction of the glass. The glass path is readily determined by rotating the entrance face AB (Fig. 3) about the axis to $A'B'$ and displacing it backward through the distance $a_4=4\sqrt{3}$ to $A''B''$. The distance of this "air image" of the entrance face from the exit face CD is the length of the glass path and is readily seen to be $6\sqrt{3}$. Assuming $\mu=1.5$, $6\sqrt{3}(\mu-1)/\mu=2\sqrt{3}$. The relative positions of object, "air image" and image are shown in Fig. 3.

The effect of a perfect prism of this type could obviously be determined much

more easily by a simple geometrical construction. Further, the quaternion computations have obviously been carried through in needless detail for a perfect prism. This has been done to show the steps which would be necessary for the purpose of establishing tolerances in determining the effect of small deviations of the faces from their correct orientation. In such computations, the scalar part of the quaternions $q_{4,3}$ and q_4 would not be zero, but small quantities representing the effect of the deviation of the prism faces from their proper orientation, making necessary the computation of the perpendicular and parallel components of vectors which, in the example given, could have been written down by inspection.

ROTOR BLADE FLAPPING MOTION*

BY

GABRIEL HORVAY

McDonnell Aircraft Corporation

1. Introduction. In an earlier paper a method was developed for the solution of a class of Hill differential equations.[1] In the present paper the method is applied to the solution of the differential equation of flapping motion of helicopter rotor blades. A brief review of the equation in Sec. 2 is followed by the solution of the homogeneous equation in Sec. 3. In Sec. 4 the stability of blade flapping motion is established for the range of the numerical parameters which usually arise in helicopter theory. The stability of the equation for large values of μ is discussed in Sec. 5. In Sec. 6 the possibility of resonance is investigated.

2. Differential equation of rotor blade flapping motion. The blades of a helicopter rotor are not attached rigidly to the rotor shaft, but are hinged so as to permit the blades to flap out of the rotor plane. This prevents transmission of severe alternating moments from the blades to the rotor shaft. The angle between a blade and the rotor plane (the plane normal to the rotor shaft) is called the flapping angle β; it is counted positive upwards.

At a standstill, the blades of the rotor rest on the droop stops. When the rotor is revolving at the angular velocity ω, the centrifugal force

$$\int_0^R dC = \int_0^R r\omega^2 dm \tag{1a}$$

(dm is the mass of the blade element at distance r from the axis of rotation, R the blade length) lifts the blades off the stops and keeps them in approximately horizontal position. The blades also experience lift forces

$$\int_0^R dL = \frac{1}{2}\int_0^R \rho c a(\varphi + \vartheta) U^2 dr. \tag{1b}$$

Here ρ is the air density, c the chord of the blade profile, a the slope of the lift curve, ϑ the blade pitch angle, $\varphi+\vartheta$ the angle of attack, and U the resultant air velocity, cf. Fig. 1a.

In *vertical flight* the equilibrium angle β of the blade is determined from the condition, cf. Fig. 1b, that the moments of lift, weight and centrifugal forces balance each other:

---

* Received Sept. 5, 1946. This paper is based on an investigation which was carried out at the McDonnell Aircraft Corporation under sponsorship of the Bureau of Aeronautics, U. S. Navy Department.

[1] G. Horvay, *Unstable solutions of a class of Hill differential equations*, Quarterly Appl. Math. **000**, 385–396 (1947). In the following, this paper will be referred to as I. (Note that A in Eq. (29) of I should be written with a superscript 2 instead of 0.) The present paper is a continuation of the study, and deals with the practical aspects of the problem. The writer's thanks are due to his colleagues, Elizabeth J. Spitzer, Kathryn Meyer, and Frances Schmitz for checking the derivations and for help with the numerical calculations.

$$\int_0^R r(dL - gdm - \beta dC) = 0.$$

(The drag has a negligible effect on the flapping motion.) It is assumed here as elsewhere that the blade is rigid, and that β is so small that the approximation $\sin\beta\sim\beta$, $\cos\beta\sim 1$ is valid. The same assumption is made also for the angles ϑ and φ.[2]

Let t denote the time and

$$\psi = \omega t \tag{2}$$

the azimuth of the blade as measured from the rearmost position. In the course of *forward flight* at the speed of $\mu\omega R$ (μ, the so-called *advance ratio*, is the ratio of forward

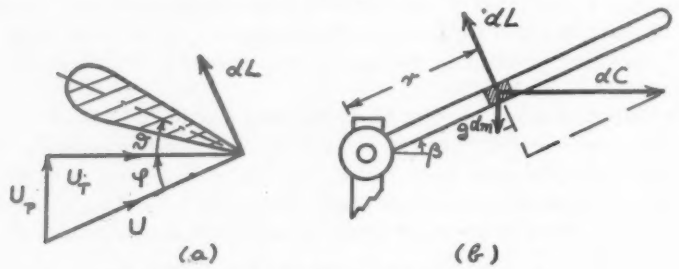

FIG. 1. Velocities and forces at a blade element.

velocity to blade tip speed), an advancing blade element ($\psi=90°$) moves with the speed $\omega(r+\mu R)$, a retreating element ($\psi=270°$) moves with the speed $\omega(r-\mu R)$. The variation in the relative air velocity brings forth a variable lift moment, and thus produces a blade flapping which varies with the azimuth ψ. The tangential component of the air velocity at element dm is

$$U_T = r\omega + \mu\omega R \sin\psi, \tag{3a}$$

and the perpendicular component is

$$U_P = \lambda\omega R - r\dot{\beta} - \mu\omega R\beta\cos\psi. \tag{3b}$$

Here $\lambda\omega R$ is the difference between the sinking speed of the helicopter and the induced velocity through the rotor disc. λ is called the *inflow ratio*.

The flapping motion of the blade is governed by the equation

$$I\ddot{\beta} = \int_0^R r(dL - gdm - \beta dC), \tag{4}$$

where

$$I = \int_0^R r^2 dm \tag{4a}$$

is the moment of inertia of the blade with respect to the flapping hinge. Observing that

[2] A brief list of the assumptions involved is given at the end of Section 4. For a more extended discussion cf. J. B. Wheatley, *Aerodynamic analysis of the autogiro rotor*, NACA Technical Report 487, 1934.

$$(\varphi + \vartheta)U^2 \simeq U_T U_P + \vartheta U_T^2 \tag{3c}$$

performing the integration (4a), and dividing by I, one arrives at the *differential equation of flapping motion*

$$\mathcal{J}(\beta) = E(\omega t), \tag{5}$$

where

$$\mathcal{J}(\beta) \equiv \ddot{\beta} + p(t)\dot{\beta} + s(t)\beta \tag{5a}$$

with

$$p(t) \equiv n\omega[1 + \tfrac{4}{3}\mu \sin \omega t], \qquad s(t) \equiv \omega^2[1 + \tfrac{4}{3}n\mu \cos \omega t + n\mu^2 \sin 2\omega t]; \tag{5b}$$

and

$$E(\omega t) \equiv -mgr_{cg}/I + n\omega^2\{\tfrac{4}{3}\lambda + (1 + \mu^2)\vartheta + (2\lambda\mu + \tfrac{8}{3}\mu\vartheta) \sin \omega t - \mu^2\vartheta \cos 2\omega t\}. \tag{5c}$$

The first term of the forcing function $E(\omega t)$ represents the moment of the blade weight (r_{cg} is the c.g. distance from the hinge), and is usually negligibly small. The remaining terms constitute the aerodynamic excitation. Control of the helicopter is effected by cyclic pitch variation:

$$\vartheta = \vartheta_0 + \vartheta_c \cos \omega t + \vartheta_s \sin \omega t. \tag{5d}$$

Here ϑ_0 is the "collective pitch" setting, ϑ_c the lateral, $-\vartheta_s$ the fore-and-aft control setting.

It will be convenient to call the equation

$$\mathcal{J}(\beta) = 0 \tag{6}$$

the "homogenized" flapping equation. The term $\ddot{\beta}$ of $\mathcal{J}(\beta)$ is the inertia term. The expression $p(t)\dot{\beta}$ represents the damping which is produced by the change in the angle of attack caused by flapping. The dimensionless quantity

$$n = \rho c a R^4/8I \tag{7}$$

can be called the *aerodynamic damping coefficient.*[3] The leading member, $\omega^2\beta$, of the spring term $s(t)\beta$ represents the restoring moment of the centrifugal force. The frequency ω of the coefficients $p(t)$ and $s(t)$ can be called the *parametric frequency.*[4] In the present problem this frequency coincides with the frequency impressed by the function $E(\omega t)$.

The solution of Eq. (5) can be written in the form

$$\beta = \beta_0 + h_1\beta_1 + h_2\beta_2 \tag{8}$$

where β_0 is the particular integral and represents the forced (steady state) response; β_1 and β_2 are the two solutions of the homogeneous equation, and represent the natural modes (transients). h_1 and h_2 are numerical coefficients determined by the initial conditions.

Two papers appear in the literature on the solution of the homogeneous equation,

---

[3] The Germans refer to $\gamma = 8n$ as the "Locksche Trägheitszahl."

[4] N. Minorsky, *On parametric excitation*, Journal Franklin Institute **250**, 25, 1945.

$\mathcal{F}(\beta)=0$. Bennett[5] has investigated the solution for the particular values $n=1.5$, $\mu=1.0$, $\beta(0)=1$, $\dot{\beta}(0)=0$, in the following manner. He determined the coefficients of the expansion

$$\beta(\psi) = \beta(0) + t\dot{\beta}(0)/1! + t^2\ddot{\beta}(0)/2! + \cdots \tag{9}$$

by repeated differentiation of Eq. (6), plotted $\beta(\psi)$ from $\psi=0$ to $\psi=4\pi$, and noted that $\beta(4\pi)/\beta(0)<1$. From this result Bennett concluded that stability is insured for all $\mu<1$. In an earlier paper Glauert and Shone[6] solved Eq. (6) by omitting the $\ddot{\beta}$ term for simplicity, and concluded that the motion is unstable.

Evidently, the above approaches to the stability problem are approximate and inconclusive.

More extended investigations are available for the particular integral. β_0 can be assumed in the form[7]

$$\beta_0 = a_0 + a_1\cos\omega t + b_1\sin\omega t + a_2\cos 2\omega t + b_2\sin 2\omega t + \cdots . \tag{10}$$

The constant part, a_0, is called the *coning angle* of the blade. The angles a_1 and b_1 determine the tilt of the cone axis (forward and to the port side, respectively, when ω is counterclockwise); the higher terms determine the motion of the blade in and out of the cone. Substituting (10) into Eq. (5), one obtains the infinite system of equations

$$\begin{aligned}
1:\quad & a_0 + \tfrac{1}{2}\mu^2 n b_2 = -mgr_{cg}/I\omega^2 + \tfrac{4}{3}n\lambda + (1+\mu^2)n\vartheta_0 + \tfrac{4}{3}\mu\eta\vartheta_s \\
\cos\psi:\quad & \tfrac{4}{3}\mu a_0 + (1+\tfrac{1}{2}\mu^2)b_1 - \tfrac{2}{3}\mu a_2 + \tfrac{1}{2}\mu^2 b_3 = (1+\tfrac{1}{2}\mu^2)\vartheta_c \\
\sin\psi:\quad & -(1-\tfrac{1}{2}\mu^2)a_1 - \tfrac{2}{3}\mu b_2 - \tfrac{1}{2}\mu^2 a_3 = 2\mu\lambda + \tfrac{8}{3}\mu\vartheta_0 + (1+\tfrac{3}{2}\mu^2)\vartheta_s \\
\cos 2\psi:\quad & \tfrac{4}{3}\mu n a_1 - 3a_2 + 2nb_2 - \tfrac{4}{3}\mu n a_3 + \cdots = -\mu^2 n\vartheta_0 - \tfrac{4}{3}\mu n\vartheta_s \\
\sin 2\psi:\quad & \mu^2 n a_0 + \tfrac{4}{3}\mu n b_1 - 2na_2 - 3b_2 - \tfrac{4}{3}\mu n b_3 + \cdots = \tfrac{4}{3}\mu n\vartheta_c \\
\cos 3\psi:\quad & \tfrac{1}{2}\mu^2 n b_1 - 2\mu n a_2 + 8a_3 - 3nb_3 + \cdots = -\tfrac{1}{2}\mu^2 n\vartheta_c \\
\sin 3\psi:\quad & \tfrac{1}{2}\mu^2 n a_1 + 2\mu n b_2 - 3na_3 - 8b_3 + \cdots = -\tfrac{1}{2}\mu^2 n\vartheta_s \\
& \cdots\cdots\cdots\cdots\cdots\cdots\cdots\cdots\cdots\cdots\cdots\cdots
\end{aligned} \tag{11}$$

in the flapping coefficients $a_0, a_1, b_1, \cdots$. Placing $a_n=b_n=0$ for $n>N$, one can solve the first $2N+1$ equations for $a_0, a_1, \cdots, a_N, b_N$. For instance, for the numerical values

$$n = 1.7,\ mgr_{cg}/I\omega^2 = 0.03,\ \lambda = -0.10,\ \vartheta_0 = 0.2,\ \vartheta_c = \vartheta_s = 0,\ \mu = 0.34738 \tag{12a}$$

which are representative for a helicopter, one finds that

$$\begin{aligned}
\beta_0(\psi) = {} & 0.124 - 0.125\cos\psi - 0.057\sin\psi - 0.012\cos 2\psi \\
& + 0.007\sin 2\psi - 0.001\cos 3\psi + \cdots
\end{aligned} \tag{12b}$$

is the forced response.

Glauert[8] initiated the above method of approach in his fundamental paper on

[5] J. A. J. Bennett, *Rotary-wing aircraft*, Aircraft Engineering, May, 1940. An account of the work of Glauert and Shone[6] is also given in this paper.

[6] Glauert and Shone, R.A.E. Report BA 1080, 1933.

[7] This is a departure from the commonly accepted notation $\beta_0=a_0-a_1\cos\omega t-b_1\sin\omega t-a_2\cos 2\omega t-b_2\sin 2\omega t-\cdots$.

[8] H. A. Glauert, *A general theory of the autogyro*, R. & M. No. 1111, British A.R.C., 1926.

rotor blade theory, and carried the expansion of β_0 to first harmonics. Subsequently Lock,[9] Wheatly[2] and others determined also the second and higher harmonic flapping coefficients. They found from numerous examples (for $\mu \lesssim 0.5$) that the convergence of β_0 is sufficiently rapid to permit termination of the series with the second harmonic terms.

Although a numerical determination of β_0 has thus been accomplished, (in contrast with the lack of similar solutions for β_1 and β_2,) the problem of forced vibrations cannot be considered as completely solved so long as the convergence of series (10) is based solely on an appeal to numerical examples. It will be shown in Section 6 that for definite values of μ and n the expansion (10) diverges. The motion β is then said to be in *resonance* with the excitation $E(\omega t)$.

3. Solution of the homogeneous equation. Determination of the transients is very simple in vertical flight. Placing $\mu = 0$ in Eq. (6) one obtains the familiar equation of damped motion

$$d^2\beta/d\psi^2 + nd\beta/d\psi + \beta = 0. \tag{13}$$

This has the solutions

$$\begin{aligned} \beta_1 &= \exp\left(-\tfrac{1}{2}n\psi\right)\cdot\cos\sqrt{1-\tfrac{1}{4}n^2}\,\psi, \\ \beta_2 &= \exp\left(-\tfrac{1}{2}n\psi\right)\cdot\sin\sqrt{1-\tfrac{1}{4}n^2}\,\psi. \end{aligned} \tag{14}$$

For $\mu > 0$ one can write in analogy

$$\begin{aligned} \beta_1 &= e_1(\psi)\mathcal{P}_1(\psi), \\ \beta_2 &= e_2(\psi)\mathcal{P}_2(\psi), \end{aligned} \tag{15a, b}$$

where

$$\begin{aligned} e_1(\psi) &= \exp\left(-\tfrac{1}{2}n_{app_1}\psi\right), \\ e_2(\psi) &= \exp\left(-\tfrac{1}{2}n_{app_2}\psi\right), \end{aligned} \tag{16a, b}$$

and $\mathcal{P}_1(\psi)$ and $\mathcal{P}_2(\psi)$ are oscillatory functions. n_{app} can be called the *apparent damping coefficient.*

The functions e_1, e_2, $\mathcal{P}_1$, $\mathcal{P}_2$ can be determined in the following manner. One substitutes[10,11]

$$\beta(\psi) = v(\psi)\cdot\epsilon(\psi), \tag{17}$$

$$\epsilon(\psi) = \exp\left(-\frac{1}{2}\int^{t} p(t)dt\right) = \exp\left(-\tfrac{1}{2}n\psi + \tfrac{2}{3}n\mu\cos\psi\right) \tag{17a}$$

into Eq. (6). This leads to an equation for the factor $v(\psi)$ in which the first derivative is absent. Replacing the trigonometric functions by exponentials, the equation can be written in the form

$$d^2v/d\psi^2 + \left[\theta_2^* e^{-2i\psi} + \theta_1^* e^{-i\psi} + \theta_0 + \theta_1 e^{i\psi} + \theta_2 e^{2i\psi}\right]v = 0, \tag{18}$$

[9] C. N. H. Lock, *Further development of autogyro theory*, R. & M. No. 1127, British A.R.C. 1928.

[10] Whittaker and Watson, *Modern analysis*, p. 194, Cambridge, 1927.

[11] The notation $\int^t$ indicates that only the upper limit, t, is to be substituted into the indefinite integral of $p(t)$.

where

$$\theta_0 = 1 - \tfrac{1}{4}n^2 - \tfrac{3}{8}\mu^2 n^2,$$
$$\theta_1 = \tfrac{1}{3}\mu n(1 + in), \qquad (19a, b, c)$$
$$\theta_2 = \mu^2 n(\tfrac{1}{8}n - \tfrac{1}{2}i),$$

and θ^* denotes the conjugate complex of θ. By writing $v(\psi)$ in the form

$$v(\psi) = e^{\sigma\psi}\sum_{-\infty}^{+\infty} C_k e^{ik\psi} \qquad (20)$$

the differential equation (18) is reduced to an infinite system of linear homogeneous equations in the C_k.

For the values

$$\pm\sigma = \frac{i}{\pi}\arctan\frac{q}{\sqrt{1-q^2}} + mi \quad \text{for} \quad -1 \leqq q \leqq 1 \qquad (21a)$$

$$= \frac{1}{\pi}\log(q + \sqrt{q^2-1}) + (m - \tfrac{1}{2})i \quad \text{for} \quad q \leqq -1,\ q \geqq 1 \qquad (21b)$$

$$= \frac{1}{\pi}\log(q' + \sqrt{q'^2+1}) + mi \quad \text{for} \quad q \text{ imaginary} \qquad (21c)$$

where

$$m = 0, \pm 1, \pm 2, \cdots \qquad (22a)$$
$$q = \sqrt{\mathcal{D}}\sin\pi\sqrt{\theta_0} \quad \text{or} \quad \sqrt{-\mathcal{D}}\sinh\pi\sqrt{-\theta_0} \qquad (22b)$$
$$q' = \sqrt{-\mathcal{D}}\sin\pi\sqrt{\theta_0} \quad \text{or} \quad \sqrt{\mathcal{D}}\sinh\pi\sqrt{-\theta_0} \qquad (22c)$$
$$y_k = 1/(\theta_0 - k^2) \qquad (22d)$$

and[12]

$$\mathcal{D} = \begin{vmatrix} \cdot & \cdot & \cdot & \cdot & \cdot & \cdot & \cdot \\ \cdot & 1 & \theta_1^* y_2 & \theta_2^* y_2 & 0 & 0 & \cdot \\ \cdot & \theta_1 y_1 & 1 & \theta_1^* y_1 & \theta_2^* y_1 & 0 & \cdot \\ \cdot & \theta_2 y_0 & \theta_1 y_0 & 1 & \theta_1^* y_0 & \theta_2^* y_0 & \cdot \\ \cdot & 0 & \theta_2 y_1 & \theta_1 y_1 & 1 & \theta_1^* y_1 & \cdot \\ \cdot & 0 & 0 & \theta_2 y_2 & \theta_1 y_2 & 1 & \cdot \\ \cdot & \cdot & \cdot & \cdot & \cdot & \cdot & \cdot \end{vmatrix}, \qquad (22e)$$

the system of equations is consistent, and the expansion coefficients C_k can be determined. Two solutions are obtained, $C_k^{(1)}$ and $C_k^{(2)}$. The first set for, say,

$$\sigma = \sigma_1 = \sigma_r + i\sigma_i, \qquad \sigma_r \geqq 0, \qquad (23a)$$

[12] It was shown in I that the infinite determinant $\mathcal{D}$ may be expanded (for small μ) into a power series in $\delta = |\theta_1|^2$, $\epsilon = |\theta_2|^2$ and $\eta = \tfrac{1}{2}(\theta_1^2\theta_2^* + \theta_1^{*2}\theta_2)$. The leading term of the expansion is 1; the higher coefficients are functions of θ_0 only and may be obtained from the Tables of I.

the second set for

$$\sigma = \sigma_2 = -\sigma_1. \tag{23b}$$

The two solutions are linearly independent, except when $\sigma_r = 0$, and $2\sigma_i =$ integer.

The trigonometric function $\mathcal{P}_1(\psi)$ is now obtained as the product

$$\mathcal{P}_1(\psi) = \exp\left(\tfrac{2}{3}n\mu \cos\psi\right) \cdot \sum_{k=-\infty}^{+\infty} C_k^{(1)} \exp i(\sigma_i + k)\psi \tag{24a}$$

and the exponential function $e_1(\psi)$ as the product

$$e_1(\psi) = \exp\left(-\tfrac{1}{2}n\psi\right) \cdot \exp\left(\sigma_r\psi\right). \tag{24b}$$

The determination of $\mathcal{P}_2(\psi)$ and $e_2(\psi)$ (call these Eqs. (25a, b)) is similar. It is seen now that e_1 involves the apparent damping coefficient

$$n_{app_1} = n - 2\sigma_r \tag{26a}$$

which is smaller than n, and e_2 involves the apparent damping coefficient

$$n_{app_2} = n + 2\sigma_r \tag{26b}$$

which is larger than n. Evidently, n_{app_1} is the critical damping coefficient.[13] It will be written without the subscript 1.

Example. Determine the flapping transients β_1 and β_2 of a helicopter for which $n = 1.7$. Choose an advance ratio μ between 0.30 and 0.35 so that the Tables of I (which cover the range $\theta_0 = -0.6$ to $+0.5$ in 0.05 steps) be directly applicable.

One finds from (19a) that for

$$n = 1.7 \tag{27a}$$

and

$$\theta_0 = 0.2 \tag{27b}$$

the advance ratio has the value

$$\mu = 0.34738. \tag{27c}$$

This yields, by (19b, c) the values

$$\theta_1 = 0.19685 + 0.33465i, \qquad \theta_2 = 0.03875 - 0.10258i. \tag{27d}$$

The characteristic exponents

$$\sigma_1 = 0.30782 + \tfrac{1}{2}i, \qquad \sigma_2 = -\sigma_1 \tag{28}$$

associated with the numerical values (27), were determined in I, Section 4. The corresponding functions $v_1(\psi)$ and $v_2(\psi)$ were also given there. Eqs. (24) and (25) now yield[14]

[13] $n - 2\sigma_r < 0$ implies instability. The arbitrariness in the value of m, Eq. (22a), is removed by making C_0 the dominant term of $v(\psi)$.

[14] The normalization is used: the sin $\frac{1}{2}\psi$ term of v_1 and the cos $\frac{1}{2}\psi$ term of v_2 are written with the coefficient 1.

$$e_1(y) = e^{-0.5422\psi}, \tag{29a}$$

$$\mathcal{P}_1(y) = -0.0733\cos\tfrac{1}{2}\psi + 0.8369\sin\tfrac{1}{2}\psi + 0.1923\cos\tfrac{3}{2}\psi + 0.1717\sin\tfrac{3}{2}\psi + 0.0268\cos\tfrac{5}{2}\psi + 0.0131\sin\tfrac{5}{2}\psi + 0.0023\cos\tfrac{7}{2}\psi + 0.0023\sin\tfrac{7}{2}\psi + 0.0002\cos\tfrac{9}{2}\psi + 0.0004\sin\tfrac{9}{2}\psi + \cdots, \tag{29b}$$

and

$$e_2(\psi) = e^{-1.1578\psi}, \tag{29c}$$

$$\mathcal{P}_2(\psi) = 1.2863\cos\tfrac{1}{2}\psi + 0.3795\sin\tfrac{1}{2}\psi + 0.4404\cos\tfrac{3}{2}\psi + 0.1028\sin\tfrac{3}{2}\psi + 0.0676\cos\tfrac{5}{2}\psi + 0.0229\sin\tfrac{5}{2}\psi + 0.0068\cos\tfrac{7}{2}\psi + 0.0050\sin\tfrac{7}{2}\psi + 0.0005\cos\tfrac{9}{2}\psi + 0.0006\sin\tfrac{9}{2}\psi + \cdots. \tag{29d}$$

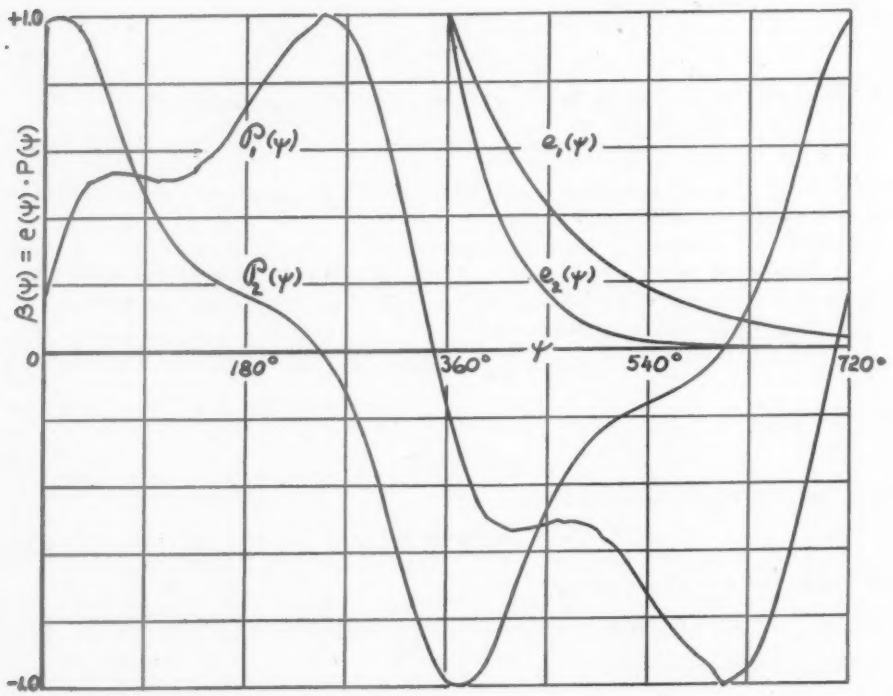

FIG. 2. Transient blade flapping modes $\beta_1(\psi) = e_1(\psi)\mathcal{P}_1(\psi)$ and $\beta_2(\psi) = e_2(\psi)\mathcal{P}_2(\psi)$ for damping coefficient $n = 1.7$ and advance ratio $\mu = 0.34738$.

The factors e_1, $\mathcal{P}_1$ and e_2, $\mathcal{P}_2$ of the transient flapping angles β_1 and β_2 are plotted in Fig. 2 as functions of ψ. $\mathcal{P}_1(\psi)$ and $\mathcal{P}(\psi)$ are drawn normalized to 1 at their maxima, $e_1(\psi)$ and $e_2(\psi)$ are drawn normalized to 1 at $\psi = 360°$. The graphs indicate that at the very large advance ratio $\mu = 0.347$ the flapping motion of the blade, as given by Eq. (6), is still so stable that a transient reduces to less than 4% of its original amplitude within one revolution. The wave form $\mathcal{P}(\psi)$ of the transient contains a pronounced

third harmonic component and unimportant higher harmonics. The frequency of the transient (or more exactly, of the dominant term of the transient) is *one half* of the rotor speed.

4. Stability of blade flapping motion. It was seen in the preceding section that the transient β_1 is associated with an apparent damping coefficient n_{app_1} which is less than n when $\sigma_r \neq 0$. σ_r can be called the "absolute degree of destabilization" of the system. For a damped system ($n>0$), like the present one, it is more convenient to characterize destabilization in terms of the ratio

$$2\sigma_r/n = 1 - n_{app}/n. \tag{30}$$

This can be called the "relative degree of destabilization" of the system, or briefly, the *degree of destabilization*. For the example of the preceding section ($n=1.7$, $\theta_0=0.2$, $\mu=0.34738$) the degree of destabilization is $2\sigma_r/n=0.362$.[15]

When

$$2\sigma_r/n = 0, \quad \text{or} \quad n_{app}/n = 1 \tag{31a}$$

a system is *completely stable*. When

$$0 < 2\sigma_r/n < 1, \quad \text{or} \quad 1 > n_{app}/n > 0 \tag{31b}$$

the system becomes partially destabilized (*transition region*), and when

$$2\sigma_r/n > 1, \quad \text{or} \quad n_{app}/n < 0 \tag{31c}$$

the system is *unstable*.

For conventional rotor blades n ranges from 1.4 to 1.9 (at sea level), and $\mu \sim 0.35$ represents the maximum attainable forward speed. By a systematic determination of σ_r associated with the values 1.4, 1.5, $\cdots$, 2.4, 2.5 of n, and the values -1, -0.9, $\cdots$, $+0.4$, $+0.5$ of θ_0 the writer computed the degree of destabilization $2\sigma_r/n$ in a μ, n region which covers the range of practical interest. The plots are shown in Figs. 3a, b. The calculated points are indicated by crosses. The points on the μ-axis (small circles in Fig. 3b) were obtained by means of an auxiliary graph giving the plot of q and q' vs. μ for various n. In Fig. 4 this construction is shown for $n=1.4, \sqrt{3}$, 1.9, 2.0, 2.1, 2.4. The intersections of the curves with horizontal lines of ordinates 0 and 1 yield the μ values for which $\sigma_r=0$.

A replot of Fig. 3, with μ as abscissa, n as ordinate and n_{app}/n as the index of the curves leads to the *stability diagram*, Fig. 5. The diagram indicates two complete stability regions, and two transition regions. The complete stability regions are characterized by $n_{app}/n=1$ and by response frequencies which vary with μ and n (between 0 and $\frac{1}{2}\omega$); the transition regions are characterized by the fixed frequencies 0 and $\frac{1}{2}\omega$, respectively, of the response, and by degrees of stability n_{app}/n which vary with μ and n (between 1 and a minimum).

From Fig. 5 it is clear that the flapping motion is very stable for $\mu<0.5$ at any n. This is in agreement with the conclusions reached in the preceding section for the special case of $n=1.7$.

---

[15] For $n=1.7$, $\theta_0=0$ one finds $\mu=0.65734$, and θ_1 and θ_2 assume the values given in I, Sec. 5. The corresponding degree of destabilization is $2\sigma_r/n=0.510$.

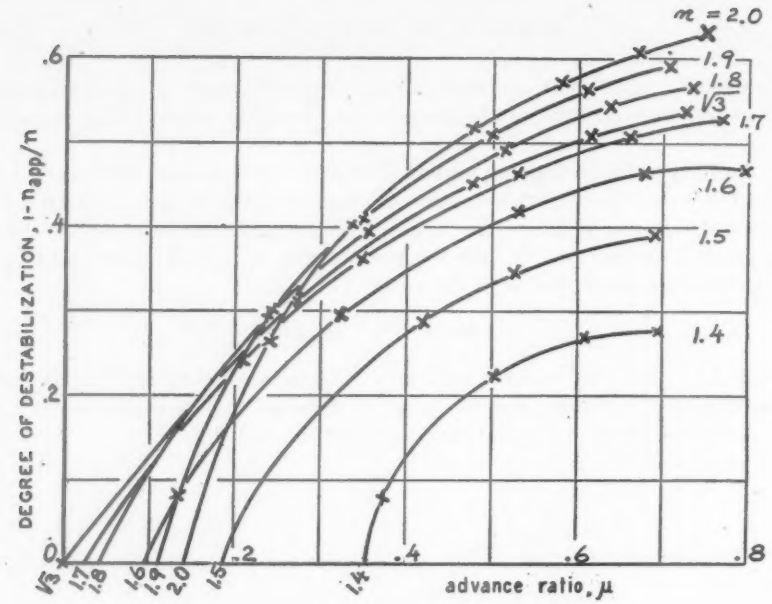

(a)

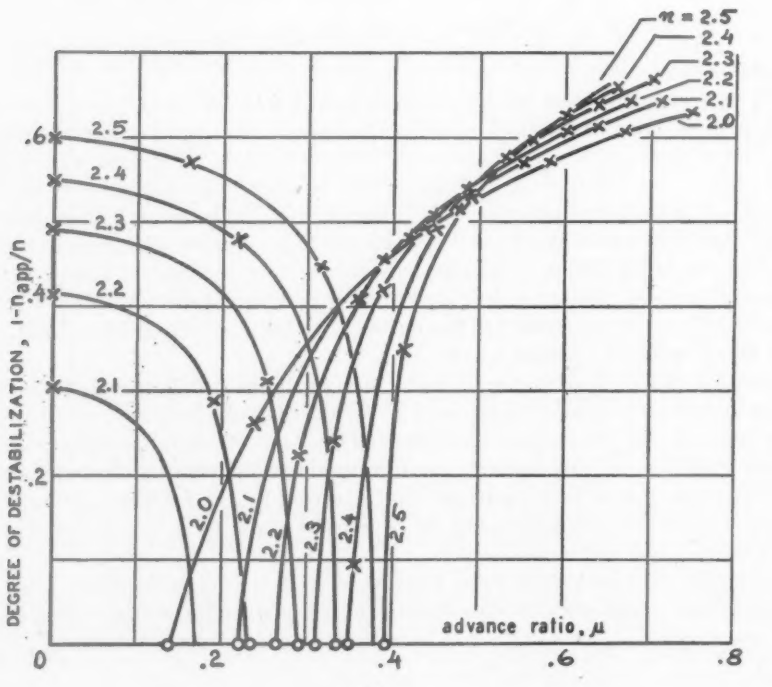

(b)

FIGS. 3a and b. Degree of destabilization of rotor blade vs. advanced ratio at various values of the aerodynamic damping coefficient n.

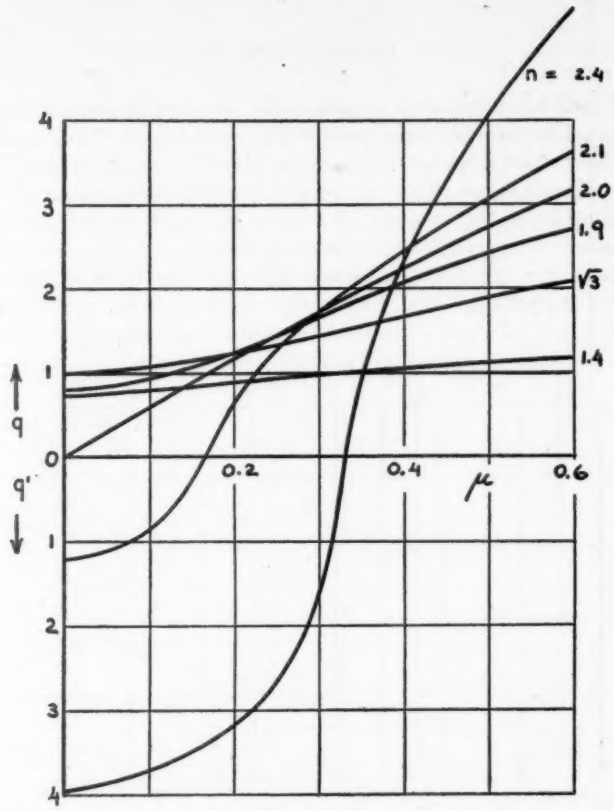

FIG. 4. The functions q and q'.

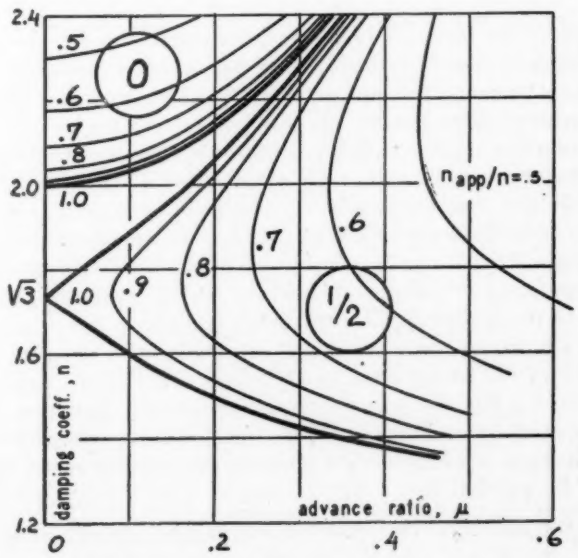

FIG. 5. Rotor blade stability diagram. Level lines indicate the relative degree of stability for various values of the damping coefficient and the advance ratio.

It may be well to recapitulate at this point the various assumptions on the basis of which the stability of flapping motion was established. The assumptions are as follows: The blades are attached to the rotor shaft by means of flapping hinges only (the freedom of oscillation of the blades in the rotor plane, about the lag hinges, is thus disregarded), and the distance of the hinges from the rotor axis is negligible. The hinge axes are perpendicular to the rotor shaft and to the respective blade span axes. The blades are untwisted, and are rigid both in bending and in twist. The chord and the lift coefficient are constant along the blades. The uniform motion of the helicopter is not affected by the oscillations of the blades. Of the aerodynamic

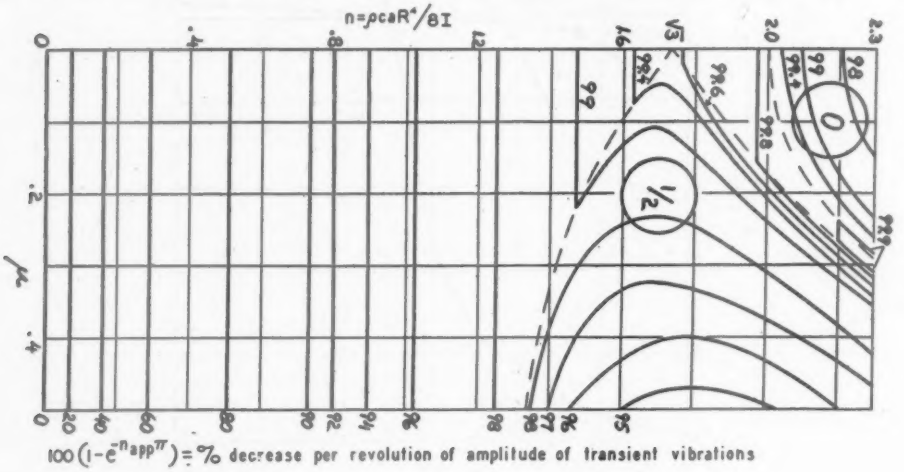

FIG. 6. Stability chart of rotor blade flapping motion.

forces which act on the blades only the velocity square lift forces are taken into account. Air velocities in the direction of the blade span are neglected. The field of induced velocities is assumed as constant over the rotor disc, and interference effects between the various blade elements are disregarded. All angles involved (but ψ) are small, in particular the angle of attack is always less than the stalling angle.

Although the above assumptions are violated by a helicopter in many respects, experience has shown that the steady state solution (10) gives a description of the flapping motion of the blades which, for $\mu \lesssim 0.35$, is in satisfactory agreement with the observations. Thus Eq. (5) can be considered as essentially correct.

From the practical point of view the plots of Fig. 6, giving the percentage decrease per revolution of the amplitude of a transient, constitute the principal result of the present paper. On the one hand the chart establishes the hitherto unsuspected and curious behavior of the flapping transients near $n=\sqrt{3}$ (the stability decreases as μ increases, the natural frequency of the flapping motion is $\frac{1}{2}\omega$ over a wide range of μ's and n's); on the other hand it also focusses attention on the sluggishness of the blades in recovering their steady state motion when the value of n is small. Blades with low n must therefore be avoided.[16]

[16] The widely held belief that "the natural frequency in flapping is equal to the speed of rotation"

The problem of blade response to control deflections leads to considerations which go beyond the question of the rate of extinction of a transient, and will therefore be taken up in a separate paper.

5. The functional relation $\sigma_r+i\sigma_i=\sigma(\mu, n)$. The characteristic exponent σ is a simple expression, (21), in the combination q (or q') of θ_0 and $\mathcal{D}$. θ_0 and $\mathcal{D}$ in turn are functions of the advance ratio μ and the damping coefficient n. As μ increases, θ_0, Eq. (19a), decreases monotonically. The variation of $\mathcal{D}$ with μ is more complicated. $\mathcal{D}$ becomes infinite for $\theta_0=0^2, 1^2, 2^2, \cdots$; for the flapping problem ($\theta_0<1$) only for $\theta_0=0$. Elsewhere $\mathcal{D}$ fluctuates between positive maxima and negative minima.[18] Correspondingly q maxima (σ_r maxima) alternate with q' maxima (σ_r maxima). (Cf. Fig. 4 which shows the $q(\mu)$, $q'(\mu)$ variation near the origin.) Complete stability exists only in the very narrow strips where $0\leqq q\leqq 1$. In these regions the ratio n_{app}/n is constant at the value 1, while the frequency varies across the region by $\frac{1}{2}\omega$. In the remainder of the μ, n diagram the dominant frequency of the transient is an integral multiple of $\frac{1}{2}\omega$, and one has either $0<2\sigma_r/n<1$ (transition region), or $2\sigma_r/n>1$ (instability region).

The relationships $\sigma_r+i\sigma_i=\sigma(\mu, n)$ can be best appraised by considering the variation of σ with μ for one particular value of n. Such a survey is carried out below, first for $n=2.4$ in the μ-range 0 to 0.5 with the aid of Fig. 5; then by an approximate method for $n=\sqrt{3}$ in the μ-range 0 to 8.0 wth the aid of Figs. 7, 8, 9. Although Eq. (5) ceases to give an approximate description of blade flapping when the stalled areas of the blades are large (when $\mu\gtrsim 0.5$), the equation is of interest, per se, also in this case, and an investigation of the behavior of the solutions of (6) for large values of μ aids in the formation of a clear picture of the variation of σ with μ and n.

For $n=2.4$, $\mu=0$, the transients β_1 and β_2 are solutions of Eq. (13), and thus can be written as

$$\beta_1 = \exp\left(-\tfrac{1}{2}n + \sqrt{\tfrac{1}{4}n^2-1}\right)\psi = \exp\left(-1.2+0.663\right)\psi, \tag{32a}$$

$$\beta_2 = \exp\left(-\tfrac{1}{2}n - \sqrt{\tfrac{1}{4}n^2-1}\right)\psi = \exp\left(-1.2-0.663\right)\psi. \tag{32b}$$

Therefore $n_{app}/n=0.447$ and $\sigma_i=0$. The same result is obtained also from the general theory. Since for $\mu=0$ one has $\mathcal{D}=1$, therefore

$$q' = \sinh \pi\sqrt{\tfrac{1}{4}n^2-1} = 3.95, \tag{32c}$$

$$\sigma = \frac{1}{\pi}\log\left(q'+\sqrt{q'^2+1}\right) = 0.663, \tag{32d}$$

and again

$$1-2\sigma_r/n = 0.447, \qquad \sigma_i = 0. \tag{32e}$$

(quotation from Bennett's Princeton University Lecture Notes *On the physical principles of the helicopter*, p. 1, 1944) is largely the result of an unfortunate misuse of the expression "natural frequency" for the frequency at which the phase displacement between impressed force and response is 90°. For many slightly damped systems with constant parameters this frequency nearly coincides with the frequency of the transient,[17] but sometimes, as in the present case, there is considerable divergence between the two.

[17] J. P. Den Hartog, *Mechanical vibrations*, p. 63, McGraw-Hill, 1940.

[18] Oscillation theorem, cf. M. J. O. Strutt, *Lamésche, Mathieusche und verwandte Funktionen in Physik und Technik*, p. 15, Springer, 1933.

As μ increases, q' decreases until it reaches zero at $\mu \sim 0.334$. Correspondingly σ_r also decreases to 0, the *characteristic curve* (the common boundary of the transition and the complete stability regions) is breached, q' changes into q, and the complete stability region is entered. Between $\mu \sim 0.334$ and $\mu \sim 0.352$, q varies from 0 to 1. Correspondingly $\sigma_r = 0$, while σ_i varies from 0 to $\frac{1}{2}$. In the transition region that follows $\sigma_i = \frac{1}{2}$, and σ_r varies from 0 to a maximum, then back to zero. (The diagram does not extend sufficiently to the right to show this variation.)

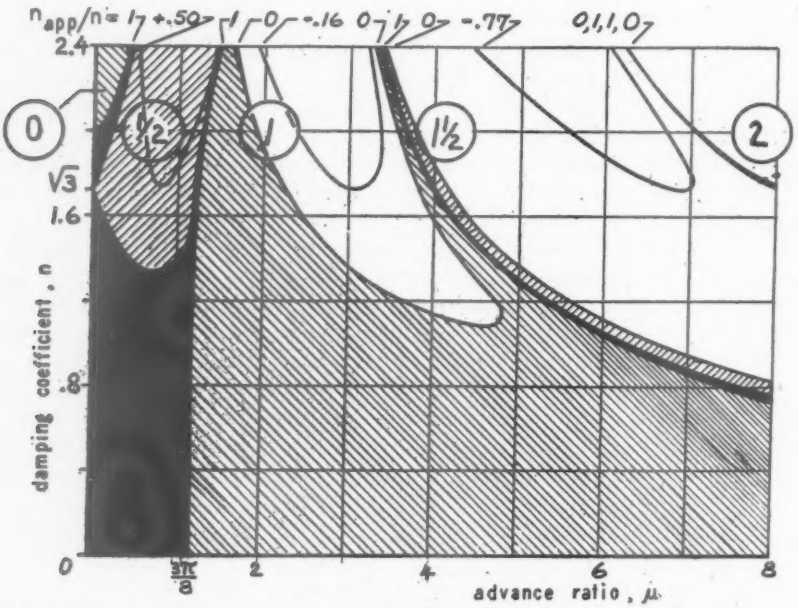

FIG. 7. Stability of the equation $\ddot{\beta}+n\omega\dot{\beta}+\omega^2(1+\frac{4}{3}n\mu\cos\omega t)\beta=0$ by the "twin-ripple method" of approximation. Complete stability regions are blackened, transition regions (bounded by the curves $n_{app}/n=1$ and $n_{app}/n=0$) are lightly shaded, and unstable regions are left blank. The encircled numbers indicate the dominant frequency of the transient (in units of ω) in the respective instability and transition regions.

Fig. 7 shows qualitatively the conditions which hold for Eq. (6) at large values of μ. This diagram was obtained by replacing the variable coefficients of $\dot{\beta}$ and β in Eq. (6) by their constant averages first in the $\psi=-\pi/2$ to $+\pi/2$ interval, then in the $\psi=\pi/2$ to $3\pi/2$ interval. The resulting pair of differential equations was solved by the method of Meissner[19] (better known as the Van der Pol-Strutt "rectangular ripple" method[20,21]) which was adapted to damped systems by Shao Wen Yuan and the writer.[22]

[19] Strutt, ibid., p. 39.

[20] Den Hartog, loc. cit., p. 389.

[21] S. Timoshenko, *Vibration problems in engineering*, p. 164, D. Van Nostrand, 1937.

[22] G. Horvay and S. W. Yuan, *Stability of rotor blade flapping motion when the hinges are tilted. Generalization of the "rectangular ripple method" of solution*, to be published soon. The procedures used in obtaining diagrams like Figs. 7, 8, 9 are also discussed in this paper.

In Fig. 7 the regions of complete stability are blackened, the transition regions are lightly shaded, and the regions of instability are left blank. Consider the ordinate $n=\sqrt{3}$. For $\mu=0$ one has the solution

$$\beta_1 = \cos \tfrac{1}{2}\psi, \qquad \beta_2 = \sin \tfrac{1}{2}\psi, \qquad n_{app}/n = 1; \tag{33}$$

the transition region $(\frac{1}{2})$ extends into the point $(\mu, n)=(0, \sqrt{3})$ of the ordinate axis. As μ increases, the stability decreases until a minimum of $n_{app}/n \sim 0.50$ is reached around $\mu \sim 0.85$. Thereafter the stability again increases.

In the present approximation of Eq. (6) complete stability ($\sigma_r=0$) sets in at $\mu \sim 1.24$ and ceases at $\mu \sim 1.28$. In the meantime σ_i has increased from $\frac{1}{2}$ to 1. In the region $\sigma_i=$ (1) (the dominant frequency of the transient is now ω) σ_r varies from 0 at $\mu \sim 1.28$ to a maximum of ~ 1.0 at $\mu \sim 3.2$ (yielding $n_{app}/n \sim -0.16$), and then back to zero at $\mu \sim 4.02$. First comes the transition interval $(1 > n_{app}/n > 0)$ from $\mu \sim 1.28$ to $\mu \sim 2.27$. This is followed by the instability interval $(n_{app}/n < 0)$ from $\mu \sim 2.27$ to $\mu \sim 3.83$. A second transition interval $(1 > n_{app}/n > 0)$ from $\mu \sim 3.83$ to $\mu \sim 4.02$ completes the (1) interval. There follows now a very narrow complete stability interval, $\mu \sim 4.02$ to $\mu \sim 4.03$, in which $\sigma_r=0$ while σ_i varies from 1 to $1\frac{1}{2}$. This is followed by the $(1\frac{1}{2})$ transition interval, this by the $(1\frac{1}{2})$ instability interval; and so on, indefinitely. Complete stability, transition, instability, transition, complete stability regions alternate, ad infinitum.

The stability regions, associated with $\sigma_r=0$ and varying σ_i, become ever narrower, the instability regions, associated with $\sigma_i=$const. and varying σ_r become wider and graver. The orders (0), $(\frac{1}{2})$, (1), $\cdots$ of the transition and instability regions are marked in the diagram. The regions (0), (1), (2), $\cdots$ can be called *even ordered regions* (the dominant frequency of the transient is 0, 2, 4, $\cdots \times \frac{1}{2}\omega$); the regions $(\frac{1}{2})$, $(1\frac{1}{2})$, $\cdots$ can be called *odd-ordered regions* (the dominant frequency of the transient is 1, 3, $\cdots \times \frac{1}{2}\omega$). The boundary curves $n_{app}/n=1$ and 0 are also indicated in Fig. 7. Level curves which touch the $n=\sqrt{3}$ horizontal line complete the picture.

It is rather interesting to note that although Eq. (6) reduces to a damped Mathieu equation when μ is very small ($\mu^2 \sim 0$), Fig. 7 shows a departure from the conventional stability diagram given for these equations. In the first place, the present diagram plots n vs. μ, whereas conventionally one plots θ_0 vs. μ. More fundamental is the change in behavior near the origin. Since the oscillating terms of the spring force $s(t)\beta$ tend to zero as $n \to 0$, no transition region, like the one at $n=\sqrt{3}$, $\mu=0$, $\theta_0=\frac{1}{2}$, wedges into the origin $n=\mu=0$, $\theta_0=1$. A second comment is also in order. The twin-ripple approximation used in obtaining Fig. 7 accounts in an approximate manner for the stiffness fluctuations produced by the $\frac{1}{2}\omega^2\mu n \cos \omega t \cdot \beta$ spring term of Eq. (6). In the process of averaging the coefficients of Eq. (6) both the $\frac{1}{2}\omega\mu n \sin \omega t \cdot \dot{\beta}$ damping term and the $\frac{1}{2}\omega^2\mu^2 n \sin 2\omega t \cdot \beta$ spring term are eliminated. However for large μ, the μ^2 term of $s(t)$ has the principal effect. This effect can also be evaluated by a "twin-ripple" approximation, provided one first omits the two μ-proportional terms of $\mathcal{J}(\beta)$, and then averages the μ^2 term in the intervals 0 to $\pi/2$ and $\pi/2$ to π. The resulting stability conditions are indicated in Fig. 8 for the value $n=\sqrt{3}$.

The diagram indicates that in the absence of the terms $\frac{1}{2}\omega\mu n \sin \psi\dot{\beta}$ and $\frac{1}{2}\omega^2\mu n \cos \psi\beta$ of $\mathcal{J}(\beta)$ the region of complete stability extends from $\mu=0$ to about $\mu \sim 1$. For $\mu > 1$ the system is mostly unstable. Comparison of Figs. 7 and 8 indicates that the high order instability regions crowd much closer to the origin than was sur-

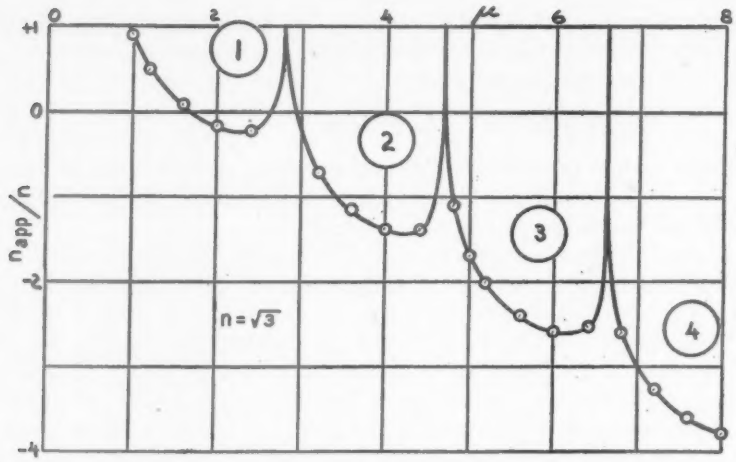

FIG. 8. Instability troughs of the equation $\ddot{\beta}+n\omega\dot{\beta}+\omega^2(1+n\mu^2 \sin 2\omega t)\beta=0$, $(n=\sqrt{3})$, by the twin-ripple method of approximation; $n_{app}/n=1$ represents complete stability, $0<n_{app}\ n<1$ represents transition, $n_{app}/n<0$ represents instability. The calculated points are indicated by small circles. The encircled numbers indicate the "orders" of the regions.

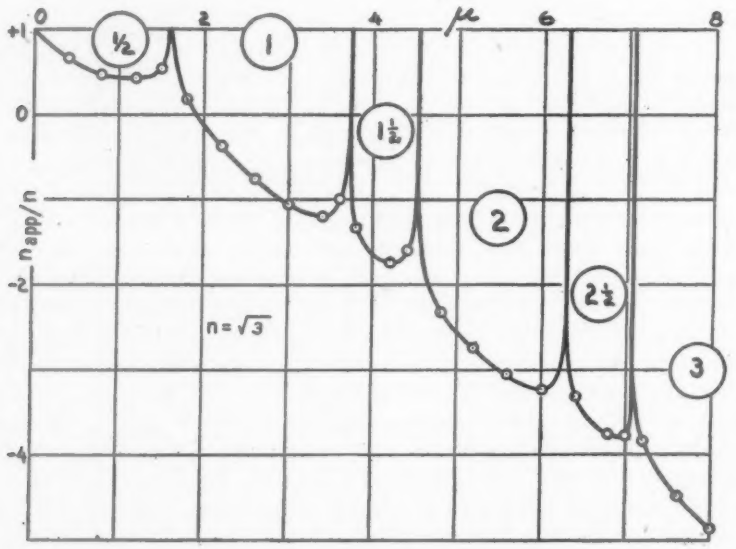

FIG. 9. Instability troughs of Eq. (6) for $n=\sqrt{3}$ by a "4-ripple approximation." The calculated points are indicated by small circles. The encircled numbers indicate the "orders" of the regions.

mised on the basis of Fig. 7. Moreover the instability caused by the μ^2 spring term is much graver than that caused by the first power μ term.

It is to be expected that in an exact solution of Eq. (6) the first power μ terms

determine the stability conditions for $\mu<1$, whereas the μ^2 term is principally responsible for the stability conditions at $\mu>1$. This is born out by Fig. 9. Fig. 9 was obtained by use of a "4-ripple" approximation. (The interval 0 to 2π is divided into 4 equal parts and the coefficients $p(t)$ of $\dot{\beta}$ and $s(t)$ of β are replaced by their averages in each interval.) This approximation takes into account the effect of all the oscillating coefficients of Eq. (6). The figure shows that for $\mu>1$ the odd ordered instability regions (which are produced solely by the μ-proportional terms) are of minor importance as compared with the even ordered instability regions.

6. Resonance.[23] The preceding sections were concerned mainly with the transient solutions of Eq. (5). The present section deals with the steady state response.

In general, the assumption (10) leads to an equation system (11) which can be solved for the Fourier coefficients $a_0, a_1, \cdots, a_N, b_N, \cdots$. When however the determinant Δ of the system vanishes, then the Ansatz (10) fails. In this case

$$\beta_0 = a_0 + a_1 \cos \omega t + b_1 \sin \omega t + a_2 \cos 2\omega t + \cdots + t[c_0 + c_1 \cos \omega t + d_1 \sin \omega t + c_2 \cos 2\omega t + \cdots] \tag{34}$$

is the correct form for the solution of the equation. Note that *the response becomes infinite even though the system is damped.*

What are the conditions for $\Delta=0$? Evidently, $\Delta=0$ implies that the homogeneous equation (6) has a solution which is of the form (10). This in turn implies

$$\sigma = \tfrac{1}{2}n \pm mi \qquad (m = 0, \tfrac{1}{2}, 2, \cdots). \tag{35}$$

Thus, *resonance occurs on the $n_{app}/n=0$ boundary lines of the even ordered transition and instability regions.* From Fig. 5 it is seen that for helicopters resonance excitation is just as remote as instability.[24]

There are two more interesting questions which arise in connection with resonance. (1) How would conditions change if the exciting force on the right side of Eq. (5) were of the form

$$E(t) = \begin{Bmatrix} \sin \\ \cos \end{Bmatrix} \nu t, \quad \text{where} \quad \nu \neq \omega, 2\omega, \cdots ? \tag{36}$$

(2) How would conditions change if the system were undamped, i.e., if the $p(t)\dot{\beta}$ term were absent from Eq. (5), but the $s(t)\beta$ expression still contained oscillating terms of frequency ω?

If $\nu=\frac{1}{2}\omega$ or an odd multiple of it, then placement of

$$\beta_0 = a_1 \cos \tfrac{1}{2}\omega t + b_1 \sin \tfrac{1}{2}\omega t + a_3 \cos \tfrac{3}{2}\omega t + b_3 \sin \tfrac{3}{2}\omega t + \cdots \tag{10'}$$

---

[23] This section is based on the paper by G. Kotowski, *Lösungen der inhomogenen Mathieuschen Differentialgleichung mit periodischer Störfunktion beliebiger Frequenz*, Z. angew. Math. Mech. **25**, 213, 1943. Kotowski credits introduction of the method to A. Erdelyi, Arch. Elektrotechn. **29**, 473, 1935.

[24] Since the response amplitudes are large near a resonance frequency the following question is of interest in many problems: how deep do the regions of large amplifications extend into the transition regions or perhaps stability regions? Kotowski answers the question for the equation $y''+(\lambda+\cos x)y = a_0+a_1 \cos x+a_2 \cos 2x$, by plotting the resonance curve. (λ is the variable parameter.) In the present problem the great distance of the helicopter operating range, $\mu\leq 0.35$, from the nearest $n_{app}/n=0$ curve eliminates the necessity for such an investigation.

into $\mathcal{F}(\beta)=E(t)$ leads to an equation system (11′), with a determinant Δ' which in general does not vanish;[25] Δ' vanishes only when the homogeneous Eq. (6) has a solution of the form (10′), i.e., when

$$\sigma = \tfrac{1}{2}n + (\tfrac{1}{2} + m)i \qquad (m = 0, \pm 1, \pm 2, \cdots) \tag{35′}$$

Thus, *for ν = odd multiple of $\frac{1}{2}\omega$, resonance, occurs on the $n_{app}/n=0$ boundary lines of the odd ordered transition and instability regions.* In this case expression (10′) plus t times a similar expression is the correct "Ansatz" for the forced response.

When ν is a fractional multiple of $\frac{1}{2}\omega$, then

$$\begin{aligned}\beta_0 = {} & \cos \nu t[a_0 + a_1 \cos \omega t + b_1 \sin \omega t + a_2 \cos 2\omega t + \cdots] \\ & + \sin \nu t[c_0 + c_1 \cos \omega t + d_1 \sin \omega t + c_2 \cos 2\omega t + \cdots]\end{aligned} \tag{10″}$$

is the correct assumption for the particular integral. The associated equation system (11″) has a determinant Δ'' which vanishes only when the homogeneous equation (6) has a solution of the form (10″), i.e., when

$$\sigma = \tfrac{1}{2}n + \left(\frac{\nu}{\omega} + m\right)i \qquad (m = 0, \pm 1, \pm 2, \cdots). \tag{35″}$$

But from Eq. (21) it is obvious that σ is never of this form, unless $n=0$. Thus, *when 2ν is a fractional multiple of the parametric frequency ω, resonance can occur only when the system is undamped.* In such a case the *response occurs along the lines $\sigma_i = m + \nu/\omega$ of the complete stability regions*, and (10″) plus t times an expression of type (10″) is the correct form for the solution.

It is to be noted that a single frequency ν excites an infinity of response frequencies ν, $\nu \pm \omega$, $\nu \pm 2\omega$, $\cdots$, and thus in a system with variable spring and damping coefficients one obtains an infinity of resonance peaks in contrast with a system characterized by a 2nd order differential equation with constant coefficients which shows only one resonance peak.

The absence of damping also modifies the results for the cases when ν is an even or odd multiple of $\frac{1}{2}\omega$. The $n_{app}/n=0$ curves now coincide with the characteristic curves of the stability diagram, and

$$\sum_0^\infty [(a_k + b_k t + c_k t^2) \cos k\omega t + (d_k + e_k t + f_k t^2) \sin k\omega t] \tag{37a}$$

and

$$\sum_0^\infty [(a_k + b_k t + c_k t^2) \cos (2k+1)\omega t + (d_k + e_k t + f_k t^2) \sin (2k+1)\omega t, \tag{37b}$$

respectively, are the proper forms for the resonant response.

The proofs of the expansions (34), etc. are based on the well-known formula[26]

$$J\epsilon^{-1}(\psi)\beta_0(\psi) = v_2(\psi)\int^{\psi} v_1(x)\epsilon^{-1}(x)E(x)dx - v_1(\psi)\int^{\psi} v_2(x)\epsilon^{-1}(x)E(x)dx \tag{38a}$$

[25] There is no need to write out the equation system.

[26] Frank-Mises, *Differential und Integralgleichungen der Physik*, Vol. I, p. 300, Fr. Vieweg u. Sohn, 1935.

where $\epsilon(\psi)$ is given by Eq. (17a); $v_1(\psi)$, $v_2(\psi)$ are the two linearly independent solutions of Eq. (18);

$$J = v_1 v_2' - v_2 v_1' = \text{const.}; \tag{38b}$$

and $E(\psi)$ is the exciting function.

When v_2 is of the form

$$e^{-n\psi/2} \sum g_k e^{ik\psi} \tag{39a}$$

and the exciting function is of the form

$$E(\psi) = \begin{Bmatrix} \cos \\ \sin \end{Bmatrix} j\psi \qquad (j = 0, 1, 2, \cdots) \tag{39b}$$

then the integrand

$$v_2(x)\epsilon^{-1}(x)E(x)$$

is a series which contains a constant term. This term integrates into ψ, and, multiplied by $-\epsilon(\psi)v_1(\psi)/J$, yields the non-periodic

$$t \sum [c_k \cos k\psi + d_k \sin k\psi]$$

terms of the expansion (34). The remainder of (38a) yields the periodic terms of (34). This proves (34). The proof of the other expansions is similar.[27]

When the exciting function is of the form

$$E(\psi) = \psi \cos \psi \tag{40}$$

then, by (38), the response is of the form

$$\beta_0(\psi) = \sum_0^\infty [(a_k + c_k\psi) \cos k\psi + (b_k + d_k\psi) \sin k\psi] \tag{41}$$

Substitution of (41) into the non-homogeneous equation $\mathfrak{F}(\beta) = E(t)$, and a comparison of the coefficients of $\cos k\psi$, $\sin k\psi$, $\psi \cos k\psi$, $\psi \sin k\psi$ on right and left, yields an infinite system of equations (11‴) for the coefficients a_k, b_k, c_k, d_k which can be solved in the manner of Eqs. (11). Use of the expansion (41) will be made in the study mentioned at the end of Sec. 4.

[27] The details (for Mathieu's equation) are given in Kotowski's paper. Kotowski also points out that there are certain exceptional cases. For instance, when a homogeneous Hill equation has a solution of the form $\sum C_k \cos k\psi$ but none of the form $\sum C_k \sin k\psi$, then the latter expression is admissible as forced response to an excitation $E(\psi) = \sin \psi$.

TORSION OF A CIRCULAR TUBE WITH LONGITUDINAL CIRCULAR HOLES*

BY

CHIH-BING LING

California Institute of Technology

Introduction. This paper presents a solution of St. Venant's torsion problem of a circular tube having a ring of uniformly distributed longitudinal circular holes of equal radii. The investigation of the stress distribution in such a tube is not only of theoretical interest but also of practical importance. The solution is found by constructing three series of harmonic functions which are invariant with respect to rotation about the axis of tube. The parametric coefficients attached to these functions are determined so as to satisfy the required boundary conditions. The case in which the central hole does not exist is also investigated. Finally, the solution is illustrated by working out several numerical examples.

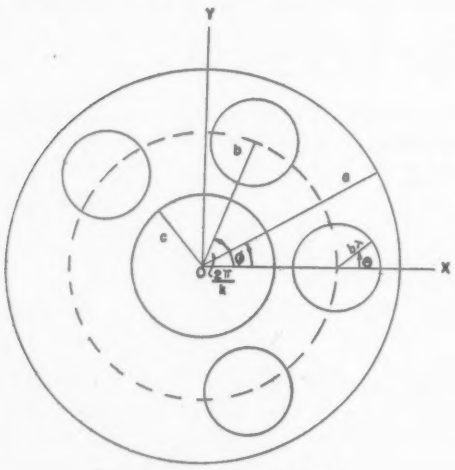

FIG. 1. Cross section of tube.

It may be mentioned that the torsion problem corresponding to the case without a central hole was solved by M. Kondo a few years ago by using the so-called stress distribution method.[1] The same method has been used by Th. v. Kármán with success to find the potential flow around an airship, but its application to the torsion problem by Kondo seems to result in great complication. In Kondo's paper, no formula for the torsional stiffness is given.

Method of solution. Consider a circular tube defined by the exterior and the interior radii a and c respectively. Let there be a ring of longitudinal circular holes parallel to axis of the tube, each of radius $b\lambda$ with their centers uniformly distributed over the circumference of a concentric circle of radius b at points represented in the Argand plane by

$$z = be^{2m\pi i/k}, \tag{1}$$

where b is the distance from the center of the tube to the center of any eccentric hole, k is the number of eccentric holes and $m = 0, 1, 2, \cdots (k-1)$; the origin being at the center of the tube. Fig. 1 shows the cross section of the tube.

Define the following two systems of polar coordinates

$$z = x + iy = are^{i\phi}, \qquad b\zeta = z - b = b\rho e^{i\theta}, \tag{2}$$

where ar, φ are polar coordinates referred to the center of the tube as origin and $b\rho$, θ

* Received Sept. 18, 1946.

[1] Masaiti Kondo, *The stresses in a twisted circular cylinder having circular holes.* Phil. Mag. (7) **22**, 1089–1108 (1936).

are polar coordinates referred to the center of one of the eccentric holes as origin, r, ρ being dimensionless. Also, for brevity, denote the ratios of the radii by

$$p = \frac{b}{a}, \qquad q = \frac{c}{a}, \qquad (q < p < 1) \tag{3}$$

where a is the radius of the exterior boundary of the tube and c is the radius of the central hole.

It is observed that the solution of St. Venant's torsion problem of the tube in question requires a harmonic function ψ, with its conjugate function single-valued, which satisfies the following three boundary conditions:

(1) on the exterior boundary of the tube where $|z| = a$

$$\Psi = \psi - (x^2 + y^2)/2 = 0; \tag{4}$$

(2) on the boundary of the central hole where $|z| = c$

$$\Psi = \text{const.} = a^2\Psi_1; \tag{5}$$

(3) on the boundaries of the ring of eccentric holes $\rho = \lambda$

$$\Psi = \text{const.} = a^2\Psi_2, \tag{6}$$

where $b\lambda$ is the radius of the eccentric hole under consideration, λ being a dimensionless quantity. Besides, by symmetry, the function ψ must be invariant with respect to rotation about the origin through angles $2m\pi/k$ and must be even with respect to the lines of symmetry.

Hence we write

$$\psi = \psi_1 + \psi_2 + \psi_3 \tag{7}$$

and construct

$$\begin{aligned} \psi_1 &= a^2 \sum_{n=0}^{\infty} A_n r^{nk} \cos nk\phi, \\ \psi_2 &= a^2 \sum_{n=1}^{\infty} \frac{B_n}{r^{nk}} \cos nk\phi, \\ \psi_3 &= a^2 \sum_{s=1}^{\infty} C_s U_s, \end{aligned} \tag{8}$$

where the quantities A, B and C are dimensionless parametric coefficients to be adjusted so as to satisfy the required boundary conditions. The class of harmonic functions U_s, first obtained by R. C. J. Howland[2] is defined by

$$\begin{aligned} W_0 &= U_0 - iV_0 = -\log (z^k - b^k), \\ W_s &= U_s - iV_s = \frac{b^s}{(s-1)!} \frac{d^s W_0}{db^s}. \end{aligned} \tag{9}$$

A brief account of these functions will be found in Appendix A. Note that in the last

[2] R. C. J. Howland, *Potential functions with periodicity in one coordinate*, Proc. Camb. Phil. Soc. **30**, 315–326 (1934).

Eq. (8) the function U_0 is rejected on the ground that it gives rise to a multi-valued conjugate function.

Now, to apply the first and the second boundary conditions, we first express ψ_3 in terms of the polar coordinates (r, ϕ) referring to the center of the tube as origin. The expansion of W_0 into a power series is different according as $|z|$ is greater or smaller than b. When $|z| > b$,

$$W_0 = -k \log z + \sum_{n=1}^{\infty} \frac{1}{n}\left(\frac{b}{z}\right)^{nk},$$

and when $|z| < b$,

$$W_0 = \pi i - k \log b + \sum_{n=1}^{\infty} \frac{1}{n}\left(\frac{z}{b}\right)^{nk}. \tag{10}$$

Differentiation gives

$$\begin{aligned} W_s &= k \sum_{n=1}^{\infty} \binom{nk-1}{s-1}\left(\frac{b}{z}\right)^{nk}, \\ W_s &= (-1)^s k \sum_{n=0}^{\infty} \binom{nk+s-1}{s-1}\left(\frac{z}{b}\right)^{nk}, \end{aligned} \tag{11}$$

respectively. It is noted that the binomial coefficient $\binom{n}{s}$ vanishes when $s > n$. Taking the real part and observing that $p = b/a$, we have

$$\begin{aligned} U_s &= k \sum_{n=1}^{\infty} \binom{nk-1}{s-1}\left(\frac{p}{r}\right)^{nk} \cos nk\phi, \\ U_s &= (-1)^s k \sum_{n=0}^{\infty} \binom{nk+s-1}{s-1}\left(\frac{r}{p}\right)^{nk} \cos nk\phi. \end{aligned} \tag{12}$$

Hence the last Eq. (8) becomes

$$\left.\begin{aligned} \psi_3 &= a^2 \sum_{n=1}^{\infty} \frac{P_n}{r^{nk}} \cos nk\phi, \quad \text{when } |z| > b \\ \psi_3 &= a^2 \sum_{n=0}^{\infty} Q_n r^{nk} \cos nk\phi, \quad \text{when } |z| < b \end{aligned}\right\} \tag{13}$$

where

$$\begin{aligned} P_n &= k p^{nk} \sum_{s=1}^{nk} \binom{nk-1}{s-1} C_s, \\ Q_n &= \frac{k}{p^{nk}} \sum_{s=1}^{\infty} (-1)^s \binom{nk+s-1}{s-1} C_s. \end{aligned} \tag{14}$$

Applying the boundary condition (4) at $|z| = a$ or $r = 1$ and using the first series for ψ_3, we find

$$0 = A_0 - \frac{1}{2} + \sum_{n=1}^{\infty} (A_n + B_n + P_n) \cos nk\phi.$$

This relation is satisfied, provided that the coefficient of each term vanishes identically, i.e., that

$$A_0 - \tfrac{1}{2} = 0, \qquad A_n + B_n + P_n = 0. \tag{15}$$

Applying the boundary condition (5) at $|z| = c$ or $r = q$ and using the second series for ψ_2, we obtain

$$\Psi_1 = A_0 + Q_0 - q^2/2 + \sum_{n=1}^{\infty} (A_n q^{nk} + B_n/q^{nk} + Q_n q^{nk}) \cos nk\phi.$$

Equating the constants from both sides and setting each coefficient equal to zero, we find

$$A_0 + Q_0 - q^2/2 = \Psi_1, \qquad A_n q^{nk} + B_n/q^{nk} + Q_n q^{nk} = 0. \tag{16}$$

To apply the third boundary condition, we first transform Ψ in terms of the polar coordinates (ρ, θ) referring to the center at $(x, y) = (b, 0)$ as origin. Thus,

$$x^2 + y^2 = b^2(1 + \rho^2 + 2\rho \cos \theta)$$

and

$$r^{nk} \cos nk\phi = R(z/a)^{nk} = p^{nk} R(1 + \rho e^{i\theta})^{nk} = p^{nk} \sum_{m=0}^{nk} \binom{nk}{m} \rho^m \cos m\theta,$$

$$\frac{\cos nk\phi}{r^{nk}} = R\left(\frac{a}{z}\right)^{nk} = \frac{1}{p^{nk}} R(1 + \rho e^{i\theta})^{-nk} \tag{17}$$

$$= \frac{1}{p^{nk}} \sum_{m=0}^{\infty} (-1)^m \binom{nk + m - 1}{m} \rho^m \cos m\theta.$$

Consequently, the first two Eq. (8) become

$$\psi_1 = a^2 \sum_{m=0}^{\infty} M_m \rho^m \cos m\theta, \qquad \psi_2 = a^2 \sum_{m=0}^{\infty} N_m \rho^m \cos m\theta, \tag{18}$$

where

$$M_m = \sum_{n=0}^{\infty} \binom{nk}{m} p^{nk} A_n, \quad N_m = (-1)^m \sum_{n=1}^{\infty} \binom{nk + m - 1}{m} B_n/p^{nk}. \tag{19}$$

Again, according to Appendix A, Eq. (A.12),

$$U_s = \cos s\theta/\rho^s + \sum_{n=0}^{\infty} (-1)^n {}^n\alpha_s \rho^n \cos n\theta.$$

Thus,

$$\psi_2 = a^2 \left\{ L_0 + \sum_{m=1}^{\infty} (C_m/\rho^m + L_m \rho^m) \cos m\theta \right\}, \tag{20}$$

where

$$L_m = (-1)^m \sum_{s=1}^{\infty} {}^m\alpha_s C_s. \tag{21}$$

Applying the boundary condition (6) at $\rho=\lambda$, we obtain

$$\Psi_2 = M_0 + N_0 + L_0 - p^2(1+\lambda^2)/2 - p^2\lambda\cos\theta + \sum_{m=1}^{\infty}(M_m\lambda^m + N_m\lambda^m + C_m/\lambda^m + L_m\lambda^m)\cos m\theta.$$

Equating the constants and setting each coefficient equal to zero, we find

$$\begin{aligned} M_0 + N_0 + L_0 - p^2(1+\lambda^2)/2 &= \Psi_2, \\ M_1\lambda + N_1\lambda + C_1/\lambda + L_1\lambda - p^2\lambda &= 0, \\ M_m\lambda^m + N_m\lambda^m + C_m/\lambda^m + L_m\lambda^m &= 0. \end{aligned} \tag{22}$$

From the first Eqs. (15), (16) and (22), we see that

$$A_0 = 1/2, \quad \Psi_1 = Q_0 + (1-q^2)/2, \quad \Psi_2 = M_0 + N_0 + L_0 - p^2(1+\lambda^2)/2 \tag{23}$$

Ψ_1 and Ψ_2 are thus determined, if the parametric coefficients can be found. The system of simultaneous linear equations represented by the other equations is just sufficient for the determination of all parametric coefficients involved. They may be rewritten as follows:

$$\begin{aligned} A_n + B_n + P_n &= 0, \qquad A_n + q^{-2nk}B_n + Q_n = 0, \\ \lambda^{-2}C_1 + M_1 + N_1 + L_1 &= p^2, \qquad \lambda^{-2m}C_m + M_m + N_m + L_m = 0. \end{aligned} \tag{24}$$

The first two equations give, for $n \geqq 1$,

$$A_n = (q^{2nk}Q_n - P_n)/(1-q^{2nk}), \qquad B_n = q^{2nk}(P_n - Q_n)/(1-q^{2nk}). \tag{25}$$

Substituting these values into M_n and N_n in the last two equations, we find with the aid of (19), (14) and (21)

$$C_1 = p^2\lambda^2 + \lambda^2\sum_{s=1}^{\infty}\beta_s C_s, \qquad C_m = \lambda^{2m}\sum_{s=1}^{\infty}{}^m\beta_s C_s, \tag{26}$$

where, in general,

$$\begin{aligned} {}^m\beta_s = &-(-1)^m\,{}^m\alpha_s \\ &+ k\sum_{n=1}^{\infty}\left\{\frac{p^{2nk}}{1-q^{2nk}}\binom{nk}{m}\left[\binom{nk-1}{s-1} - (-1)^s\left(\frac{q}{p}\right)^{2nk}\binom{nk+s-1}{s-1}\right]\right. \\ &\left. + \frac{(-1)^m q^{2nk}}{(1-q^{2nk})p^{2nk}}\binom{nk+m-1}{m}\left[(-1)^s\binom{nk+s-1}{s-1} - p^{2nk}\binom{nk-1}{s-1}\right]\right\}. \end{aligned} \tag{27}$$

This system of linear equations can be solved by successive approximations as follows. Write

$$C_m = \sum_{t=0}^{\infty} C_m^{(t)}, \tag{28}$$

where

$$C_1^{(0)} = p^2\lambda^2, \qquad C_m^{(0)} = 0,$$

and, by iteration,

$$C_m^{(t)} = \lambda^{2m} \sum_{s=1}^{\infty} {}^m\beta_s C_s^{(t-1)}. \tag{29}$$

With the values of C_m thus found, the coefficients A_n and B_n can be obtained without difficulty from (25) with the aid of (14).

It is to be observed that the validity of the solution by successive approximations depends upon the convergence of the series (28). From physical considerations alone, it seems likely that there will be convergence as long as the boundaries do not overlap, i.e.,

$$q + p\lambda < p < 1 - p\lambda, \qquad \lambda < \sin(\pi/k). \tag{30}$$

To establish convergence of such a series analytically is usually difficult. However, we may proceed by first using some inequalities for the coefficients so that the series (29) can be summed, and then applying the ratio test to ascertain the range of convergence. Obviously some convergence is lost in thus using the inequalities, but it is often possible to establish a considerable range of convergence in this way. In the interest of brevity, no details will be given here.

Torsional stiffness. The torsional stiffness of the tube is given by

$$H = 2\iint \Psi dxdy + 2\pi c^2 a^2 \Psi_1 + 2k\pi\lambda^2 b^2 a^2 \Psi_2, \tag{31}$$

where the double integration is extended over the entire cross-sectional area of the tube, excluding the holes. Let

$$H_j = 2\iint \psi_j dxdy, \quad (j = 1, 2, 3), \qquad H_4 = \iint (x^2 + y^2)dxdy.$$

Then,

$$2\iint \Psi dxdy = H_1 + H_2 + H_3 - H_4. \tag{32}$$

These integrals, save H_3, can be evaluated by ordinary methods of integration without difficulty. The following results are obtained:

$$H_1 = \pi a^4(1 - q^2 - kp^2\lambda^2), \qquad H_2 = 0, \tag{33}$$

$$H_4 = \pi a^4\{1 - q^4 - kp^4\lambda^2(2 + \lambda^2)\}/2.$$

The integration of H_3 by ordinary methods fails since there exist singularities at the centers of the eccentric holes. However, H_3 can be evaluated by using the following relation derived from Green's theorem, in which F is a function of the complex variable z regular in the domain S enclosed by a contour C.

$$\iint_S \frac{dF}{dz} dS = \frac{1}{2} i \int_C F d\bar{z}, \tag{34}$$

the contour C being taken in a counter-clockwise direction. In this equation set $W_3 = dF/dz$, so that

$$F = \int^{z} W_s dz, \tag{35}$$

and let the contour C be taken around the sector of $1/2k$ of the cross section, as shown in Fig. 2. Then

$$\iint U_s dxdy = 2kR \iint_S W_s dS = kRi \int_C F d\bar{z}. \tag{36}$$

Using the appropriate series of W_s in different parts of the contour, we find that this integral vanishes identically for all values of s except for $s=1$. The term arising from $1/\zeta$ in W_1 does not vanish when the integration is taken along the semicircle $\rho=\lambda$. Here

$$F = \int \frac{dz}{\zeta} = b \log \zeta,$$

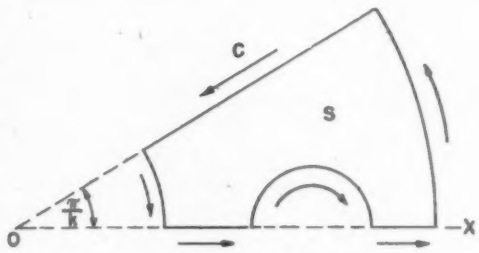

FIG. 2. Contour C of $1/2k$ of section.

and when $\rho=\lambda$,

$$F = b(\log \lambda + i\theta), \qquad d\bar{z} = b\lambda de^{-i\theta}.$$

We thus find

$$\int_{\pi}^{0} F d\bar{z} = b^2\lambda(2 + 2 \log \lambda + i\pi).$$

Hence,

$$\iint U_1 dxdy = -\pi k\lambda b^2, \tag{37}$$

and consequently,

$$H_2 = 2a^2 \sum_{s=1}^{\infty} C_s \iint U_s dxdy = -2\pi k\lambda b^2 a^2 C_1. \tag{38}$$

Summing up, we find the torsional stiffness

$$H = \pi a^4 \{(1-q^2)^2 + kp^4\lambda^2(2+\lambda^2) - 2kp^2\lambda(2C_1+\lambda) + 4q^2\Psi_1 + 4kp^2\lambda^2\Psi_2\}/2. \tag{39}$$

The resulting twisting couple is given by

$$T = \mu\tau H, \tag{40}$$

where μ is the modulus of rigidity of the material and τ is the angle of twist per unit length of the tube.

Stress components. The non-vanishing stress components of the tube are two shear stress components given in terms of the polar coordinates (r, ϕ) by the following

$$z_r = \frac{\mu\tau}{ar} \frac{\partial\Psi}{\partial\phi}, \qquad z_\phi = -\frac{\mu\tau}{a} \frac{\partial\Psi}{\partial r}, \tag{41}$$

while in terms of the polar coordinates (ρ, θ), they are

$$z_\rho = \frac{\mu\tau}{b\rho}\frac{\partial\Psi}{\partial\theta}, \qquad z_\theta = -\frac{\mu\tau}{b}\frac{\partial\Psi}{\partial\rho}. \tag{42}$$

It is now a straightforward matter to find the stress at any point of the cross section. By using appropriate series, the shear stresses on the three boundaries are found as follows:

$$\begin{aligned}
[z_\phi]_{r=1} &= \mu\tau a\left(1 - 2k\sum_{n=1}^{\infty} nA_n \cos nk\phi\right),\\
[z_\theta]_{\rho=\lambda} &= \mu\tau a\left(p\lambda + \frac{2}{p\lambda}\sum_{m=1}^{\infty}\frac{mC_m}{\lambda^m}\cos m\theta\right),\\
[z_\phi]_{r=q} &= \mu\tau a\left(q + \frac{2k}{q}\sum_{n=1}^{\infty}\frac{nB_n}{q^{nk}}\cos nk\phi\right).
\end{aligned} \tag{43}$$

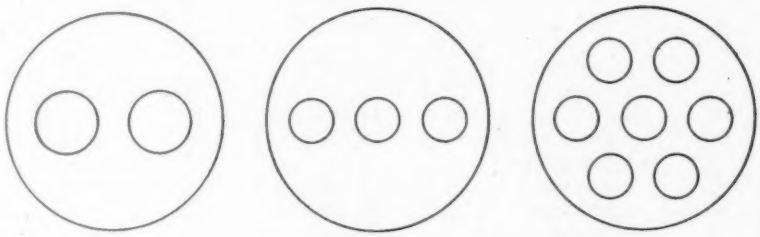

FIG. 3. Illustrative examples.

The maximum shear stress occurs on the boundary across the narrowest sections. Due to the presence of the holes, the greatest shear stress does not necessarily occur on the exterior boundary.

The case without central hole. It is interesting to investigate also the case in which the central hole of the tube does not exist. A solution is obtained for ψ by merely omitting ψ_2 in Eq. (7), such that

$$\psi = \psi_1 + \psi_3. \tag{44}$$

Consequently, the relations obtained from the boundary conditions become

$$A_0 = \tfrac{1}{2}, \qquad \Psi_2 = M_0 + L_0 - \tfrac{1}{2}p^2(1 + \lambda^2), \tag{45}$$

$$A_n = -P_n, \qquad \lambda^{-2}C_1 + M_1 + L_1 = p^2, \qquad \lambda^{-2m}C_m + M_m + L_m = 0,$$

so that the coefficient in (27) is simplified to

$${}^m\beta_s = -(-1)^m\,{}^m\alpha_s + k\sum_{n=1}^{\infty}\binom{nk}{m}\binom{nk-1}{s-1}p^{2nk}. \tag{46}$$

Numerical examples. The foregoing method of solution will be illustrated by working out the following three examples:

Case	k	p	q	λ	No. of Holes
I	2	$\frac{3}{7}$	0	$\frac{2}{3}$	2
II	2	$\frac{3}{5}$	$\frac{1}{5}$	$\frac{1}{3}$	3
III	6	$\frac{3}{5}$	$\frac{1}{5}$	$\frac{1}{3}$	7

The arrangements are shown in Fig. 3. In each case the holes have equal radii and the nearest distance between any two adjacent boundaries is equal to the radius of one hole. These cases probably represent the most crucial ones ever met in practice. Tables of the coefficients ${}^m\beta_s$ are first prepared, with which the parametric coefficients C_m are found by the method of successive approximations; the results being shown in Appendix B and in the accompanying Table I. The shear stresses along the boundaries are then computed and shown in Table II. Fig. 4 shows the results diagrammatically.

TABLE I. The coefficients C_m

m	Case I	Case II	Case III
1	7.8560×10^{-2}	4.2392×10^{-2}	3.0593×10^{-2}
2	3.1549×10^{-3}	3.1240×10^{-4}	5.8718×10^{-4}
3	-3.0714×10^{-4}	1.9115×10^{-5}	4.9273×10^{-5}
4	9.6791×10^{-5}	3.2509×10^{-7}	-7.4587×10^{-6}
5	-1.7036×10^{-5}	1.8686×10^{-7}	4.9622×10^{-7}
6	3.9811×10^{-6}	-1.2587×10^{-8}	5.9963×10^{-8}
7	-8.0836×10^{-7}	2.5340×10^{-9}	-1.0635×10^{-8}
8	1.7422×10^{-7}	-2.7810×10^{-10}	4.7674×10^{-10}

TABLE II. Shear stress/$\mu\tau a$ along boundaries.

$k\phi$ or θ	Case I		Case II			Case III		
	Exterior boundary	Eccentric holes	Exterior boundary	Eccentric holes	Central hole	Exterior boundary	Eccentric holes	Central hole
0	1.185	1.194	1.308	1.547	0.459	1.127	1.247	0.214
30°	1.125	1.049	1.124	1.327	0.402	1.105	1.053	0.212
60°	1.022	0.660	0.967	0.793	0.277	1.050	0.583	0.207
90°	0.956	0.198	0.930	0.145	0.160	0.988	0.068	0.200
120°	0.928	−0.199	0.928	−0.451	0.081	0.938	−0.259	0.193
150°	0.918	−0.396	0.931	−0.871	0.039	0.907	−0.529	0.188
180°	0.916	−0.392	0.932	−1.033	0.026	0.897	−0.678	0.186

It appears that in all the cases the greatest shear stress occurs at those points on the boundaries of the holes which are nearest to the exterior boundary. The magnitudes are equal to 1.194, 1.547 and 1.247 respectively except for a factor $\mu\tau a$. The points of greatest shear stress will, however, shift to the exterior boundary if the eccentric holes are sufficiently remote from the exterior boundary. It is seen that in each case there exist two null points or points of zero stress on the boundary of each hole at an angle θ numerically between 90° and 120° or, to be more precise, at 105°,

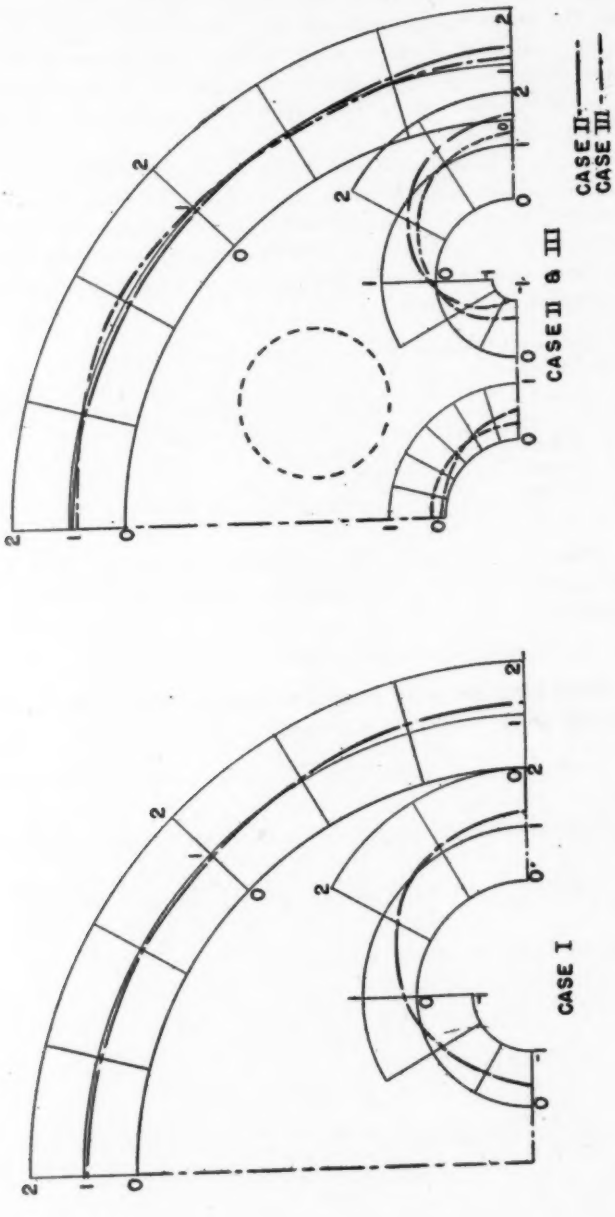

FIG. 4. Shear stress/$\mu\tau a$ along boundaries.

96° and 95° respectively. It is also seen that due to the presence of holes the maximum shear stress on the exterior boundary is increased by 18.5%, 30.8% and 12.7% respectively. From the stress distribution on the boundaries it appears that among the three cases the case II is the most unfavorable arrangement in which, it is recalled, the centers of the holes are situated collinearly on the same diameter of the section. The stress distribution on the boundary of the central hole is less important since the magnitude is smaller.

Table III shows the cross-sectional area A and the torsional stiffness H of the tube, in which the last two columns indicate their percentage reductions due to the presence of holes respectively. The relative reductions in torsion stiffness due to 1% reduction in area are equal to 0.729%, 1.589% and 0.963% respectively. Again, it appears that the case II is the most unfavorable arrangement among the three where the effectiveness of torsion modulus is concerned.

TABLE III. Cross-sectional area A and torsional stiffness H.

Case	$A/\pi a^2$	$H/\frac{1}{2}\pi a^4$	% reduction of A	% reduction of H
I	0.8367	0.8809	16.33	11.91
II	0.8800	0.8093	12.00	19.07
III	0.7200	0.7305	28.00	26.95

The author wishes to express his deep appreciation to Dr. H. S. Tsien of the Guggenheim Aeronautical Laboratory, California Institute of Technology, for helpful criticism and suggestions.

APPENDIX A

Class of functions invariant with respect to rotation. Let there be on the circle $|z| = b$ in the Argand plane a series of k points

$$z = be^{2m\pi i/k}, \tag{A.1}$$

where $m = 0, 1, 2, \cdots, (k-1)$.

A function with a logarithmic singularity at each such point is defined by

$$W_0 = -\log (z^k - b^k) = -\log (z - b) - \sum_{m=1}^{k-1} \log (z - be^{2m\pi i/k}). \tag{A.2}$$

Writing $z - b = b\zeta$, we have except for a constant

$$W_0 = -\log \zeta - \sum_{m=1}^{k-1} \log (1 - u_m\zeta), \tag{A.3}$$

where

$$1/u_m = 1 - e^{2m\pi i/k},$$

such that u_m is a root of the equation

$$(u - 1)^k - u^k = 0. \tag{A.4}$$

Expansion yields

$$W_0 = -\log \zeta + \sum_{n=1}^{\infty} (-1)^n {}^n\alpha_0 \zeta^n, \tag{A.5}$$

where

$$ {}^{n}\alpha_0 = \frac{1}{n}\sum_{m=1}^{k-1} u_m^n = \sigma_n/n, $$

σ_n denoting the sum of the nth power of the roots of Eq. (A.4), which may be calculated for any given values of k and n.

It is readily shown that functions derived from Eq. (A.2) by differentiation with respect to b are invariant with respect to rotation about the origin through angles $2m\pi/k$. If we define

$$ W_s = \frac{b^s}{(s-1)!}\frac{d^s W_0}{db^s}, \tag{A.7} $$

we find

$$ W_s = \frac{1}{\zeta^s} + \sum_{m=1}^{k-1}\frac{(1-u_m^{-1})^s}{(u_m^{-1}+\zeta)^s} = \frac{1}{\zeta^s} + \sum_{m=1}^{k-1}(u_m-1)^s\sum_{n=0}^{\infty}(-1)^n\binom{n+s-1}{n}(u_m\zeta)^n, $$

or

$$ W_s = \frac{1}{\zeta^s} + \sum_{n=0}^{\infty}(-1)^n\,{}^{n}\alpha_s\zeta^n, \tag{A.8} $$

where

$$ \begin{aligned} {}^{n}\alpha_s &= \binom{n+s-1}{n}\sum_{m=1}^{k-1}(u_m-1)^s u_m^n = \binom{n+s-1}{n}\sum_{t=0}^{s}(-1)^t\binom{s}{t}\sigma_{n+s-t} \\ &= \binom{n+s-1}{n}\Delta^s\sigma_n, \end{aligned} \tag{A.9} $$

$\Delta^s\sigma_n$ being the sth finite difference of the series $\sigma_n, \sigma_{n+1}, \sigma_{n+2}, \cdots$. From Eq. (A.4) we obtain

$$ u^{n+mk} = \sum_{t=0}^{mk}(-1)^t\binom{mk}{t}u^{n+mk-t}, $$

where m is an integer. Summing over the roots,

$$ \sigma_{n+mk} = \sum_{t=0}^{mk}(-1)^t\binom{mk}{t}\sigma_{n+mk-t} = \Delta^{mk}\sigma_n. $$

Hence

$$ \Delta^{mk+s}\sigma_n = \Delta^s\Delta^{mk}\sigma_n = \Delta^s\sigma_{n+mk}, \tag{A.10} $$

so that all the coefficients can be found from the values of σ_n and its first $(k-1)$th finite differences.

Now, if we define

$$ W_0 = U_0 - iV_0, \qquad W_s = U_s - iV_s \tag{A.11} $$

and $\zeta = \rho e^{i\theta}$, we find by equating the real and imaginary parts

$$
\begin{aligned}
U_0 &= -\log\rho + \sum_{n=1}^{\infty}(-1)^n\,{}^n\alpha_0\rho^n\cos n\theta \\
V_0 &= \theta - \sum_{n=1}^{\infty}(-1)^n\,{}^n\alpha_0\rho^n\sin n\theta, \\
U_s &= \frac{\cos s\theta}{\rho^s} + \sum_{n=0}^{\infty}(-1)^n\,{}^n\alpha_s\rho^n\cos n\theta \\
V_s &= \frac{\sin s\theta}{\rho^s} = \sum_{n=1}^{\infty}(-1)^n\,{}^n\alpha_s\rho^n\sin n\theta.
\end{aligned}
\tag{A.12}
$$

APPENDIX B. TABLES OF COEFFICIENTS ${}^m\beta_s$

CASE I. $k=2$, $p=3/7$, $q=0$

s	$m=1$	$m=2$	$m=3$	$m=4$
1	-1.0547×10^{-1}	2.0736×10^{-1}	-5.1703×10^{-2}	3.4879×10^{-2}
2	4.1472×10^{-1}	-7.2751×10^{-2}	1.6111×10^{-1}	-6.4085×10^{-2}
3	-1.5511×10^{-1}	2.4167×10^{-1}	-1.1142×10^{-1}	1.4009×10^{-1}
4	1.3952×10^{-1}	-1.2817×10^{-1}	1.8679×10^{-1}	-1.1476×10^{-1}
5	-7.4973×10^{-2}	1.2605×10^{-1}	-1.2240×10^{-1}	1.5170×10^{-1}
6	4.7899×10^{-2}	-7.8758×10^{-2}	1.1563×10^{-1}	-1.1495×10^{-1}
7	-2.7106×10^{-2}	5.5633×10^{-2}	-7.7962×10^{-2}	1.0623×10^{-1}
8	1.5692×10^{-2}	-3.4860×10^{-2}	5.9407×10^{-2}	-7.9025×10^{-2}
s	$m=5$	$m=6$	$m=7$	$m=8$
1	-1.4995×10^{-2}	7.9832×10^{-3}	-3.8723×10^{-3}	1.9615×10^{-3}
2	5.0421×10^{-2}	-2.6253×10^{-2}	1.5891×10^{-2}	-8.7149×10^{-3}
3	-7.3439×10^{-2}	5.7816×10^{-2}	-3.4184×10^{-2}	2.2278×10^{-2}
4	1.1797×10^{-1}	-7.8946×10^{-2}	5.5966×10^{-2}	-3.9978×10^{-2}
5	-1.1196×10^{-1}	1.0893×10^{-1}	-7.7443×10^{-2}	6.1346×10^{-2}
6	1.3072×10^{-1}	-1.0718×10^{-1}	1.0010×10^{-1}	-7.7385×10^{-2}
7	-1.0842×10^{-1}	1.1678×10^{-1}	-1.0180×10^{-1}	9.3473×10^{-2}
8	9.8847×10^{-2}	-1.0237×10^{-1}	1.0703×10^{-1}	-9.6648×10^{-2}

CASE II. $k=2$, $p=3/5$, $q=1/5$

s	$m=1$	$m=2$	$m=3$	$m=4$
1	4.9867×10^{-1}	5.8617×10^{-1}	3.2014×10^{-1}	4.0272×10^{-2}
2	1.1751	1.3668	9.7830×10^{-1}	1.2483
3	9.6041×10^{-1}	1.4633	2.9506	1.7326
4	1.6086×10^{-1}	2.4953	2.3101	6.1916
5	1.2869	4.4025×10^{-1}	5.6549	4.1153
6	-9.9512×10^{-1}	3.1571	9.7328×10^{-1}	1.2122×10
7	2.0139	−1.6578	7.6527	2.5465
8	−2.3208	4.4190	−2.9699	1.7278×10

s	$m=5$	$m=6$	$m=7$	$m=8$
1	2.5737×10^{-1}	-1.6585×10^{-1}	2.8770×10^{-1}	-2.9011×10^{-1}
2	1.7611×10^{-1}	1.0524	-4.6363×10^{-1}	1.1047
3	3.3929	4.8664×10^{-1}	3.3914	-1.1137
4	3.2923	8.0811	1.4551	8.6392
5	1.2917×10	6.6271	1.8327×10	4.0214
6	7.9600	2.6963×10	9.7852	4.0734×10
7	2.5212×10	1.6097×10	5.6595×10	2.9178×10
8	7.3042	7.4312×10	2.6870×10	1.1962×10^{2}

CASE III. $k=6$, $p=3/5$, $q=1/5$

s	$m=1$	$m=2$	$m=3$	$m=4$
1	-2.8379	1.6559	1.0945	-1.7600
2	3.3118	-5.8522	5.9408	5.8842
3	3.2836	8.9112	-1.7916×10	1.8392×10
4	-7.0400	1.1769×10	2.4523×10	-6.6469×10
5	5.6284	-2.8311×10	3.8057×10	7.6789×10
6	6.0363	2.2409×10	-1.0871×10^{2}	1.3393×10^{2}
7	-1.3620×10	2.8477×10	8.8391×10	-4.1222×10^{2}
8	7.9354	-7.0520×10	1.2148×10^{2}	3.4151×10^{2}

s	$m=5$	$m=6$	$m=7$	$m=8$
1	1.1569	1.0060	-1.9457	9.9193×10^{-1}
2	-1.1324×10	7.4698	8.1366	-1.7630×10
3	2.2834×10	-5.4335×10	3.7881×10	4.5598×10
4	6.1432×10	8.9290×10	-2.3555×10^{2}	1.7075×10^{2}
5	-2.4343×10^{2}	2.2150×10^{2}	3.4389×10^{2}	-9.8099×10^{2}
6	2.6581×10^{2}	-9.0308×10^{2}	8.1328×10^{2}	1.3199×10^{3}
7	4.8145×10^{2}	9.4883×10^{2}	-3.3856×10^{3}	3.0419×10^{3}
8	-1.5696×10^{3}	1.7598×10^{3}	3.4764×10^{3}	-1.2761×10^{4}

ANALYSIS OF THE TURBULENT BOUNDARY LAYER FOR ADVERSE PRESSURE GRADIENTS INVOLVING SEPARATION*

BY

W. S. COLEMAN

Research Department, Blackburn Aircraft

PART 1.

1. Introduction. In a recent paper by von Doenhoff and Tetervin,[1] and subsequently in another by Garner,[2] a new differential equation of an empirical character has been advanced, whereby the analysis of turbulent boundary layer development, and the prediction of turbulent separation, are greatly facilitated. The present paper deals with the problem theoretically, and, from considerations of the fundamental equations of motion, establishes an analogous expression which, though analytically different from that proposed by the above authors, contains the same parameters. It is further shown how this equation may be solved numerically by an approximate method of a rather complex character.

On comparing results with those obtained from the empirical relations, it appears that there is good agreement when the pressure gradient is small, but that discrepancies are more serious for larger gradients tending to separation. In this respect there is a notable divergence between the results given by von Doenhoff's formula on the one hand, and that of Garner on the other, the former being appreciably smaller at values of H in the region of separation. It appears, however, that Garner's relation involves the three basic parameters of the theoretical equation, whereas, in the case of von Doenhoff and Tetervin, only two are apparent. There is reason to think, therefore, that Garner's treatment may be the more reliable, a conclusion which is supported by the theoretical calculations, in that they are in very much better agreement with Garner's predictions than with those of von Doenhoff and Tetervin. Nevertheless, despite the above discrepancies, step-by-step integration of the empirical equations, in conjunction with the momentum equation, leads to estimates of the boundary layer characteristics in good agreement with experiment, so that the errors appear to be less important in the final result.

So far as the theoretical treatment is concerned, it would seem of value in establishing the essential parameters associated with the new equation, but for ease and rapidity of calculation in practical cases the empirical approach may prove more attractive.

We shall now proceed to elaborate the fundamental arguments leading to the equation concerned.

---

* Received March 22, 1946.

[1] A. E. von Doenhoff and N. Tetervin, *Determination of general relations for the behaviour of turbulent boundary layers*, Nat. Ad. Comm. for Aeron. confidential report No. 3G13 (1943). Also reprinted by Aeron. Res. Comm., Report 6845, F.M.597, Ae. 2255 (1943).

[2] H. C. Garner, *The development of turbulent boundary layers*, Aeron. Res. Comm., Report 7814, F.M. 705 (1944).

2. Equations of fully developed, turbulent flow. The Reynolds equations[3] of turbulent motion in a two dimensional field of incompressible, viscous flow take the well known form

$$\frac{D\bar{u}}{Dt} = \frac{1}{\rho}\left[\frac{\partial}{\partial x}(\bar{p}_{xx} - \rho\overline{uu'}) + \frac{\partial}{\partial y}(\bar{p}_{yx} - \rho\overline{u'v'})\right], \tag{2.1}$$

$$\frac{D\bar{v}}{Dt} = \frac{1}{\rho}\left[\frac{\partial}{\partial x}(\bar{p}_{xy} - \rho\overline{u'v'}) + \frac{\partial}{\partial y}(\bar{p}_{yy} - \rho\overline{v'v'})\right]. \tag{2.2}$$

There is also the equation of continuity,

$$\frac{\partial\bar{u}}{\partial x} + \frac{\partial\bar{v}}{\partial y} = 0, \tag{2.3}$$

where bars denote temporal mean values and primes the fluctuating components.

Adopting Boussinesq's procedure[4] of representing the Reynolds stresses $\rho\overline{u'u'}$, $\rho\overline{v'v'}$, $\rho\overline{u'v'}$ by an apparent increase of viscosity, we replace the natural coefficient of viscosity μ by $(\mu+\rho\epsilon)$, where ϵ is the measure of the momentum interchange due to turbulence, and must therefore be considered to vary with respect to the space co-ordinates. The Reynolds stresses are further treated in exactly the manner prescribed by the general theory of stress. Accordingly,

$$\left.\begin{aligned} \bar{p}_{xx} - \rho\overline{u'u'} &= -\bar{p} + 2(\mu+\rho\epsilon)\frac{\partial\bar{u}}{\partial x} \\ \bar{p}_{yy} - \rho\overline{v'v'} &= -\bar{p} + 2(\mu+\rho\epsilon)\frac{\partial v}{\partial y} \\ \bar{p}_{xy} - \rho\overline{u'v'} = \bar{p}_{yx} - \rho\overline{u'v'} &= (\mu+\rho\epsilon)\left(\frac{\partial\bar{v}}{\partial x} + \frac{\partial\bar{u}}{\partial y}\right) \end{aligned}\right\}. \tag{2.4}$$

and Eqs. (2.1), (2.2) become

$$\frac{D\bar{u}}{Dt} = -\frac{1}{\rho}\frac{\partial\bar{p}}{\partial x} + (\nu+\epsilon)\nabla^2\bar{u} + 2\frac{\partial\epsilon}{\partial x}\frac{\partial\bar{u}}{\partial x} + \frac{\partial\epsilon}{\partial y}\left(\frac{\partial\bar{v}}{\partial x} + \frac{\partial\bar{u}}{\partial y}\right), \tag{2.5}$$

$$\frac{D\bar{v}}{Dt} = -\frac{1}{\rho}\frac{\partial\bar{p}}{\partial y} + (\nu+\epsilon)\nabla^2\bar{v} + 2\frac{\partial\epsilon}{\partial y}\frac{\partial\bar{v}}{\partial y} + \frac{\partial\epsilon}{\partial x}\left(\frac{\partial\bar{v}}{\partial x} + \frac{\partial\bar{u}}{\partial y}\right), \tag{2.6}$$

whence the bars denoting mean quantities are no longer necessary, and will therefore be omitted in what follows.

3. Curved flow. Intrinsic form of the equations. Equations (2.5), (2.6) will now be referred to the curvilinear co-ordinates of Fig. 1. Let AB be a segment of any streamline of the mean flow, and let PN be the orthogonal curve through the point P on the streamline where the resultant velocity is q. Let ds, dn be elements of arc of AB and PN respectively, and finally, let θ be the angle the tangent to PN at P makes with the axis of X.

[3] O. Reynolds, *On the dynamical theory of incompressible viscuous fluids and the determination of the criterion*, Phil. Trans. (A) **186**, 123–164 (1895).

[4] T. V. Boussinesq, *Essai sur la théorie des eaux courantes*, Mém. Sav. Étrang. **23**, No. 1 (1877).

Then

$$u = -q\sin\theta, \qquad v = q\cos\theta;$$

$$\frac{\partial}{\partial x} = -\sin\theta\frac{\partial}{\partial s} + \cos\theta\frac{\partial}{\partial n}, \qquad \frac{\partial}{\partial y} = \cos\theta\frac{\partial}{\partial s} + \sin\theta\frac{\partial}{\partial n};$$

$$\nabla^2 = \frac{\partial^2}{\partial s^2} - \frac{\partial\theta}{\partial n}\frac{\partial}{\partial s} + \frac{\partial\theta}{\partial s}\frac{\partial}{\partial n} + \frac{\partial^2}{\partial n^2},$$

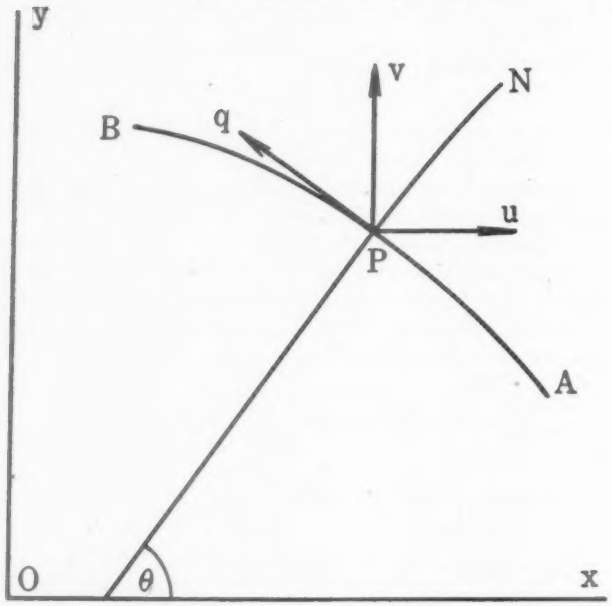

FIG. 1.

and the equations of motion for steady flow take the form

$$q\frac{\partial q}{\partial s} = -\frac{1}{\rho}\frac{\partial p}{\partial s} + (\nu+\epsilon)\left[\frac{\partial^2 q}{\partial s^2} - \frac{\partial q}{\partial s}\frac{\partial\theta}{\partial n} - q\left\{\left(\frac{\partial\theta}{\partial s}\right)^2 + \left(\frac{\partial\theta}{\partial n}\right)^2\right\} + \frac{\partial q}{\partial n}\frac{\partial\theta}{\partial s} + \frac{\partial^2 q}{\partial n^2}\right]$$
$$+ 2\frac{\partial\epsilon}{\partial s}\frac{\partial q}{\partial s} + \frac{\partial\epsilon}{\partial n}\left(\frac{\partial q}{\partial n} - q\frac{\partial\theta}{\partial s}\right), \tag{3.1}$$

$$q^2\frac{\partial\theta}{\partial s} = \frac{1}{\rho}\frac{\partial p}{\partial n} + (\nu+\epsilon)\left[2\frac{\partial q}{\partial s}\frac{\partial\theta}{\partial s} + q\left\{\frac{\partial^2\theta}{\partial s^2} + \frac{\partial^2\theta}{\partial n^2}\right\} + 2\frac{\partial q}{\partial n}\frac{\partial\theta}{\partial n}\right]$$
$$+ 2q\frac{\partial\epsilon}{\partial n}\frac{\partial\theta}{\partial n} - \frac{\partial\epsilon}{\partial s}\left(\frac{\partial q}{\partial n} - q\frac{\partial\theta}{\partial s}\right); \tag{3.2}$$

whilst the equation of continuity leads to

$$\frac{\partial q}{\partial s} - q\frac{\partial\theta}{\partial n} = 0. \tag{3.3}$$

4. Application to the boundary layer. Integral equation for θ. In applying the equations of motion to the boundary layer, we make the usual assumptions that

(a) the fluid is of small viscosity;

(b) the boundary layer thickness δ is small, $O(\nu^{1/5})$;*

(c) the curvatures $\partial\theta/\partial s$, $\partial\theta/\partial n$ are nowhere large, $O(\nu^{-1/2})$.

Then, with the usual Prandtl approximation[5] of neglecting all terms other than those of first order magnitude, Eqs. (3.1), (3.2) reduce to

$$q\frac{\partial q}{\partial s} = -\frac{1}{\rho}\frac{\partial p}{\partial s} + (\nu+\epsilon)\frac{\partial^2 q}{\partial n^2} + \frac{\partial \epsilon}{\partial n}\frac{\partial q}{\partial n}, \tag{4.1}$$

$$q^2\frac{\partial \theta}{\partial s} = \frac{1}{\rho}\frac{\partial p}{\partial n}, \tag{4.2}$$

the equation of continuity remaining as in (3.3).

Further, Eq. (4.2) can generally be neglected, since the total change of pressure along a normal must be $O(\delta^2)$. The derivatives of p with respect to s may accordingly be replaced by the total differentials. It will also be legitimate, on the basis of (b) and (c) above, to regard s as measured along the surface, and n along normals to the surface.

Substitute, now, (3.3) in (4.1) and integrate with respect to n. Then

$$\rho\int_0^n q^2\frac{\partial\theta}{\partial n}dn + n\frac{dp}{ds} + C = (\mu+\rho\epsilon)\frac{\partial q}{\partial n}, \tag{4.3}$$

C being the integration constant.

For brevity, write τ for the total shear stress $(\mu+\rho\epsilon)(\partial q/\partial n)$. Then C is equal to the surface value τ_0, and (4.3) may be expressed as

$$f \equiv \frac{\tau}{\tau_0} = 1 + \omega_\delta\eta + \frac{\rho}{\tau_0}\int_0^\eta q^2\frac{\partial\theta}{\partial\eta}d\eta, \tag{4.4}$$

with $\omega_\delta \equiv \delta dp/\tau_0 ds$, $\eta \equiv n/\delta$. Hence, from (4.4)

$$\frac{\partial\theta}{\partial\eta} = \frac{\tau_0}{\rho q^2}\left(\frac{\partial f}{\partial\eta} - \omega_\delta\right),$$

or putting $X^2 \equiv \tau_0/\rho q_1^2$, where q_1 is the velocity at the outer limit of the boundary layer,

$$\frac{\partial\theta}{\partial\eta} = \frac{X^2}{\left(\frac{q}{q_1}\right)^2}\left(\frac{\partial f}{\partial\eta} - \omega_\delta\right), \tag{4.5}$$

---

* It is usual in the dimensional analysis of the equations of motion to regard δ as $O(\nu^{1/2})$, which is the case if the viscous terms are taken to be of the same order as the inertia terms. However, it is known in the case of the turbulent boundary layer that δ is proportional to $\nu^{1/5}$. Cf. S. Goldstein, *Modern developments in fluid dynamics*, vol. 2, University Press, Oxford, 1938, p. 362.

[5] L. Prandtl, *Über Flüssigkeitsbewegungen bei sehr kleiner Reibung*, Verhand. des dritten internat. Math.-Kongress, Heidelberg, pp. 484–491 (1904).

so that

$$\theta = X^2 \int_0^\eta \frac{1}{\left(\frac{q}{q_1}\right)^2} \left(\frac{\partial f}{\partial \eta} - \omega_s\right) d\eta + \text{const.} \tag{4.6}$$

5. Equation of the boundary layer parameter H. If the constant of integration in (4.6) is chosen so that θ is zero at the surface ($\eta = 0$), it follows that $-\theta$ will be equal to the angle between the tangent of the streamline at the point P (Fig. 1) and the tangent to the surface where the orthogonal through P strikes the surface; or in less precise terms, $-\theta$ measures the divergence of the mean flow with respect to the surface.

Let θ_1 be the value of θ at $\eta = 1$, s_1 the distance along the outer edge of the boundary layer, and let the value ψ_1 of the stream function ψ be defined as

$$\psi_1 = \int_0^\delta q dn. \tag{5.1}$$

Then, since

$$\frac{d\psi_1}{ds_1} = \frac{\partial \psi_1}{\partial s} \frac{\partial s}{\partial s_1} + \frac{\partial \psi_1}{\partial n} \frac{\partial n}{\partial s_1},$$

we have, to the order of accuracy of the boundary layer equations ($s_1 \doteq s$),

$$\frac{d\psi_1}{ds} = q_1 \left(\theta_1 + \frac{d\delta}{ds}\right),$$

or

$$\psi_1 = \int q_1 \left(\theta_1 + \frac{d\delta}{ds}\right) ds + \text{const.} \tag{5.2}$$

Now introduce the displacement length δ_1 which, in terms of δ, may be written non-dimensionally as

$$\frac{\delta_1}{\delta} = \int_0^1 \left(1 - \frac{q}{q_1}\right) d\eta. \tag{5.3}$$

With respect to (5.1) we have, therefore,

$$\psi_1 = q_1(\delta - \delta_1), \tag{5.4}$$

so that from (5.2) and (5.4)

$$\int q_1 \left(\theta_1 + \frac{d\delta}{ds}\right) ds = q_1(\delta - \delta_1) + \text{const.}, \tag{5.5}$$

and, on differentiating (5.5) with respect to s and rearranging,

$$\frac{d\delta_1}{ds} + \frac{\delta_1}{q_1} \frac{dq_1}{ds} = \frac{\delta}{q_1} \frac{dq_1}{ds} - \theta_1. \tag{5.6}$$

There is also the momentum equation which takes the well known form

$$\frac{d\vartheta}{ds}+\frac{\vartheta}{q_1}\frac{dq_1}{ds}(H+2)=\frac{\tau_0}{\rho q_1^2}=X^2, \tag{5.7}$$

where the momentum length ϑ is defined as

$$\vartheta=\int_0^\delta \frac{q}{q_1}\left(1-\frac{q}{q_1}\right)dn,$$

and $H=\delta_1/\vartheta$. Hence

$$\frac{dH}{ds}=\frac{d}{ds}\left(\frac{\delta_1}{\vartheta}\right)=\frac{1}{\vartheta}\left(\frac{d\delta_1}{ds}-\frac{\delta_1}{\vartheta}\frac{d\vartheta}{ds}\right),$$

and therefore

$$\vartheta\frac{dH}{ds}=\frac{d\delta_1}{ds}-H\frac{d\vartheta}{ds}. \tag{5.8}$$

Now substitute for $d\delta_1/ds$ from (5.6) and for $d\vartheta/ds$ from (5.7). It is then found that Eqs. (5.6), (5.7) may be written alternatively as

$$\vartheta\frac{dH}{ds}=-X^2[\omega_\delta+H\{1+\omega_\vartheta(H+1)\}]-\theta_1, \tag{5.9}$$

$$\frac{d\vartheta}{ds}=X^2[1+\omega_\vartheta(H+2)], \tag{5.10}$$

in which $\omega_\delta\equiv\delta dp/\tau_0 ds$ and $\omega_\vartheta\equiv\vartheta dp/\tau_0 ds$.

6. Discussion of Eqs. (5.9), (5.10) in relation to the empirical formulae of von Doenhoff, Tetervin and Garner. It is shown in Part 2, Sec. 12, that Eq. (5.9) can be reduced to the form

$$\vartheta\frac{dH}{ds}=F_1(\omega_\vartheta, R_\vartheta, H), \tag{6.1}$$

R_ϑ being the Reynolds number $q_1\vartheta/\nu$. This is of interest in that von Doenhoff and Tetervin[1] recently introduced an empirical equation in terms of ω_ϑ and H, that is to say,

$$\vartheta\frac{dH}{ds}=F_2(\omega_\vartheta, H), \tag{6.2}$$

though analytically their expression differs appreciably from the theoretical relation. Following a similar procedure, Garner[2] has derived another empirical equation which, functionally, is of precisely the same form as the theoretical result (6.1), but which otherwise bears a close resemblance to the formula of von Doenhoff and Tetervin. Garner's solution, therefore, is of particular interest in relation to Eq. (5.9), and it may be useful to summarize briefly these empirical developments. We will begin by considering the original work of von Doenhoff and Tetervin.

They observe first that the velocity profile determines H, and point out that the

converse statement cannot be proved theoretically. They accordingly proceed to subject the hypothesis to experimental test, and, from a considerable volume of experimental data, show that there is very convincing evidence to support the assumption that H uniquely defines the velocity profile. On the strength of this conclusion that the distribution is a uni-parametric function, they then consider how the external forces acting on the boundary layer are related to H. The argument is advanced that the rate of change of H, rather than H itself, is the determining factor, and it is further pointed out that this assumption has the desirable effect of connecting conditions downstream from a point with those upstream of the point. The problem which von Doenhoff and Tetervin investigate, therefore, is the degree of correlation between dH/ds, the pressure gradient dp/ds and the surface friction τ_0. In the first instance they attempt to establish a relation between the gradients of H and p when expressed non-dimensionally as* $\vartheta dH/ds$ and $-\vartheta d(p/\frac{1}{2}\rho q_1^2)/ds$, thus leaving the frictional term as an independent entity. From their analysis, however, the authors conclude that there is no general relationship of this kind, a systematic variation with Reynolds number being noted. They then consider the ratio of the dimensionless pressure gradient, given above, to the friction intensity which they write in the non-dimensional form $\tau_0/\rho q_1^2$. This ratio, it will be seen, is equal to $-2\vartheta dp/\tau_0 ds$. It is therefore proportional to ω_ϑ. In determining the above quantity, von Doenhoff and Tetervin tentatively assume the flat plate skin friction law, as given by Squire and Young,[6] irrespective of the pressure gradient. Allowing for the fact that dH/ds and dp/ds were obtained by graphical differentiation of the experimental results, they conclude that, at a constant value of H, there is an approximately linear relationship between $\vartheta dH/ds$ and $\vartheta dp/\tau_0 ds$, and consequently arrive at the general result indicated by Eq. (6.2). Finally, by analyzing their data at a number of prescribed values of H, they are able to formulate an arbitrary, analytical expression for (6.2) which, in terms of the present notation, is given in section 13, Eq. (13.1).

Garner follows essentially the line of development instigated by von Doenhoff and Tetervin. He expresses the momentum equation in the form first used by Howarth,[7] and, as a result, prefers a power law for the skin friction.[8] He also takes into account the effect of pressure gradients on the skin friction, whereas von Doenhoff and Tetervin are content in general with the plane flow approximation. Using Θ and Γ as basic variables, where** $\Theta \equiv \vartheta R_\vartheta^{1/n}$, and $\Gamma \equiv \Theta dq_1/q_1 ds$, Garner then obtains an equation for $\Theta dH/ds$ which is analytically similar to that of ref. 1. In the existing notation it may be expressed, however, in the alternative form given in section 13, Eq. (13.2), from which it will be seen, since X is a function of R_ϑ, that it is entirely consistent with Eq. (6.1).

---

* The presence of the negative sign will be clear when it is recalled that von Doenhoff and Tetervin adopt the alternative form $\vartheta dq/q ds$, where, in their notation, q is the dynamic pressure at the outer limit of the boundary layer.

** The index is subsequently taken as $n=6$ in conformity with the choice of Falkner's equation for the skin friction.

[6] H. B. Squire and A. D. Young, *The calculation of the profile drag of aerofoils*, Tech. Rep. of the Aeron. Res. Comm., R & M. No. 1838 (1938).

[7] L. Howarth, *The theoretical determination of the lift coefficient for a thin elliptic cylinder*, Proc. Roy. Soc. (A) **149**, 574–575 (1935).

[8] V. M. Falkner, *A new law for calculating drag*, Airc. Eng., **15**, 65–69 (1943).

The empirical equation for $\vartheta dH/ds$, the momentum equation and a relation for the skin friction are then sufficient to enable the development of the turbulent boundary layer to be analyzed. The solution depends on a step-by-step integration which Garner elaborates in great detail by the finite difference calculus. It assumes that the static pressure distribution is given, and that the initial values of ϑ and H are known, e.g. at transition. This problem is discussed thoroughly in both refs. 1 and 2, and need not concern us further. The integration then yields ϑ and H at the beginning of each interval. Hence, we seek a form of Eq. (5.9) purely in terms of ϑ, H and p. This is the subject of Part 2.

Part 2.

7. Approximations regarding the turbulent and laminar layers. Boundary conditions. It is inevitable that a theoretical approach to the problem of the turbulent boundary layer must be appreciably more complex than the simple, empirical treatment of von Doenhoff and Tetervin. The difficulty of solving the fundamental equations of motion, even when the flow is laminar, is here increased by the fact that we have to consider an "apparent viscosity" which varies from point to point in the fluid. In order to deal with this feature of the flow, some kind of turbulent mechanism must be specified and incorporated into the basic equations. The very considerable difficulties of a rigorous treatment of this aspect of the problem are well known, and even an approximate and much simplified theory, as adopted in the present paper, leads to a rather complicated solution which does not yield an analytical function for $\vartheta dH/ds$. Indeed, it has not been possible to present the arguments advanced in the following pages in the form of a unified theory. Rather the investigation has been divided into a series of associated problems which are considered individually, and it is then shown how the results may be combined in a numerical solution to provide the data for the step-by-step integration referred to in section 6. As a consequence, it will probably assist the reader to give a statement as to the procedure now to be followed, and the nature of the approximations involved.

In the first place it will be assumed that the flow may be sub-divided into a turbulent layer, where the effects of fluid viscosity are negligible, and a thin surface layer (laminar sub-layer) where viscosity is predominant, the transition from the one flow to the other being regarded as occurring instantaneously, i.e. in zero length η. Neglect of ν when the motion is fully turbulent implies that $\epsilon \gg \nu$ (see Eq. 4.3), an assumption which is valid for sufficiently large Reynolds numbers, and one commonly made in considering this region.[9] It will also be convenient at first to take ω_δ as independent variable, and we will subsequently derive a method of transforming from ω_δ to ω_ϑ which is the variable required in performing the numerical integration of Eqs. (5.9), (5.10).

On the above basis, we shall then proceed to our first objective, namely the establishment of the velocity distribution in the turbulent and sub-laminar layers, the two cases being considered independently, but in such a manner that the essential boundary conditions are satisfied, and further, that the velocity is continuous at the transition from the laminar to turbulent states. Secondly, the important quantity θ_1 of Eq. (5.9) will be investigated. This, it will be shown, depends primarily on the condi-

[9] See, e.g., S. Goldstein (editor), *Modern developments in fluid dynamics*, vol. 2, University Press, Oxford, 1938, pp. 331–332.

tions in the laminar sub-layer, which cannot be entirely neglected for this reason. To a less, but appreciable degree, it also affects the magnitude of the parameter H. Finally, we develop a method whereby Eq. (5.9) may be evaluated numerically in terms of ϑ, H and p (or q_1, which is related to p by Bernoulli's theorem).

Turning, now, to the approximate nature of the analysis, we have first the simple theory of diffusion upon which the flow in the turbulent layer is based. It is assumed that the intensity components of the turbulent fluctuations do not differ appreciably (or at any rate are proportional to one another), and that the scale may be sufficiently represented by a mean length which is a function of the space co-ordinates. Although the subsequent development of this simplified conception of the turbulent mechanism near a surface in no way depends on a physical model, it is mathematically equivalent, nevertheless, to Prandtl's momentum transfer theory,[10] and is further closely connected with von Kármán's similarity theory[11] which appears as a special case in the present treatment.

Without entering into the details of the argument, it is finally shown that the turbulent velocity distribution may be expressed in terms of two functions f and g, and the surface friction X, namely,

$$\frac{\partial}{\partial \eta}\left(\frac{q}{q_1}\right) = \frac{X}{\lambda f^{-1/2}},$$

where

$$\lambda f^{-1/2} = -\int_0^{\eta} g f^{-1/2} d\eta + \text{const.},$$

λ being a function of the correlation between the longitudinal and lateral velocity fluctuations, and the scale of the turbulence.

Strictly, when the natural viscosity of the fluid can not be ignored, f and g are dependent on ω_s, η and the Reynolds number, but, when the flow is fully trubulent, we neglect, in accordance with our initial assumptions, the viscous terms, and treat both f and g purely as functions of ω_s and η. The stress function f may then be equated to f_R, where f_R denotes the component due to the Reynolds shear stress. Hence, assuming for the moment that X is known, the problem of calculating the velocity distribution in the turbulent layer reduces to the determination of f_R and g. To this end, we first make use of an argument advanced in section 8 (a), namely that approximate solutions for f_R and g are sufficient provided $\lambda f_R^{-1/2}$ is itself correctly established. Accordingly, we express both f_R and g as a power series in η with coefficients which are to be purely functions of ω_s. In the case of f_R the coefficients are chosen to satisfy all the known boundary conditions, with the exception of terms dependent on viscosity which are regarded as referring to the laminar sub-layer only. This leads to a solution in quartic form. In addition to the series for g, two particular solutions for λ are considered, viz. (a) when g = function of ω_s only $= -\Lambda$, (b) when λ = function of ω_s only $= \lambda_1$. It is then suggested that (a) holds near the surface, while (b) is applicable to-

[10] L. Prandtl, *Bericht über Untersuchungen zur ausgebildeten Turbulenz*, Zeitschr. angew. Math. Mech. 5, 136–139 (1925).

[11] T. v. Kármán, *Mechanische Ähnlichkeit und Turbulenz*, Nachr. Ges. Wiss. Göttingen, Math-Phys. Klasse, 58–76 (1930).

wards the outer edge of the boundary layer. By identifying λ_1 with λ when $\eta=1$, and assuming that $\partial\lambda/\partial\eta$ is then zero, a solution for λ, in terms of Λ and λ_1 may then be obtained, if g is expressed as a quadratic, to satisfy condition (a) when $\eta=0$, and condition (b) when $\eta=1$. The resulting distribution of λ for intermediate values of η is then regarded provisionally as a valid approximation. Further, when $\omega_3=0$, it appears that the corresponding value of Λ (designated Λ_0) is then identical to von Kármán's constant K of the similarity theory.[11] Its value is therefore known. In addition, we obtain immediately an integral relation for Λ/Λ_0 purely in terms of f_R. Hence, apart from X, λ_1 is the only remaining unknown. As a first approximation, but nevertheless one which appears to be well substantiated by experiment, we assume that λ_1 is independent of ω_3. Like Λ_0, it must then be regarded as a fundamental constant to be determined experimentally, the value in the present instance being calculated to give the best agreement between the theoretical and experimental velocity profiles for flow in parallel wall channels. Finally, neglecting second order terms, we obtain a very simple relation for the variation of X with ω_3, namely $X/X_0=\Lambda/\Lambda_0$, where X_0 refers to the condition $\omega_3=0$, and is therefore calculable from either von Kármán's logarithmic skin friction equation,[11,12] or from a power law such as Falkner has published.[8] We thus establish a general solution for the velocity distribution in the turbulent part of the boundary layer.

As regards the treatment of the laminar sub-layer, little need be said. It is essentially in the nature of a linear (double link) interpolation which satisfies the main wall condition, and preserves continuity with the turbulent flow solution at the point of transition. It makes no reference, therefore, to the equations of motion. On the other hand, the approach is justified on the grounds that, when the Reynolds number is moderate or large, the laminar layer is quite thin, and further, that the velocity distribution is then mainly linear throughout the region concerned.

The solution for θ_1, however, requires a little more attention. As already pointed out, it is primarily dependent on conditions in the laminar layer; it is also largely determined by the stress function. Hence, the relation for f_R considered in the study of the turbulent velocity profile is certainly no longer tenable near the surface. We accordingly develop the stress function, which must now be written as f, as a new power series, applicable for small values of η only, and including the effects of viscosity.

The procedure for determining the coefficients of the series is similar to that adopted in dealing with the turbulent layer, except that in this case the boundary conditions are restricted to the surface. The series is also limited to a quartic in view of the fact that η is to be regarded as quite small; at the same time it is desirable on account of the increasingly involved character of the coefficients relating to higher powers of η. The distribution of f in the outer part of the boundary layer is then represented by a second, independent series which satisfies the conditions at $\eta=1$, and is continuous with the distribution of f near the wall. The fact that this "inner and outer" solution is not altogether consistent with the previous solution for f, when viscosity was entirely neglected, is regarded as unimportant, for in the first place both approaches are only approximate, and secondly, so far as θ_1 is concerned, it is the distribution of f in the laminar sub-layer which is critical, whilst the relatively large

[12] T. v. Kármán, *Turbulence and skin friction*, J. Aer. Sci. 1, 1–20 (1934).

error which probably arises in the turbulent region has only slight significance. In the former case there is reason to believe that, when viscosity is included, the treatment leads to results of good accuracy.

Finally, having established θ_1, numerical estimates of $\vartheta dH/ds$ may be made from Eq. (5.9) in terms of ω_s. An additional equation relating ω_s and ω_ϑ is also given. Hence Eq. (5.9) may be integrated step-by-step according to ref. (1) or (2).

8. (a) Turbulent diffusion in the boundary layer. The first step towards the transformation of Eq. (5.9) is to develop a theory of turbulent diffusion, valid for the boundary layer. This is greatly complicated by the fact that the flow is anisotropic. Nevertheless, an approximate treatment, which has yielded valuable results in the case of turbulent flow over plane surfaces and in pipes, rests on the assumption that the intensity components $\sqrt{\overline{u'^2}}$, $\sqrt{\overline{v'^2}}$ do not differ appreciably, and further that the correlation may still be represented by a single scalar function. Extending this hypothesis to the case of flow in the presence of pressure gradients generally, we write

$$\epsilon \doteq l\sqrt{\overline{v'^2}}, \tag{8.1}$$

where l is the length defining the average scale of the turbulence at any point. To the order of accuracy of the boundary layer equation $\rho\epsilon\partial q/\partial n$ is equal to the original Reynolds stress $-\rho\overline{u'v'}$. Denote this component by τ_R. Then

$$\frac{\tau_R}{\rho} = \epsilon\frac{\partial q}{\partial n} = -\overline{u'v'} = R_{uv}\sqrt{\overline{u'^2}}\sqrt{\overline{v'^2}}, \tag{8.2}$$

where the correlation coefficient R_{uv} is here defined as

$$R_{uv} = -\frac{\overline{u'v'}}{\sqrt{\overline{u'^2}}\sqrt{\overline{v'^2}}} = -\frac{\overline{u'v'}}{\overline{v'^2}},$$

since, by hypothesis, $\overline{u'^2} \doteq \overline{v'^2}$.

From (8.2) we then have

$$\overline{v'^2} = \frac{\epsilon}{R_{uv}}\frac{\partial q}{\partial n}, \tag{8.3}$$

and combining (8.3) with (8.1),

$$\epsilon = \frac{l^2}{R_{uv}}\frac{\partial q}{\partial n}, \tag{8.4}$$

so that the Reynolds stress may be written non-dimensionally as

$$\frac{\tau_R}{\rho q_1^2} = \frac{1}{R_{uv}}\left(\frac{l}{\delta}\right)^2\left|\frac{\partial}{\partial\eta}\left(\frac{q}{q_1}\right)\right|\frac{\partial}{\partial\eta}\left(\frac{q}{q_1}\right) = \lambda^2\left|\frac{\partial}{\partial\eta}\left(\frac{q}{q_1}\right)\right|\frac{\partial}{\partial\eta}\left(\frac{q}{q_1}\right), \tag{8.5}$$

the function $\lambda \equiv R_{uv}^{-\frac{1}{2}}(l/\delta)$ being, in general, a function of η, ω_s and the Reynolds number, since the turbulent mechanism is influenced by viscosity near the surface. It follows that

$$f_R \equiv \frac{\tau_R}{\tau_0} = \frac{\lambda^2}{X^2}\left|\frac{\partial}{\partial\eta}\left(\frac{q}{q_1}\right)\right|\frac{\partial}{\partial\eta}\left(\frac{q}{q_1}\right). \tag{8.6}$$

We now seek to express λ in terms of the stress function f_R. First differentiate (8.6) with respect to η. Then

$$\frac{\partial \lambda}{\partial \eta} + \left[\frac{\partial^2 q}{\partial \eta^2} \Big/ \frac{\partial q}{\partial \eta} - \frac{1}{2f_R}\frac{\partial f_R}{\partial \eta}\right]\lambda = 0. \tag{8.7}$$

Without loss of generality we may also write

$$\lambda = g \frac{\partial q}{\partial \eta} \Big/ \frac{\partial^2 q}{\partial \eta^2}, \tag{8.8}$$

g being also a function of η, ω_s and the Reynolds number. Hence, combining (8.7), (8.8)

$$\frac{\partial \lambda}{\partial \eta} - \frac{1}{2f_R}\frac{\partial f_R}{\partial \eta}\lambda = -g, \tag{8.9}$$

which on integration yields

$$\lambda = -f_R^{1/2}\left[\int_0^\eta g f_R^{-1/2} d\eta + \text{const.}\right], \tag{8.10}$$

or writing $I_1 \equiv -\int_0^\eta g f_R^{-1/2} d\eta + \text{const.}$,

$$\lambda = f_R^{1/2} I_1. \tag{8.11}$$

Ignoring for the present the integration constant in (8.10), consider, now, the solution when g is a function only of ω_s and Reynolds number, so that with respect to η

$$g = \text{constant} = -\Lambda. \tag{8.12}$$

Then

$$\lambda = \Lambda f_R^{1/2} \int_0^\eta f_R^{-1/2} d\eta, \tag{8.13}$$

for which there is a maximum at $\eta = \eta_1$ such that

$$f_{R\eta_1}^{-1/2}\left(\frac{\partial f_R}{\partial \eta}\right)_{\eta_1} \int_0^{\eta_1} f_R^{-1/2} d\eta = -2. \tag{8.14}$$

Again, the solution which makes

$$\lambda = \text{constant} = \lambda_1 \tag{8.15}$$

for all values of η is given by

$$g = \frac{1}{2f_R}\frac{\partial f_R}{\partial \eta}\lambda_1. \tag{8.16}$$

Now assign to λ_1 the value of λ when $\eta = 1$. If, further, we make the reasonable assumption $\partial\lambda/\partial\eta \to 0$ as $\eta \to 1$, then a solution for λ is obtained, which satisfies the above conditions, by equating (8.11) to λ_1 when $\eta = \eta_1$, with $\lambda = \lambda_1$ in the range $\eta_1 < \eta < 1$.

Whether or not this solution for λ leads to boundary layer characteristics in accordance with fact can only be decided by test, but for the present we will regard it provisionally as satisfactory. Hence the necessary and sufficient conditions are

$$\left.\begin{aligned} \eta &= 0, \qquad \lambda = 0, \qquad g = -\Lambda \\ \eta &= \eta_1, \qquad \lambda = \lambda_1, \qquad g = \frac{1}{2f_{R\eta_1}}\left(\frac{\partial f_R}{\partial \eta}\right)_{\eta_1}\lambda_1 \end{aligned}\right\}. \tag{8.17}$$

In general write

$$g = -\Lambda\left(1 + \sum_{n=1}\Lambda_n\eta^n\right), \tag{8.18}$$

where Λ_n are arbitrary constants. Then (8.17) will be satisfied by the series

$$g = -\Lambda(1 + \Lambda_1\eta + \Lambda_2\eta^2), \tag{8.19}$$

so that from (8.10)

$$\lambda = \Lambda f_R^{1/2}\left[\int_0^\eta f_R^{-1/2}d\eta + \Lambda_1\int_0^\eta \eta f_R^{-1/2}d\eta + \Lambda_2\int_0^\eta \eta^2 f_R^{-1/2}d\eta\right], \tag{8.20}$$

and

$$\frac{\partial\lambda}{\partial\eta} = \Lambda\left[(1 + \Lambda_1\eta + \Lambda_2\eta^2) + \tfrac{1}{2}f_R^{-1/2}\frac{\partial f_R}{\partial\eta}\left(\int_0^\eta f_R^{-1/2}d\eta + \Lambda_1\int_0^\eta \eta f_R^{-1/2}d\eta + \Lambda_2\int_0^\eta \eta^2 f_R^{-1/2}d\eta\right)\right]. \tag{8.21}$$

Let

$$G_0 \equiv f_{R\eta_1}^{1/2}\int_0^{\eta_1} f_R^{-1/2}d\eta, \qquad G_1 \equiv f_{R\eta_1}^{1/2,}\int_0^{\eta_1}\eta f_R^{-1/2}d\eta,$$

$$G_2 \equiv f_{R\eta_1}^{1/2}\int_0^{\eta_1}\eta^2 f_R^{-1/2}d\eta,$$

and

$$H_0 \equiv 1 + \tfrac{1}{2}f_{R\eta_1}^{-1/2}\left(\frac{\partial f_R}{\partial\eta}\right)_{\eta_1}\int_0^{\eta_1} f_R^{-1/2}d\eta,$$

$$H_1 \equiv \eta_1 + \tfrac{1}{2}f_{R\eta_1}^{-1/2}\left(\frac{\partial f_R}{\partial\eta}\right)_{\eta_1}\int_0^{\eta_1}\eta f_R^{-1/2}d\eta,$$

$$H_2 \equiv \eta_1^2 + \tfrac{1}{2}f_{R\eta_1}^{-1/2}\left(\frac{\partial f_R}{\partial\eta}\right)_{\eta_1}\int_0^{\eta_1}\eta^2 f_R^{-1/2}d\eta.$$

Then (8.14) makes

$$H_0 = 0, \tag{8.22}$$

and, to satisfy (8.17), we have from (8.20), (8.21)

$$\left.\begin{aligned} G_0 + G_1\Lambda_1 + G_2\Lambda_2 &= \frac{\lambda_1}{\Lambda} \\ H_1\Lambda_1 + H_2\Lambda_2 &= 0 \end{aligned}\right\}. \tag{8.23}$$

Therefore,

$$\Lambda_1 = \frac{H_2\left(\frac{\lambda_1}{\Lambda} - G_0\right)}{(G_1H_2 - G_2H_1)}, \tag{8.24}$$

$$\Lambda_2 = -\frac{H_1}{H_2}\Lambda_1. \tag{8.25}$$

Hence, by the definition of I_1, when $0<\eta<\eta_1$,

$$I_1 = \Lambda\int_0^{\eta}(1 + \Lambda_1\eta + \Lambda_2\eta^2)f_R^{-1/2}d\eta + \text{const.}; \tag{8.26}$$

and when $\eta_1<\eta<1$,

$$I_1 = \lambda_1 f_R^{-1/2} + \text{const.} \tag{8.27}$$

It follows from Eqs. (8.6), (8.11) that

$$\frac{\partial}{\partial\eta}\left(\frac{q}{q_1}\right) = \frac{X}{I_1}, \tag{8.28}$$

whence, integrating along normals from the outer edge of the boundary layer towards the surface, and allowing for the condition $q\to q_1$ as $n\to\delta$,

$$\frac{q}{q_1} = 1 + I_2X, \tag{8.29}$$

where $I_2 \equiv \int_1^{\eta} I_1^{-1}d\eta$. Hence, the velocity profile is determined primarily, not by the individual values of f_R and λ, but only by the product $\lambda f_R^{-1/2}$, for which there will be a unique distribution across any section of the boundary layer, depending on the flow conditions. We may therefore seek approximate solutions, of an arbitrary character, for f_R and λ, provided that, when combined in the above manner, they yield a solution of (8.29) in accordance with the physical facts.

In the next section we shall make use of this argument to obtain a general solution of the velocity distribution in the turbulent layer.

8. (b) Velocity distribution in the turbulent layer. It has been shown experimentally[12,14,15] that, for moderate or large Reynolds numbers, fully developed turbulent flow in the absence of a pressure gradient, or when the gradient is small (as in pipe

---

[13] H. Darcy, *Recherches expérimentales relatives au mouvement de l'eau dans les tuyaux*, Mém. Sav. Étrang. **15**, 141–403 (1858).

[14] T. Stanton, *The mechanical viscosity of fluids*, Proc. Roy. Soc. (A) **85**, 366–376, (1911).

[15] W. Fritsch, *Der Einfluss der Wandrauhigkeitsverteilung in Rinnen*, Zeitschr. angew. Math. Mech. **8**, 199–216 (1928).

flow), does not depend on viscosity. This fact is expressed quantitatively by the well known velocity defect law which, in the present notation, becomes*

$$-I_2 = \frac{1}{X}\left(1 - \frac{q}{q_1}\right) = \phi(\eta), \tag{8.30}$$

or, extending (8.30) to include the case when the pressure gradient is not negligibly small ($\omega_s \neq 0$),

$$-I_2 = \frac{1}{X}\left(1 - \frac{q}{q_1}\right) = \phi(\omega_s, \eta). \tag{8.31}$$

Hence,

$$\frac{\partial I_2}{\partial \eta} = \frac{1}{I_1} = \frac{f_R^{1/2}}{\lambda} = \phi'(\omega_s, \eta). \tag{8.32}$$

But, from the preceding section, we have obtained λ, and therefore I_1, in terms of f_R and the variables Λ and λ_1 which are purely functions of ω_s. Hence, it follows that in the turbulent region, for which Eqs. (8.31), (8.32) are valid, f_R must be a function of ω_s and η only. Moreover, we may then write $f \doteq f_R$, and therefore f is also simply a function of ω_s and η.

We will now obtain an expression for I_1, which satisfies the turbulent velocity distribution generally, by the argument advanced in the last section. This, it will be recalled, depends only on the approximate determination of both f_R and λ, provided that $\lambda f_R^{-1/2}$ is correctly established. First, therefore, express f_R in an arbitrary form. The problem then reduces to the determination of Λ and λ_1 so as to satisfy the above conditions for I_1. Accordingly, proceeding to the approximate development of f_R, we note first that Eq. (4.4) has the alternative form

$$f = 1 + \omega_s \eta + \frac{\delta}{X^2}\int_0^\eta \left(\frac{q}{q_1}\right)\frac{\partial}{\partial s}\left(\frac{q}{q_1}\right) d\eta. \tag{8.33}$$

Successive differentiation of (8.33) also gives

$$\frac{\partial f}{\partial \eta} = \omega_s + \frac{\delta}{X^2}\left(\frac{q}{q_1}\right)\frac{\partial}{\partial s}\left(\frac{q}{q_1}\right),$$

$$\frac{\partial^2 f}{\partial \eta^2} = \frac{\delta}{X^2}\left[\frac{\partial}{\partial \eta}\left(\frac{q}{q_1}\right)\frac{\partial}{\partial s}\left(\frac{q}{q_1}\right) + \left(\frac{q}{q_1}\right)\frac{\partial}{\partial s}\frac{\partial}{\partial \eta}\left(\frac{q}{q_1}\right)\right],$$

$$\frac{\partial^3 f}{\partial \eta^3} = \frac{\delta}{X^2}\left[\frac{\partial^2}{\partial \eta^2}\left(\frac{q}{q_1}\right)\frac{\partial}{\partial s}\left(\frac{q}{q_1}\right) + 2\frac{\partial}{\partial \eta}\left(\frac{q}{q_1}\right)\frac{\partial}{\partial s}\frac{\partial}{\partial \eta}\left(\frac{q}{q_1}\right) + \left(\frac{q}{q_1}\right)\frac{\partial}{\partial s}\frac{\partial^2}{\partial \eta^2}\left(\frac{q}{q_1}\right)\right],$$

etc.

Consider, next, the known boundary conditions. They are:

* This equation is commonly written in the form $(U_c - U)/U_\tau = f(y/h)$.

$$\eta = 0, \qquad \frac{q}{q_1} = 0, \qquad \frac{\partial}{\partial s}\left(\frac{q}{q_1}\right) = 0, \qquad \frac{\partial}{\partial \eta}\left(\frac{q}{q_1}\right) = \frac{q_1\delta}{\nu} X^2 = R_\delta X^2;$$

$$\eta = 1, \qquad \frac{q}{q_1} = 1, \qquad q_1 \frac{dq_1}{ds} = -\frac{1}{\rho}\frac{dp}{ds}, \qquad \frac{\partial}{\partial \eta}\left(\frac{q}{q_1}\right) = 0.$$

Hence, for f and the known derivatives, we have

$$\eta = 0, \qquad f = 1, \qquad \frac{\partial f}{\partial \eta} = \omega_\delta, \qquad \frac{\partial^2 f}{\partial \eta^2} = 0,$$

$$\frac{\partial^3 f}{\partial \eta^3} = 4X R_\delta^2 \delta \left[\frac{dX}{ds} + \frac{X}{q_1}\frac{dq_1}{ds}\right],$$

and when

$$\eta = 1, \qquad f = 0, \qquad \frac{\partial f}{\partial \eta} = 0.$$

These conditions must be satisfied in addition to that discussed earlier, namely, for fully developed turbulence, the flow is independent of the Reynolds number when moderate or large. It also follows that f_R may then be taken equal to f. Express, therefore, f_R as a power series in η, with coefficients which are purely functions of ω_δ. If, in addition, f_R is to satisfy the boundary conditions, we must ignore those in which the Reynolds number occurs explicitly, the argument implying that such terms are only important in the laminar sub-layer. This leaves five boundary conditions to be satisfied. Accordingly, we write*

$$f_R = A_0 + A_1\eta + A_2\eta^2 + A_3\eta^3 + A_4\eta^4. \tag{8.34}$$

Hence,

$$A_0 = 1, \qquad A_1 = \omega_\delta, \qquad A_2 = 0, \tag{8.35}$$

and

$$\left.\begin{aligned} A_0 + A_1 + A_2 + A_3 + A_4 &= 0 \\ A_1 + 2A_2 + 3A_3 + 4A_4 &= 0 \end{aligned}\right\}$$

which on solution yield

$$\left.\begin{aligned} A_3 &= -4 - 3\omega_\delta \\ A_4 &= 3 + 2\omega_\delta \end{aligned}\right\}. \tag{8.36}$$

We must now consider the boundary functions Λ and λ_1. First, with respect to λ_1, let us provisionally assume that it has a unique value for the fully developed turbulent boundary layer (i.e. it is constant for all positive values of ω_δ). It then follows from (8.13) that

---

* The above series, to fit the same boundary conditions, was first suggested by Fediaevsky. See K. Fediaevsky, *Turbulent boundary layer of an aerofoil*, J. Aer. Sci. **4**, 491–498 (1937).

$$\frac{\Lambda}{\Lambda_0} = \frac{\left[f_{R\eta_1}^{1/2} \int_0^{\eta_1} f_R^{-1/2} d\eta \right]_0}{f_{R\eta_1}^{1/2} \int_0^{\eta_1} f_R^{-1/2} d\eta}, \tag{8.37}$$

the suffix 0 to Λ and the bracket of the numerator on the right hand side of the equation denoting the condition $\omega_s = 0$. Hence, it remains to determine Λ_0 and λ_1. From Eqs. (8.8), (8.19) we see that, when $\eta = 0$,

$$\lambda = -\Lambda \frac{\partial q}{\partial \eta} \Big/ \frac{\partial^2 q}{\partial \eta^2}, \tag{8.38}$$

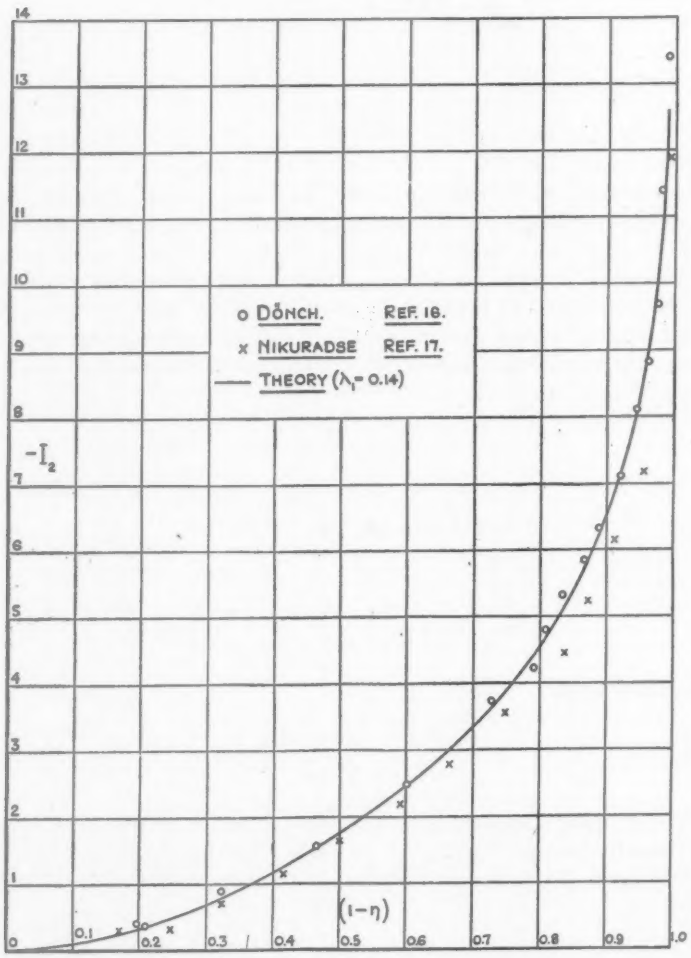

FIG. 2.

which is recognized as a form of von Kármán's equation for the length l in the similarity theory.[11] Accordingly, when $\omega_s = 0$, Λ must be equal to the Kármán constant K whose value, from the logarithmic skin friction law for plane flow (see section 8 (c), Eq. 8.47) is 0.392. Thus, when

$$\omega_s = 0, \qquad \Lambda = \Lambda_0 = K = 0.392.$$

Finally, if λ_1 is to be independent of ω_s, we may determine its value for any arbitrary condition of turbulent flow, e.g. for the case of plane flow. Like Λ_0, it must also be regarded as a constant, only ascertainable numerically by experiment. We will therefore assign to λ_1 that value which gives the best theoretical agreement with the data[16,17] of Fig. 2. This leads to $\lambda_1 = 0.14$, when it will be seen that the distribution of I_2 ($\omega_s = 0$) calculated from the numerical integration of Eqs. (8.26), (8.27), in conjunction with Eqs. (8.34), (8.35), (8.36), agrees very well with the experimental curves for all values of η outside the laminar sub-layer.

The validity of the assumption $\lambda_1 =$ constant, and hence of Eq. (8.37), is discussed in section 8 (c). Further evidence appears from the general comparison of the theoretical and experimental velocity profiles in section 10.

8. (c) Consideration of the general skin friction law ($\omega_s \geqq 0$). The present development of the theory of turbulent flow near a surface depends essentially on the three boundary terms Λ, λ_1 and X, of which Λ and λ_1 have already been considered. As regards X, which determines the surface value of the shear stress, or skin friction intensity, previous investigators have mainly been content to ignore the effect of pressure gradients on X, and to take one of the well attested laws strictly applicable for plane flow only. We shall now show, however, that a simple, approximate relation may be derived to account for the variation of X with ω_s, i.e. for the influence of pressure gradients on skin friction. This leads to the consideration of the flow conditions very near the surface, namely for very small values of η. Eq. (8.34) then reduces to

$$f_R = 1 + \omega_s \eta, \tag{8.39}$$

and, equally, Eq. (8.19) approximates to

$$g = -\Lambda. \tag{8.40}$$

Substituting, now, (8.39), (8.40) in (8.26) and integrating, we find

$$I_1 = \frac{2\Lambda}{\omega_s}(\sqrt{1 + \omega_s \eta} - 1), \tag{8.41}$$

the constant of integration satisfying the condition $I_1 = \eta = 0$. Or, since $\omega_s \eta$ is small in relation to unity, (8.41) may be expanded to give simply

$$I_1 = \Lambda \eta. \tag{8.42}$$

Hence, by definition,

---

[16] F. Dönsch, *Divergente und konvergente turbulente Strömung mit kleinen Öffnungswinkeln*, Forschungsber. Ver. Deutsch. Ing., p. 282 (1926).

[17] J. Nikuradse, *Untersuchungen über die Strömungen des Wassers in konvergenten und divergenten Kanälen*, Forschungsber. Ver. Deutsch. Ing., p. 289 (1929).

$$I_2 \equiv \int \frac{1}{I_1}\, d\eta = \frac{1}{\Lambda}\int \frac{1}{\eta}\, d\eta,$$

$$= \frac{1}{\Lambda} \log_e \eta + \text{const.},$$

$$= h_0 + h_1 \log_{10} \eta, \tag{8.43}$$

where h_0 = constant for any given value of ω_s, and $h_1 = 2.3026/\Lambda$. Owing to the fact that viscosity has been neglected, Eq. (8.43) leads to the well known result that $q = -\infty$ when $\eta = 0$, or, alternatively, that $q = 0$ at some small distance η_0 from the surface, η_0 being clearly of the order of thickness of the laminar sub-layer. As shown in the appendix, the original boundary layer equation (4.3) indicates that η_0 is proportional to $1/R_s X$, and we therefore write

$$\eta_0 = \frac{\Omega}{R_s X}, \tag{8.44}$$

where Ω, the factor of proportionality, is clearly a function of ω_s. It is also immediately apparent from (8.29) that, for the approximate condition $\eta = \eta_0$, $q = 0$,

$$(I_2)_{\eta_0} = -\frac{1}{X}. \tag{8.45}$$

Hence, combining Eqs. (8.43), (8.44), (8.45),

$$\frac{1}{X} = -(h_0 + h_1 \log \Omega) + h_1 \log R_s X, \tag{8.46}$$

which has the form of von Kármán's skin friction law for plane flow.[11,12] Thus, when $\omega_s = 0$, Eq. (8.46) must be consistent with von Kármán's semi-empirical relation

$$\frac{1}{c_f^{1/2}} = 3.60 + 4.15 \log_{10} R_s c_f^{1/2}, \tag{8.47}$$

where $c_f^{1/2} = \sqrt{2}X$ and, by identifying (8.46) with (8.47), it follows, when h_0 and h_1 are determined from Eqs. (8.34), (8.35), (8.36) for $\omega_s = 0$, that Ω has the value 0.131 which compares with values given by Prandtl[13] varying between 0.089 and 0.111. Eq. (8.46) then reduces to

$$\frac{1}{X_0} = 5.97 + 5.88 \log R_s X_0, \tag{8.48}$$

and it follows immediately from the relation $K = \Lambda_0 = 2.3026/(h_1)_0$ that $\Lambda_0 = 0.392$.

For the case when $\omega_s \neq 0$, it is necessary to know Ω as a function of ω_s in order to obtain X from Eq. (8.46). The difficulty of establishing this relation theoretically may be avoided, however, in the following approximate treatment, which appears to be reasonably valid up to values of ω_s at which separation is imminent.

On splitting the product of Reynolds number and skin friction coefficient in (8.46), we have the alternative arrangement

[13] L. Prandtl in W. F. Durand, *Aerodynamic theory*, vol. 3, J. Springer Berlin, p. 140 (1935).

$$\frac{1}{X} = h_1 \log R_\delta + h_1 \log X - (h_0 + h_1 \log \Omega), \tag{8.49}$$

or by writing

$$h_1 \log X - (h_0 + h_1 \log \Omega) = \sigma h_1,$$

where σ is also a function of ω_δ,

$$\frac{1}{X} = h_1(\log R_\delta + \sigma). \tag{8.50}$$

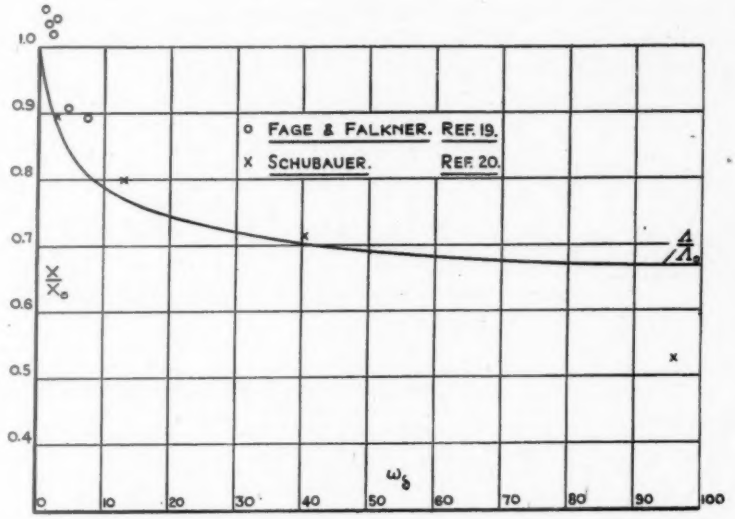

FIG. 3. Comparison of X/X_0 and Λ/Λ_0.

Consider, now, the variation of X with ω_δ when R_δ remains constant. Then

$$\frac{X}{X'} = \frac{h_1'(\log R_\delta + \sigma')}{h_1(\log R_\delta + \sigma)}, \tag{8.51}$$

where h_1, X, σ correspond with ω_δ, and h_1', X', σ' with ω_δ'.

It further appears from experiment that σ varies only slightly, and is small in relation to $\log R_\delta$, provided R_δ is moderate or large. Hence, for the ratio (8.51) no serious error is introduced in neglecting σ, and we then have the simple relation

$$\frac{X}{X'} = \frac{h_1'}{h_1} = \frac{\Lambda}{\Lambda'}, \tag{8.52}$$

which, when $\omega_\delta' = 0$, becomes

$$\frac{X}{X_0} = \frac{\Lambda}{\Lambda_0}, \tag{8.53}$$

Λ/Λ_0 being given by (8.37) and X_0 by (8.48).

Evidence[19,20] as to the validity of (8.53) is shown in Fig. 3.

From the very limited data at present available, it would appear that (8.53) is a reasonably good approximation in the range $0<\omega_3<50$, but clearly a good deal more experimental information is required before the precise significance of Eq. (8.53) can be ascertained.

9. Laminar sub-layer. The solution of Eqs. (5.9), (5.10) depends on a knowledge of the momentum thickness, and the parameters H and θ_1, each of which is a function of the velocity profile. If, however, the laminar sub-layer is neglected in evaluating these quantities, appreciable errors will arise, and it is necessary, therefore, to consider the flow in this region as well as in the fully developed turbulent part of the boundary layer. Before doing so, it will be convenient to express the displacement and momentum lengths in the non-dimensional forms

$$\frac{\delta_1}{\delta} = \int_0^1 \left(1 - \frac{q}{q_1}\right) d\eta = \alpha X; \tag{9.1}$$

$$\frac{\vartheta}{\delta} = \int_0^1 \frac{q}{q_1}\left(1 - \frac{q}{q_1}\right) d\eta = \alpha X - \beta X^2, \tag{9.2}$$

where, from Eq. (8.29), $\alpha \equiv -\int_0^1 I_2 d\eta$, $\beta \equiv \int_0^1 I_2^2 d\eta$. Consequently,

$$\frac{\vartheta}{\delta} = \frac{\alpha^2}{\beta}\left(\frac{H-1}{H^2}\right), \tag{9.3}$$

$$H = \frac{1}{1 - \frac{\beta}{\alpha} X}. \tag{9.4}$$

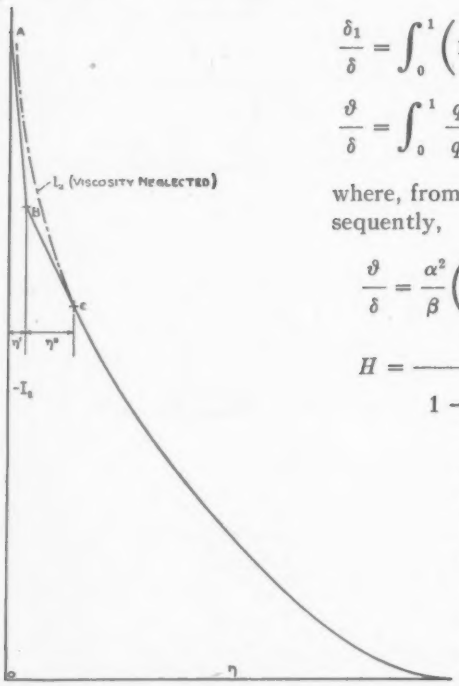

FIG. 4. Distribution of I_2 in laminar sub-layer.

Turning our attention, now, to the laminar sub-layer, we note first that, for moderate or large Reynolds numbers, it is quite thin. Since, also, the velocity distribution in this region is mainly linear, a good approximation to the corresponding distribution of I_2 may be represented by the discontinuous curve ABC (Fig. 4). The characteristics of his curve will be determined by satisfying the essential

[19] A. Fage and V. M. Falkner, *An experimental determination of the intensity of friction on the surface of an aerofoil*, Proc. Roy. Soc. (A) **129**, 378–410 (1930); also Tech. Rep. of the Aeron. Res. Comm., R & M. No. 1315, **1**, 117–140 (1930).

[20] G. B. Schubauer, *Airflow in the boundary layer of an elliptic cylinder*, Twenty-fifth Ann. Rep. Nat. Ad. Comm. for Aeron. Rep. No. 652, 207–226 (1939).

wall conditions, and by preserving continuity with the solution (ν neglected) where the laminar flow merges with the turbulent flow. For

$$0 < \eta < \eta',$$

let

$$I_2 = j_0 + j_1\eta, \tag{9.5}$$

and for

$$\eta' < \eta < (\eta' + \eta''),$$
$$I_2 = j_0 + (j_1 - j_2)\eta' + j_2\eta, \tag{9.6}$$

where j_0, j_1, j_2 are coefficients satisfying the necessary boundary conditions, and η', η'' are defined in Fig. 4. Then, if η_l is the nominal thickness of the laminar sub-layer,

$$\eta_l = \eta' + \eta'' = \frac{\sqrt{m}}{\Lambda R_\delta X} \tag{9.7}$$

according to the appendix.

Also, from Eqs. (8.45), (9.5), we have, when the approximate condition $\eta = \eta_0$ is replaced by the correct condition $\eta = 0$,

$$j_0 = -\frac{1}{X}, \tag{9.8}$$

and, from the differentiation of (9.5)

$$j_1 = \left(\frac{\partial I_2}{\partial \eta}\right)_{\eta=0} = \left(\frac{1}{I_1}\right)_{\eta=0}.$$

But, according to Eq. (8.28)

$$\left(\frac{1}{I_1}\right)_{\eta=0} = \frac{1}{X}\left[\frac{\partial}{\partial \eta}\left(\frac{q}{q_1}\right)\right]_{\eta=0},$$

which, from the boundary condition

$$\left[\frac{\partial}{\partial \eta}\left(\frac{q}{q_1}\right)\right]_{\eta=0} = R_\delta X^2,$$

gives

$$j_1 = \frac{1}{X}\left[\frac{\partial}{\partial \eta}\left(\frac{q}{q_1}\right)\right]_{\eta=0} = R_\delta X. \tag{9.9}$$

Finally, if the distribution of I_2 in the laminar layer is to be continuous with that in the turbulent region, we have from (9.6)

$$j_2 = \left(\frac{\partial I_2}{\partial \eta}\right)_{\eta_l} = \left(\frac{1}{I_1}\right)_{\eta_l}, \tag{9.10}$$

where $(I_1)_{\eta_l}$, $(I_2)_{\eta_l}$ are the values of I_1 and I_2 at $\eta=\eta_l$ given by the solution of sections 8 (a), 8 (b) when ν is neglected.

It follows from (9.7), (9.9) that

$$\eta_l = \eta' + \eta'' = \frac{\sqrt{m}}{\Lambda j_1}, \tag{9.11}$$

and hence, from the relation

$$j_0 + j_1\eta' = (I_2)_{\eta_l} - j_2\eta'',$$

that

$$\eta' = \frac{(I_2)_{\eta_l} - j_0 - j_2\sqrt{m}/j_1\Lambda}{(j_1 - j_2)}. \tag{9.12}$$

Hence, by definition,

$$\alpha = -\int_0^{\eta'} (j_0 + j_1\eta)d\eta - \int_{\eta'}^{\eta_l} \{j_0 + (j_1 - j_2)\eta' + j_2\eta\}d\eta - \int_{\eta_l}^{1} I_2 d\eta,$$

$$= -j_0\eta_l - \tfrac{1}{2}(j_1\eta'^2 + 2j_1\eta'\eta'' + j_2\eta''^2) - \int_{\eta_l}^{1} I_2 d\eta, \tag{9.13}$$

and

$$\beta = \int_0^{\eta'} (j_0 + j_1\eta)^2 d\eta + \int_{\eta'}^{\eta_l} \{j_0 + (j_1 - j_2)\eta' + j_2\eta\}^2 d\eta + \int_{\eta_l}^{1} I_2^2 d\eta,$$

$$= j_0^2\eta_l + j_1(j_0 + j_1\eta'')\eta'^2 + j_2(j_0 + j_1\eta')\eta''^2$$

$$+ 2j_0j_1\eta'\eta'' + \tfrac{1}{3}(j_1^2\eta'^3 + j_2^2\eta''^3) + \int_{\eta_l}^{1} I_2^2 d\eta. \tag{9.14}$$

10. Velocity profiles. Comparison of theory and experiment. Von Doenhoff and Tetervin[1] have analyzed a large amount of data from velocity measurements in the turbulent boundary layer, and it is of interest, therefore, to compare their empirical curves with the theoretical conclusions of the present paper. For this purpose it has been most convenient to take the actual velocity distribution in the form $q/q_1 = f(n/\vartheta)$ as a basis of comparison, the experimental data being obtained from cross-plots of Fig. 9, of the paper quoted in Footnote 1, where q/q_1 is plotted with respect to H for a series of values of n/ϑ = constant.

Fig. 5 gives typical results at $\omega_s = 30$ and for $\log R_s = 3.5$ and $\log R_s = 6.0$. In making the theoretical calculations, I_2 for the turbulent layer (ν neglected) is first determined from the numerical integration of the reciprocals of Eqs. (8.26), (8.27) in conjunction with Eqs. (8.34), (8.35), (8.36) and (8.37); X then follows from (8.37), (8.48), (8.53), and hence the velocity distribution in the turbulent part of the boundary layer from (8.29). The integrals α, β are next evaluated in the turbulent region by numerical integration of I_2 and I_2^2 respectively, and thence for the laminar layer by direct calculation from Eqs. (9.11), (9.12), (9.13), (9.14). Finally, H follows from Eq. (9.4), ϑ/δ from (9.3) and hence n/ϑ from

$$\frac{n}{\vartheta} = \eta \Big/ \left(\frac{\vartheta}{\delta}\right).$$

The results of Fig. 5, which are representative of a number of such calculations, indicate satisfactory agreement between theory and experiment up to values of H in the region of separation.

11. Approximate treatment of Eq. (4.6) in the solution of Eq. (5.9). We are now in a position to consider the solution of Eq. (5.9). This equation contains the important term θ_1, which, as will be seen from Eq. (4.6), depends on the ratio of $(\partial f/\partial\eta - \omega_s)$

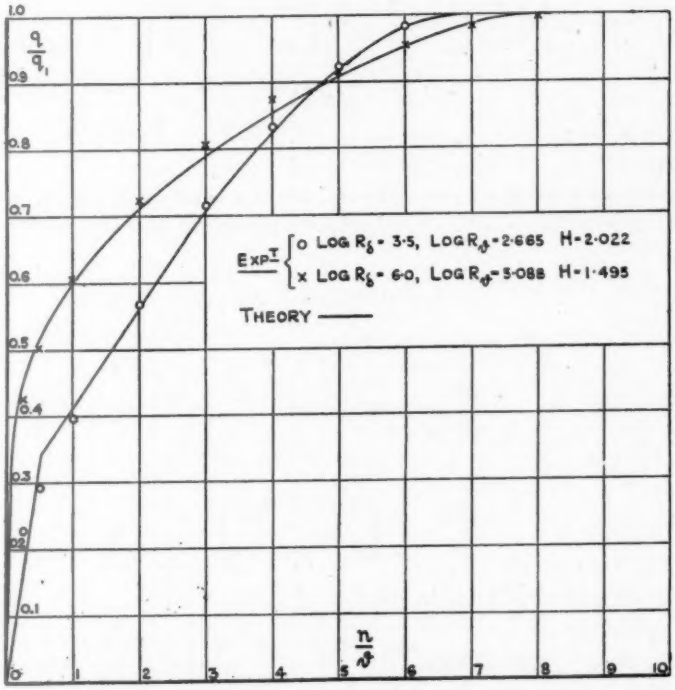

FIG. 5. Theoretical and experimental velocity profiles.

to $(q/q_1)^2$. Near the surface, within the laminar sub-layer, $\partial\theta/\partial\eta$ becomes large, and it appears that the value of θ_1 is critically dependent on the distribution of $\partial\theta/\partial\eta$ in this region. Consequently, viscosity is by no means a negligible factor, and it must be taken into account, not only with regard to the local velocity distribution, already considered in section (9), but also in so far as it affects the stress function f. In this respect, the solution is in marked contrast to that of the turbulent, velocity distribution, for which f may be equated to f_R. Hence, Eq. (8.34) is no longer tenable, and we must consider a more accurate form, at least for small values of η, when the solution will depend predominantly on the viscous terms previously ignored. In dealing first with the term θ_1, we shall accordingly divide the analysis into two parts; (a) that in

which the effects of viscosity are all important, (b) that region outside the laminar sub-layer where, again, viscosity may be neglected. As before, let us represent the stress function near the surface by a power series, namely,

$$f = B_0 + B_1\eta + B_2\eta^2 + \cdots, \tag{11.1}$$

and solve for the B coefficients from the boundary conditions at $\eta=0$. Then, as before (see Sec. 8 (b))

$$B_0 = A_0 = 1, \qquad B_1 = A_1 = \omega_\delta, \qquad B_2 = A_2 = 0, \tag{11.2}$$

$$B_3 = \frac{1}{6}\left(\frac{\partial^3 f}{\partial\eta^3}\right)_{\eta=0} = \frac{2}{3}XR_\delta^2\delta\left[\frac{dX}{ds} + \frac{X}{q_1}\frac{dq_1}{ds}\right],$$

$$= \frac{2}{3}XR_\delta^2\delta\left[\frac{dX}{dR_\vartheta}\frac{dR_\vartheta}{ds} + \frac{X}{q_1}\frac{dq_1}{ds}\right], \tag{11.3}$$

where $R_\vartheta = q_1\vartheta/\nu$.

To a first approximation we now take the relation between X and R_ϑ as that for a flat plate, and determine dX/dR_ϑ from Falkner's power law form.[8] This in terms of R_ϑ may be written

$$X = 0.0808R_\vartheta^{-1/12}, \tag{11.4}$$

so that

$$\frac{dX}{dR_\vartheta} = -0.00673R_\vartheta^{-13/12}. \tag{11.5}$$

Also,

$$\frac{dR_\vartheta}{ds} = \frac{q_1}{\nu}\left[\frac{d\vartheta}{ds} + \frac{\vartheta}{q_1}\frac{dq_1}{ds}\right]. \tag{11.6}$$

Hence, substituting (11.5), (11.6) in (11.3)

$$\frac{3}{2}B_3 = -0.00673XR_\vartheta^{-13/12}R_\delta^2\left[\frac{d\vartheta}{ds} + \frac{\vartheta}{q_1}\frac{dq_1}{ds}\right] + \frac{\delta}{q_1}\frac{dq_1}{ds}X^2R_\delta^2,$$

or, from Eq. (5.10) and the Bernoulli relation

$$\frac{1}{q_1}\frac{dq_1}{ds} = -\frac{1}{\rho q_1^2}\frac{dp}{ds},$$

$$\frac{3}{2}B_3 = -0.00673XR_\vartheta^{-13/12}R_\delta^2\left[X^2\left\{1 + \omega_\delta(H+2) - \frac{\vartheta}{\rho q_1^2X^2}\frac{dp}{ds}\right\}\right]$$

$$-\frac{\delta}{\rho q_1^2X^2}\frac{dp}{ds}X^4R_\delta^2,$$

so that

$$3B_2 = -2X^2R_\delta^2[0.00673R_\delta R_\vartheta^{-13/12}\{1+\omega_\vartheta(H+1)\}+\omega_\delta X],$$
$$= -2X^2R_\delta^2\left[0.00673\left(\frac{\vartheta}{\delta}\right)^{-13/12}R_\delta^{-1/12}\{1+\omega_\vartheta(H+1)\}+\omega_\delta X\right]. \quad (11.7)$$

We also obtain a relation for B_4 as follows. Equation (4.3) may be written

$$1+\omega_\delta\eta+\frac{1}{X^2}\int_0^\eta\left(\frac{q}{q_1}\right)^2\frac{\partial\theta}{\partial\eta}\,d\eta=\frac{1}{X^2R_\delta}\frac{\partial}{\partial\eta}\left(\frac{q}{q_1}\right)$$
$$+\frac{\lambda^2}{X^2}\left|\frac{\partial}{\partial\eta}\left(\frac{q}{q_1}\right)\right|\frac{\partial}{\partial\eta}\left(\frac{q}{q_1}\right), \quad (11.8)$$

which on differentiation with respect to η gives

$$\left(\frac{q}{q_1}\right)^2\frac{\partial\theta}{\partial\eta}=\frac{1}{R_\delta}\frac{\partial^2}{\partial\eta^2}\left(\frac{q}{q_1}\right)+2\lambda\frac{\partial\lambda}{\partial\eta}\left|\frac{\partial}{\partial\eta}\left(\frac{q}{q_1}\right)\right|\frac{\partial}{\partial\eta}\left(\frac{q}{q_1}\right)$$
$$+2\lambda^2\left|\frac{\partial}{\partial\eta}\left(\frac{q}{q_1}\right)\frac{\partial^2}{\partial\eta^2}\left(\frac{q}{q_1}\right)-\omega_\delta X^2,\right. \quad (11.9)$$

and when $\eta=0$, $q=\lambda=0$; therefore, from (11.9),

$$\frac{1}{R_\delta}\left[\frac{\partial^2}{\partial\eta^2}\left(\frac{q}{q_1}\right)\right]_{\eta=0}=\omega_\delta X^2,$$

or

$$\left[\frac{\partial^2}{\partial\eta^2}\left(\frac{q}{q_1}\right)\right]_{\eta=0}=X^2R_\delta\omega_\delta. \quad (11.10)$$

We also have from Sec. 8 (b)

$$\frac{\partial^4 f}{\partial\eta^4}=\frac{\delta}{X^2}\left[\frac{\partial^3}{\partial\eta^3}\left(\frac{q}{q_1}\right)\frac{\partial}{\partial s}\left(\frac{q}{q_1}\right)+3\frac{\partial^2}{\partial\eta^2}\left(\frac{q}{q_1}\right)\frac{\partial}{\partial s}\frac{\partial}{\partial\eta}\left(\frac{q}{q_1}\right)\right.$$
$$\left.+3\frac{\partial}{\partial\eta}\left(\frac{q}{q_1}\right)\frac{\partial}{\partial s}\frac{\partial^2}{\partial\eta^2}\left(\frac{q}{q_1}\right)+\left(\frac{q}{q_1}\right)\frac{\partial}{\partial s}\frac{\partial^3}{\partial\eta^3}\left(\frac{q}{q_1}\right)\right],$$

and when $\eta=0$

$$\left(\frac{\partial^4 f}{\partial\eta^4}\right)_{\eta=0}=\frac{3\delta}{X^2}\left[\frac{\partial^2}{\partial\eta^2}\left(\frac{q}{q_1}\right)\frac{\partial}{\partial s}\frac{\partial}{\partial\eta}\left(\frac{q}{q_1}\right)+\frac{\partial}{\partial\eta}\left(\frac{q}{q_1}\right)\frac{\partial}{\partial s}\frac{\partial^2}{\partial\eta^2}\left(\frac{q}{q_1}\right)\right]. \quad (11.11)$$

From (11.1) there is also the relation

$$B_4=\frac{1}{24}\left(\frac{\partial^4 f}{\partial\eta^4}\right)_{\eta=0}. \quad (11.12)$$

Then, from (11.10), (11.11), the first term of (11.12) yields

$$\frac{1}{8}\frac{\delta}{X^2}\frac{\partial^2}{\partial\eta^2}\left(\frac{q}{q_1}\right)\frac{\partial}{\partial s}\frac{\partial}{\partial\eta}\left(\frac{q}{q_1}\right)=\frac{1}{4}XR_\delta^2\omega_\delta\delta\left[\frac{dX}{ds}+\frac{X}{q_1}\frac{dq_1}{ds}\right],$$

$$=\frac{3}{8}B_3\omega_\delta, \tag{11.13}$$

according to Eq. (11.3).

Again, for the second term of (11.12), we note first that (11.10) may be written alternatively as

$$\left[\frac{\partial^2}{\partial\eta^2}\left(\frac{q}{q_1}\right)\right]_{\eta=0}=\frac{R_\delta\delta}{\rho q_1^2}\frac{dp}{ds},$$

and therefore

$$\frac{1}{8}\frac{\delta}{X^2}\frac{\partial}{\partial\eta}\left(\frac{q}{q_1}\right)\frac{\partial}{\partial s}\frac{\partial^2}{\partial\eta^2}\left(\frac{q}{q_1}\right)=\frac{1}{8}R_\delta^2\frac{\delta^2}{\rho q_1^2}\frac{d^2p}{ds^2},$$

or, since $\omega_\delta=\delta dp/\tau_0 ds=(\delta/X^2\rho q_1^2)(dp/ds)$, we have, substituting for δ in terms of ω_δ,

$$\frac{1}{8}\frac{\delta}{X^2}\frac{\partial}{\partial\eta}\left(\frac{q}{q_1}\right)\frac{\partial}{\partial s}\frac{\partial^2}{\partial\eta^2}\left(\frac{q}{q_1}\right)=\frac{1}{8}R_\delta^2\omega_\delta^2X^4\rho q_1^2\frac{d^2p}{ds^2}\Big/\left(\frac{dp}{ds}\right)^2.$$

Further,

$$\frac{dp}{ds}=-\rho q_1\frac{dq_1}{ds},$$

$$\frac{d^2p}{ds^2}=-\rho\left[\left(\frac{dq_1}{ds}\right)^2+q_1\frac{d^2q_1}{ds^2}\right],$$

and if the Bernoulli velocity distribution is assumed to be linear, which in general is a reasonable approximation,

$$\frac{d^2p}{ds^2}\Big/\left(\frac{dp}{ds}\right)^2=-\frac{1}{\rho q_1^2}.$$

Hence,

$$\frac{1}{8}\frac{\delta}{X^2}\frac{\partial}{\partial\eta}\left(\frac{q}{q_1}\right)\frac{\partial}{\partial s}\frac{\partial^2}{\partial\eta^2}\left(\frac{q}{q_1}\right)=-\frac{1}{8}X^3R_\delta^2\omega_\delta^2X.$$

But from (11.7)

$$X^3R_\delta^2=\frac{3B_3}{2\left[0.00673\left(\frac{\vartheta}{\delta}\right)^{-13/12}R_\delta^{-1/12}\{1+\omega_\vartheta(H+1)+\omega_\delta X\}\right]}.$$

For brevity write now

$$a \equiv 2\left[0.00673\left(\frac{\vartheta}{\delta}\right)^{-13/12} R_\delta^{-1/12}\{1 + \omega_\vartheta(H+1) + \omega_\delta X\}\right],$$

$$b \equiv 3B_3 = -aX^3R_\delta^2. \tag{11.14}$$

Then the second term of (11.12) reduces to

$$\frac{1}{8}\,\frac{\delta}{X^2}\,\frac{\partial}{\partial\eta}\left(\frac{q}{q_1}\right)\frac{\partial}{\partial s}\,\frac{\partial^2}{\partial\eta^2}\left(\frac{q}{q_1}\right) = \frac{1}{8}\,\frac{b}{a}\,\omega_\delta^2 X, \tag{11.15}$$

and adding (11.13), (11.15),

$$B_4 = \frac{1}{8}\,b\omega_\delta\left(1 + \frac{\omega_\delta X}{a}\right). \tag{11.16}$$

Higher coefficients become progressively more complex, but in view of the fact that the values of η concerned are very small, we may, to a sufficient approximation, restrict the series (11.1) to a quartic, in which case we have

$$\frac{\partial f}{\partial\eta} - \omega_\delta = 3B_3\eta^2 + 4B_4\eta^3,$$

$$= b\eta^2\left[1 + \frac{1}{2}\,\omega_\delta\left(1 + \frac{\omega_\delta X}{a}\right)\eta\right]. \tag{11.17}$$

This equation, substituted in (4.6), then enables the distribution of θ near the surface to be calculated.

For the corresponding distribution in the turbulent part of the boundary layer, we should, to be consistent, correlate Eq. (11.1) with Eq. (8.34), but, as already pointed out, the value of θ_1 depends primarily on the conditions near the surface, and the precise form of $(\partial f/\partial\eta) - \omega_\delta$ at larger values of η appears to be less important, provided the essential conditions relating to f in the turbulent region are satisfied. We will therefore write a second approximation for f outside the laminar layer as

$$f = B_0' + B_1'(1-\eta) + B_2'(1-\eta)^2, \tag{11.18}$$

and satisfy the conditions at $\eta = 1$ and $\eta = \eta^*$, where η^* (see Fig. 6) represents the effective thickness of the laminar sub-layer. Then, from (11.1), (11.2), (11.14), (11.16), (11.17), we have, when $\eta = \eta^*$,

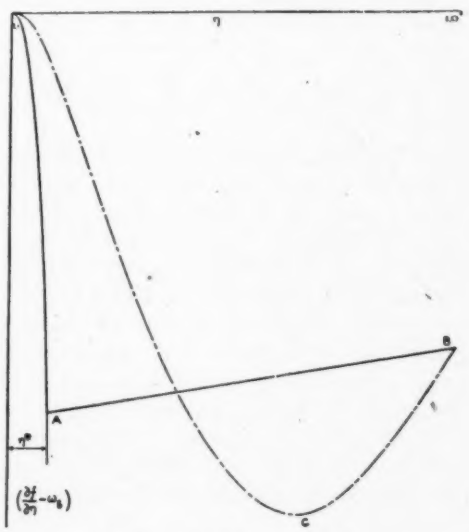

FIG. 6.

$$f = 1 + \omega_s\eta^* + \frac{1}{3}b\eta^{*3}\left[1 + \frac{3}{8}\omega_s\left(1 + \frac{\omega_s X}{a}\right)\eta^*\right],$$

$$\frac{\partial f}{\partial \eta} = \omega_s + b\eta^{*2}\left[1 + \frac{1}{2}\omega_s\left(1 + \frac{\omega_s X}{a}\right)\eta^*\right],$$

and when $\eta = 1$, $f = \partial f/\partial\eta = 0$.

Hence, equating f and $\partial f/\partial\eta$, as given by (11.18), to the above boundary conditions at $\eta = \eta^*$ and $\eta = 1$, we obtain

$$B_0' = B_1' = 0,$$

$$B_2' = -\frac{1}{2}\left[\frac{\omega_s + b\eta^{*2}\left\{1 + \frac{1}{2}\omega_s\left(1 + \frac{\omega_s X}{a}\right)\eta^*\right\}}{(1 - \eta^*)}\right], \tag{11.19}$$

and

$$1 + \omega_s + \frac{1}{3}b\eta^{*3}\left[1 + \frac{3}{8}\omega_s\left(1 + \frac{\omega_s X}{a}\right)\eta^*\right] + \frac{1}{2}\left[b\eta^{*2}\left\{1 + \frac{1}{2}\omega_s\left(1 + \frac{\omega_s X}{a}\right)\eta^*\right\} - \omega_s\right](1 - \eta^*) = 0, \tag{11.20}$$

which are the two equations from which to solve for B_2' and η^*.

The distribution of the quantity $(\partial f/\partial\eta) - \omega_s$ in the turbulent layer is then given by the linear relationship

$$\left(\frac{\partial f}{\partial \eta} - \omega_s\right) = -\omega_s - 2B_2'(1 - \eta). \tag{11.21}$$

This is illustrated in Fig. 6, where the line AB represents the solution in the turbulent region (Eq. 11.21), and the curve OA the corresponding solution in the laminar layer, as given by Eq. (11.17). The chain curve OCB has been included for comparison, and is the solution developed in section 8 (b). The curves are approximately to scale, and refer to the same flow conditions. The effect of viscosity near the surface evidently has a large influence on the initial distribution of the shear stress, and hence upon θ_1. For small values of η there is no reason to doubt the accuracy of the curve OA, but further from the surface the treatment of section 8 (b) is probably a closer approximation than that afforded by the series (11.18). The true solution would therefore appear to be represented by a transition curve linking OA as $\eta \to 0$ with OCB as $\eta \to 1$.

One final point needs consideration. When $\eta = 0$, so also $(\partial f/\partial\eta) - \omega_s = q = 0$, and therefore the initial value of $\partial\theta/\partial\eta$ becomes indeterminate. This may be circumvented by the following argument. From (11.16)

$$\mathop{\mathcal{L}}_{\eta\to 0}\left(\frac{\partial f}{\partial \eta} - \omega_s\right) = b\eta^2.$$

Likewise,

$$\mathop{\mathcal{L}}_{\eta\to 0}\left(\frac{q}{q_1}\right)^2 = R_\delta^2 X^4 \eta^2.$$

Hence, from Eq. (4.5),

$$\mathop{\mathcal{L}}_{\eta\to 0}\left(\frac{\partial\theta}{\partial\eta}\right) = \frac{b}{R_\delta^2 X^2} = -aX.$$

12. Solution of Eq. (5.9) for $\vartheta dH/ds$. Since, by definition,

$$\omega_\vartheta = \omega_\delta\left(\frac{\vartheta}{\delta}\right),$$

we have, according to Eq. (9.3),

$$\omega_\vartheta = \omega_\delta \frac{\alpha^2}{\beta}\left(\frac{H-1}{H^2}\right). \tag{12.1}$$

Combining, now, Eqs. (4.6), (8.29), (8.53), (12.1) with Eq. (5.9),

$$\vartheta\frac{dH}{ds} = -X_0^2\left(\frac{\Lambda}{\Lambda_0}\right)^2\left[\omega_\delta + H\left\{1+\omega_\delta\frac{\alpha^2}{\beta}\left(\frac{H^2-1}{H^2}\right)\right\} + \int_0^1 \frac{\left(\frac{\partial f}{\partial\eta}-\omega_\delta\right)}{\left(1+I_2X_0\frac{\Lambda}{\Lambda_0}\right)^2}d\eta\right], \tag{12.2}$$

where I_2, α, β are found as described in section (10), and $(\partial f/\partial\eta)-\omega_\delta$ is given by Eq. (11.17) in the range $0<\eta<\eta^*$, and by Eq. (11.21) in the range $\eta^*<\eta<1$.

Considering the functional nature of the terms, excluding H for the moment, on the right hand side of Eq. (12.2), it is evident that they are either functions of ω_δ and R_δ, or of ω_δ or R_δ separately. Hence we may write

$$\vartheta\frac{dH}{ds} = \phi_1(\omega_\delta, R_\delta, H). \tag{12.3}$$

Actually, from Eq. (9.4), H is also a function of ω_δ and R_δ, so that (12.3) reduces to

$$\vartheta\frac{dH}{ds} = \phi_2(\omega_\delta, R_\delta). \tag{12.4}$$

For the numerical integration of Eqs. (5.9), (5.10) along the lines of refs. (1) and (2), however, it is desirable to retain the form (12.3).

We now show how (12.2) may be evaluated in terms of the data discussed in section (6), namely, when the static pressure and the initial values of ϑ and H at each step are known.

From Eqs. (9.3), (9.4) we have

$$\delta = \frac{\vartheta H}{\alpha X} = \frac{\vartheta H}{\alpha X_0 \dfrac{\Lambda}{\Lambda_0}}, \tag{12.5}$$

or,

$$\omega_\vartheta = (\omega_\vartheta)_0 \frac{H}{\alpha X_0 \left(\dfrac{\Lambda}{\Lambda_0}\right)^3}, \tag{12.6}$$

where

$$(\omega_\vartheta)_0 = \frac{\vartheta}{\rho q_1^2 X_0^2} \frac{dp}{ds} = -\frac{\vartheta}{X_0^2} \frac{1}{q_1} \frac{dq_1}{ds}.$$

Eq. (12.5), or (12.6), can be solved as follows. Given ϑ, X_0 is determined from the law relating X_0 and R_ϑ, i.e. Falkner's power law,[8] or the logarithmic law of Squire and Young.[6] Now assume a value of ω_δ; hence we obtain Λ/Λ_0 (which is purely a function of ω_δ) by calculation according to section 8 (b), or, alternatively, from Fig. 3. X then follows. This enables a value of δ to be found consistent with the assumed value of ω_δ, and the corresponding value of R_δ is calculated. Finally, knowing both ω_δ and R_δ, we obtain α from section (9), and, since H is given, a second approximation for δ (or ω_δ) follows from Eqs. (12.5), (12.6). Hence, by trial and error, or by pre-established families of curves, we may solve for the relation between δ and ϑ. By virtue of Eqs. (12.5), (12.6), therefore, (12.2) is expressible in terms of ϑ, H and the pressure distribution, so that formally we have

$$\vartheta \frac{dH}{ds} = \phi_3[(\omega_\vartheta)_0, R_\vartheta, H]. \tag{12.7}$$

In conclusion it is worth noting that $(\omega_\vartheta)_0$ is a multiple of Garner's variable Γ, as it is of von Doenhoff's corresponding term. Thus, Garner takes

$$\Gamma \equiv \vartheta R_\vartheta^{1/6} \frac{1}{q_1} \frac{dq_1}{ds}, \tag{12.8}$$

and assumes Falkner's power law for the skin friction, viz.

$$X_0^2 = 0.006534 R_\vartheta^{-1/6}, \tag{12.9}$$

so that combining (12.8), (12.9)

$$\Gamma = 0.006534 \frac{\vartheta}{X_0^2} \frac{1}{q_1} \frac{dq_1}{ds},$$

$$= -0.006534(\omega_\vartheta)_0.$$

Similarly, von Doenhoff's term, which we will denote by Γ', is

$$\Gamma' = 2 \frac{\vartheta}{X_0^2} \frac{1}{q_1} \frac{dq_1}{ds} = -2(\omega_\vartheta)_0.$$

Consequently, as discussed in section (6), both the theoretical Eq. (12.2) and the empirical equations for $\vartheta dH/ds$ of refs. (1) and (2) contain the same basic parameters.

13. Comparison of Eq. (12.2) with the corresponding relations of von Doenhoff and Garner. For comparison we have taken, as examples, the case (a) when $\omega_\delta = 0$, (b) when $\omega_\delta = 30$, the range of $\log R_\delta$ considered being in both cases $3.5 < \log R_\delta < 6.0$. For (b) this range of Reynolds number allows a wide variation of flow conditions to be studied, from virtually the plane flow state up to separation, which is imminent when H exceeds 1.8.

TABLE 1.

$\omega_\delta = 0$

Log $q_1\delta/\nu$	α	β	X	H	ϑ/δ	Log $q_1\vartheta/\nu$	$\vartheta dH/ds \times 10^3$		
							Ref. 1	Ref. 2	Theory
3.5	2.845	20.21	0.0526	1.596	0.0937	2.471	−0.996	−2.731	−0.047
4.0	2.724	17.29	0.0464	1.421	0.0896	2.952	−0.190	−0.102	+0.306
4.5	2.682	16.10	0.0413	1.330	0.0835	3.422	−0.041	+0.179	0.298
5.0	2.667	15.57	0.0371	1.277	0.0776	3.890	+0.007	0.202	0.271
5.5	2.662	15.31	0.0338	1.242	0.0727	4.362	0.027	0.182	0.190
6.0	2.660	15.23	0.0309	1.215	0.0677	4.831	0.038	0.155	0.157

TABLE 2.

$\omega_\delta = 30$

Log $q_1\delta/\nu$	α	β	X	H	ϑ/δ	Log $q_1\vartheta/\nu$	$\vartheta dH/ds \times 10^3$		
							Ref. 1	Ref. 2	Theory
3.5	7.770	103.49	0.0379	2.020	0.1460	2.665	35.6	72.7	62.0
4.0	8.086	114.81	0.0334	1.902	0.1421	3.153	20.7	35.1	40.9
4.5	8.187	119.66	0.0297	1.770	0.1376	3.639	12.65	15.4	24.6
5.0	8.223	121.68	0.0267	1.654	0.1328	4.123	7.58	7.58	14.9
5.5	8.233	122.36	0.0243	1.566	0.1279	4.607	5.06	4.34	9.23
6.0	8.237	122.67	0.0222	1.495	0.1224	5.088	3.60	2.62	5.68

Tables 1 and 2 and Fig. 7 summarize the results, those of refs. (1) and (2) having been calculated from the formulae there given, which, for the present purpose, may be most conveniently expressed in the notation of the present paper as follows:

Von Doenhoff and Tetervin[1]

$$\vartheta \frac{dH}{ds} = e^{4.68(H-2.975)}\left[2(\omega_\vartheta)_0 - 2.035(H - 1.286)\right], \tag{13.1}$$

with X_0 given by Squire's and Young's formula

$$X_0^2 = \left[5.890 \log_{10} (4.075 R_\vartheta)\right]^{-2};$$

Garner[2]

$$\vartheta \frac{dH}{ds} = X_0^2 e^{5(H-1\cdot4)}\left[(\omega_\vartheta)_0 - 2.068(H - 1.4)\right], \tag{13.2}$$

where X_0 is based on Falkner's formula

$$X_0^2 = 0.006534 R_\vartheta^{-1/6}.$$

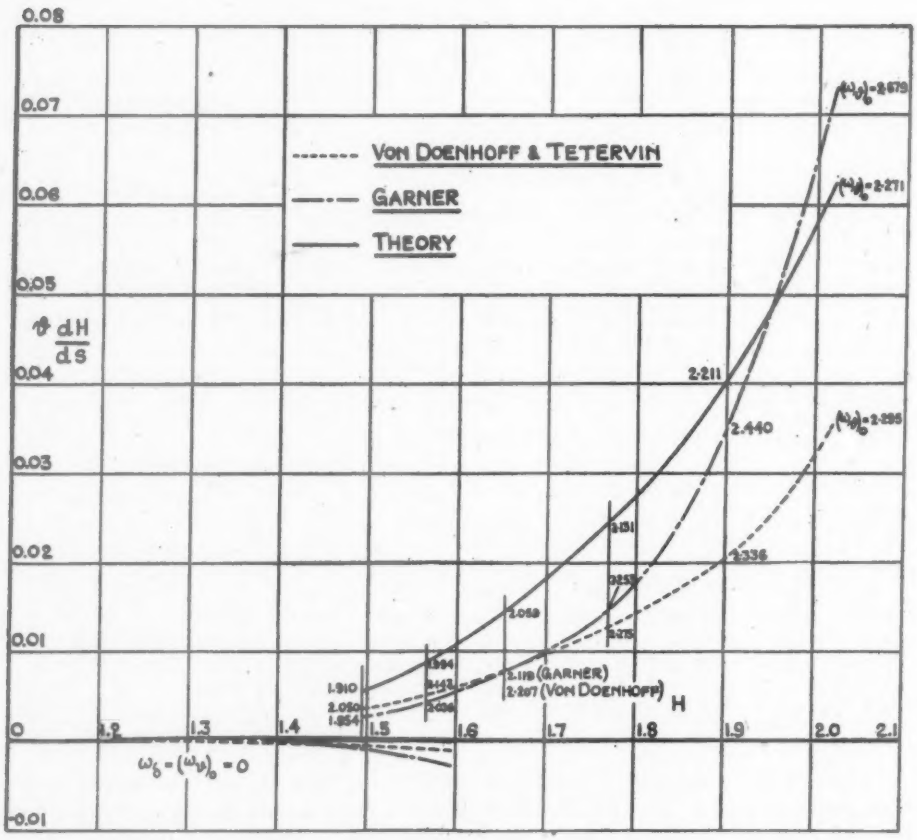

FIG. 7. Comparison of theoretical and empirical solutions for $\vartheta dH/ds$.

In estimating $(\omega_\vartheta)_0$, when $\omega_\delta = 30$, the skin friction law adopted in each case has been adhered to. Thus, for theoretical values of $(\omega_\vartheta)_0$ Eq. (8.48) applies, whilst for the empirical formulae of von Doenhoff and Garner the particular skin friction equations given above have been used. This leads to slight variations of $(\omega_\vartheta)_0$ under otherwise similar conditions, as will be seen from Fig. 7, where the appropriate value of $(\omega_\vartheta)_0$ is indicated against each point to facilitate comparison.

For plane flow ($\omega_\delta = 0$), both the theoretical and empirical results are in good agreement at large Reynolds numbers, but there is some discrepancy at lower values when H becomes abnormally large due to the very thick laminar sub-layer. Under these circumstances the theory is probably unreliable, so that some deviation is to be expected. The condition that $dH/ds \doteqdot 0$, or, as is generally assumed, $H = \text{constant}$ when the pressure gradient is zero or small, is, however, well substantiated by theory.

Under conditions of a pronounced pressure gradient, tending to separation, agreement is less satisfactory, not only between the theoretical and semi-empirical solutions, but also between von Doenhoff's and Garner's results.

Some comment on these discrepancies was made in the introduction. It was there pointed out that the theory is consistent with Garner's relation in that both indicate $\vartheta dH/ds$ to be a function of ω_ϑ, R_ϑ and H, whereas the von Doenhoff-Tetervin equation does not contain R_ϑ as an independent parameter. Consequently, in this respect, theoretical calculations might be expected to agree (as is the case) more nearly with Eq. (13.2) than with Eq. (13.1), the latter probably being less generally representative on account of the above restriction.

A further point of interest in regard to the empirical formulae is the value of H when $dH/ds = \omega_\delta = \omega_\vartheta = 0$. From (13.1), (13.2) it will be noted that, according to von Doenhoff and Tetervin, H then has the value 1.286, whereas Garner, after investigating the variation of H at transition in some detail, concludes that the value 1.4 is a better approximation. As already observed, $\vartheta dH/ds$ is very small within the normal range of H when ω_δ is zero, so that any slight discrepancy to which the above quantity may be subject will introduce a large change in the value of H at which dH/ds is precisely zero. In the empirical approach dH/ds was obtained graphically, and therefore the difference between the values of H under the afore-mentioned conditions, as given in refs. (1) and (2), is probably due to errors in the graphical method. By interpolation of the theoretical results in Table 1, the corresponding value of H is found to be about 1.56. Allowing for the approximate nature of the theory, which may accordingly imply errors in the above H value of the same order as for the empirical formulae, it follows, nevertheless, that Garner's figure of 1.4 is perhaps a better estimate than that of von Doenhoff and Tetervin.

In conclusion, the general form of the equation for $\vartheta dH/ds$ appears to be established, and a method of analyzing the growth of the turbulent boundary layer has been developed. In practice, however, it is laborious to use, though by extensive graphical treatment it is considered that the work could be reduced to reasonable proportions. Alternatively, if some degree of empiricism is acceptable, a reasonably reliable, simple and rapid means of reaching a solution is possible on the lines of refs. (1) and (2).

Appendix

According to Eq. (11.8)

$$\frac{\tau}{\rho q_1^2} = \frac{1}{R_\delta}\frac{\partial}{\partial \eta}\left(\frac{q}{q_1}\right) + \lambda^2\left|\frac{\partial}{\partial \eta}\left(\frac{q}{q_1}\right)\right|\frac{\partial}{\partial \eta}\left(\frac{q}{q_1}\right). \tag{A}$$

The first term on the right hand side of (A) represents the true viscous shear stress, whilst the second term represents the Reynolds stress. Where the laminar sub-layer merges with the fully turbulent layer, the former stress becomes vanishingly small in

relation to the latter. Let η_l denote the value of η at which the viscous stress is virtually negligible, and let the ratio of Reynolds stress to viscous stress at this point be m. Then

$$\lambda^2 \left| \frac{\partial}{\partial \eta}\left(\frac{q}{q_1}\right) \right| \frac{\partial}{\partial \eta}\left(\frac{q}{q_1}\right) = \frac{m}{R_\delta} \frac{\partial}{\partial \eta}\left(\frac{q}{q_1}\right). \tag{B}$$

Also near the surface

$$\lambda = \Lambda \eta, \tag{C}$$

and approximately we may write

$$\frac{\partial}{\partial \eta}\left(\frac{q}{q_1}\right) = R_\delta X^2. \tag{D}$$

Hence, by combining (B), (C), (D) and re-arranging, we have

$$\eta_l = \frac{\sqrt{m}}{\Lambda R_\delta X}, \tag{E}$$

so that if η_0 of section 8 (c) is regarded as proportional to η_l,

$$\eta_0 \sim \eta_l \sim \frac{1}{R_\delta X}. \tag{F}$$

By writing $\sqrt{m}/\Lambda$ = constant, Eq. (E) becomes identical with von Kármán's equation[12] for the non-dimensional thickness of the laminar sub-layer. For the constant von Kármán finds the approximate value 30. Then if we take the condition of plane flow, when

$$\Lambda = \Lambda_0 = 0.392,$$

we see that

$$\sqrt{m} = 30 \times 0.392 = 11.76.$$

or

$$m = 138.3.$$

Thus the viscous stress is locally 1/138.3 of the Reynolds stress, i.e. it amounts to slightly less than 1% of it.

—NOTES—

THE PRODUCT OF THREE REFLECTIONS*

By H. S. M. COXETER (*University of Toronto*)

1. Introduction. This paper completes a trilogy, as it is a sequel to Synge's "Reflection in a corner formed by three plane mirrors" and Tuckerman's "Multiple reflections by plane mirrors."[1] However, it is written in such a way as to be self-contained.

The product of reflections in two intersecting planes is easily seen to be a rotation about the line of intersection of the planes through twice the angle between them. Hence the product of three reflections is, in general, a *rotatory reflection*: the product of a rotation and a reflection. We shall see (in §2) that, by a suitable displacement of the mirrors, without altering the final effect, we can arrange for the axis of the rotation to be perpendicular to the plane of the remaining reflection, so that the rotation and reflection are commutative. [An exception arises in the case of three "vertical" mirrors, all perpendicular to one plane. Then the product is a *glide-reflection*: the combination of a translation and a reflection. We shall discuss that case in Sec. 8.]

If the three mirrors have a common point, we represent them by the great circles which they cut out on the unit sphere around the point. Of the eight spherical triangles formed by the three great circles, just one is distinguished by having the three "fronts" of the mirrors all facing inwards. We shall call this the *mirror triangle* and denote it by **ABC**. [Similarly, if the three mirrors are all vertical, we represent them by the sides of the plane triangle **ABC** which they cut out on a horizontal plane.]

Let $\mathbf{AA_1}$, $\mathbf{BB_1}$, $\mathbf{CC_1}$ be the *altitudes* of triangle **ABC**; then $\mathbf{A_1B_1C_1}$ is called the *pedal triangle* (or "orthic triangle") of **ABC**. (See Fig. 1.) We shall find that the product of reflection in the three sides of an acute-angled triangle **ABC**, in any particular order, is a rotatory reflection [or glide-reflection] consisting of the reflection in one side of the pedal triangle combined with a rotation [or translation] along that side, of an amount equal to the perimeter of the pedal triangle. The three sides of the pedal triangle, with two senses along each, account for the six possible orders of the three reflections. We shall reconcile this with the results of Synge and Tuckerman, and finish with a brief statement concerning the analogous problem in m dimensions.

Steiner remarked in 1837 that the pedal triangle of an acute-angled spherical triangle **ABC** is the triangle of minimum perimeter inscribed in **ABC**. The present treatment was suggested by Schwarz's beautiful proof of the corresponding theorem for plane triangles.[2]

For simplicity, all the spherical triangles in the diagrams have been drawn as

---

* Received Sept. 11, 1946.

[1] This Quarterly **4**, 166–176 (1946), **5**, 133–148 (1947).

[2] Steiner, *Aufgaben und Lehrsätze*, Gesammelte Werke, vol. 2, Berlin, 1882, p. 45 (No. 7). Schwarz, *Beweis des Satzes, dass unter allen einem spitzwinkligen Dreiecke eingeschriebenen Dreiecken das Dreieck der Höhenfusspunkte den kleinsten Umfang hat*, Gesammelte Mathematische Abhandlungen, vol. 2, Berlin, 1890, pp. 344–345.

plane triangles. This economy is justified by the fact that the results remain valid in the case of three vertical mirrors.

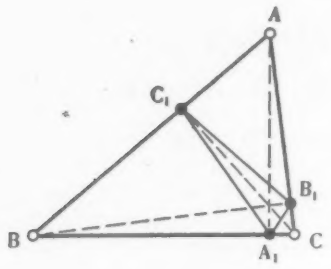

FIG. 1

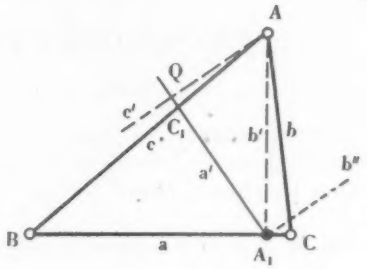

FIG. 2

The author wishes to express his gratitude to Professor Synge for many helpful suggestions in connection with this work.

2. The sides of the pedal triangle. If a congruent transformation of the sphere leaves a great circle invariant (as a whole, but not necessarily point by point) it is either the reflection in the plane of the great circle, or a rotation about the perpendicular line (which we call a rotation *along* the great circle), or the combination of both: a rotatory reflection. In the last case we shall call the great circle the *line of action* of the rotatory reflection. In general it is unique: no other great circle is invariant under the given transformation. The only exception is when the rotation is a half-turn, or rotation through π; then the rotatory reflection reduces to the *central inversion*, which reverses all vectors and transforms each point of the sphere into its antipodal point.

Let A, B, C denote the reflections in the sides $\mathbf{a}$, $\mathbf{b}$, $\mathbf{c}$ of the mirror triangle $\mathbf{ABC}$. The product BC (first B, then C) is a rotation through $-2A$ about the vertex $\mathbf{A}$ (or about the line to $\mathbf{A}$ from the center of the sphere). This can just as well be expressed as the product of reflections in *any* two great circles through $\mathbf{A}$ making this same angle A, say $\mathbf{b}'$ and $\mathbf{c}'$. Choosing $\mathbf{b}'$ to be the altitude $\mathbf{AA}_1$, as in Fig. 2, we have $ABC=AB'C'$, where AB' is a half-turn: the product of reflections in two perpendicular great circles through $\mathbf{A}_1$. But this half-turn can just as well be expressed as the product of reflections in *any* two perpendicular great circles through $\mathbf{A}_1$, say $\mathbf{a}'$ and $\mathbf{b}''$. Choosing $\mathbf{a}'$ to be $\mathbf{A}_1\mathbf{Q}$ perpendicular to $\mathbf{c}'$, we have $AB'C'=A'B''C'$, where $\mathbf{a}'$ is perpendicular to both $\mathbf{b}''$ and $\mathbf{c}'$. Thus $ABC=A'B''C'$: the product of the reflection A' and the commutative rotation $B''C'$.

This shows that the line of action of the rotatory reflection ABC passes through $\mathbf{A}_1$. Similarly that of CBA passes through $\mathbf{C}_1$. But ABC and CBA, being inverse transformations, have the same line of action (in opposite senses). Therefore this line of action is the great circle $\mathbf{A}_1\mathbf{C}_1$. Moreover, the sense of the rotation $B''C'$ is from $\mathbf{A}_1$ towards $\mathbf{C}_1$. Hence

THEOREM 2.1. *The six rotatory reflections* ABC, CBA, BCA, ACB, CAB, BAC *consist of reflections in the sides of the pedal triangle* $\mathbf{A}_1\mathbf{B}_1\mathbf{C}_1$ *combined with rotations along those sides in the senses* $\mathbf{A}_1\mathbf{C}_1$, $\mathbf{C}_1\mathbf{A}_1$, $\mathbf{B}_1\mathbf{A}_1$, $\mathbf{A}_1\mathbf{B}_1$, $\mathbf{C}_1\mathbf{B}_1$, $\mathbf{B}_1\mathbf{C}_1$.

The amount of rotation, being twice the angle between $\mathbf{b}''$ and $\mathbf{c}'$, is equal to $2\mathbf{A}_1\mathbf{Q}$, which is less than π for a sufficiently small triangle **ABC**, and consequently (by continuity) less than π for any triangle except a trirectangular one; for that is the only case where it can attain the value π(which gives the central inversion).

3. Two geometrical theorems. The rearrangement of reflections that led to the equation $ABC = A'B''C'$ provides a kinematical proof for

THEOREM 3.1. *If* $\mathbf{A}_1\mathbf{B}_1\mathbf{C}_1$ *is the pedal triangle of a spherical triangle* **ABC**, *the perpendicular from* **A** *to* $\mathbf{A}_1\mathbf{C}_1$ *makes an angle* A *with the altitude* $\mathbf{AA}_1$.

Similarly the perpendicular from **A** to $\mathbf{A}_1\mathbf{B}_1$ makes this same angle A with $\mathbf{AA}_1$. (See Fig. 3.) Thus $\mathbf{AA}_1$ bisects the angle between the perpendiculars to $\mathbf{A}_1\mathbf{C}_1$ and $\mathbf{A}_1\mathbf{B}_1$. Consequently it also bisects the angle between $\mathbf{A}_1\mathbf{C}_1$ and $\mathbf{A}_1\mathbf{B}_1$ themselves. Thus $\mathbf{AA}_1$ is the internal bisector of $\angle \mathbf{B}_1\mathbf{A}_1\mathbf{C}_1$, and **BC** is the external bisector. Hence

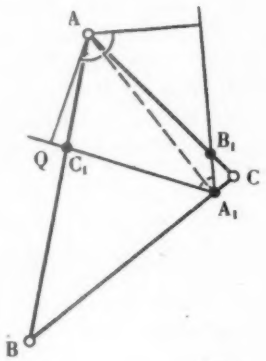

FIG. 3

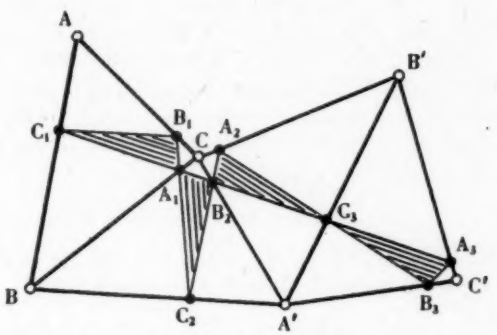

FIG. 4

THEOREM 3.2. *The orthocenter and vertices of a spherical triangle* **ABC** *are the incenter and excenters of its pedal triangle* $\mathbf{A}_1\mathbf{B}_1\mathbf{C}_1$.

This theorem can hardly be new, as its plane analogue is so familiar (see Fig. 1); but some of the standard textbooks fail to mention it. We have considered an acute-angled triangle **ABC**; but the effect of an obtuse C is merely to make **C** the incenter of $\mathbf{A}_1\mathbf{B}_1\mathbf{C}_1$ (so that the orthocenter of **ABC** is an excenter of $\mathbf{A}_1\mathbf{B}_1\mathbf{C}_1$).

The converse is, of course, obvious: If the external bisectors of the angles of any triangle $\mathbf{A}_1\mathbf{B}_1\mathbf{C}_1$ form a triangle **ABC**, the internal bisectors are the altitudes of **ABC**.

4. The perimeter of the pedal triangle. (For this part of the work we cannot allow any of the angles A, B, C to be obtuse.) By Theorem 3.2, **A** is the center of an excircle of triangle $\mathbf{A}_1\mathbf{B}_1\mathbf{C}_1$ (viz., the excircle beyond the side $\mathbf{B}_1\mathbf{C}_1$). The arc $\mathbf{A}_1\mathbf{Q}$ (Fig. 3), being one of the tangents from $\mathbf{A}_1$ to this small circle, is equal to s_1, the semiperimeter of triangle $\mathbf{A}_1\mathbf{B}_1\mathbf{C}_1$. As we saw at the end of §2, this arc is half the amount of the rotation $B''C'$. Hence

THEOREM 4.1. *The amount of rotation involved in the product of reflections in the sides of an acute-angled spherical triangle* **ABC**, *in any order, is equal to the perimeter of the pedal triangle* $\mathbf{A}_1\mathbf{B}_1\mathbf{C}_1$.

The right triangle $\mathbf{AA_1Q}$ has side $\mathbf{A_1Q} = s_1$ and hypotenuse $\mathbf{AA_1} = h_a$. Hence[3]

$$\sin s_1 = \sin h_a \sin A$$

$$= 2N = -2\frac{\cos S}{\tan R} = \frac{2 \sin \Delta/2}{\tan R} \tag{4.2}$$

where Δ is the area (or spherical excess) of triangle **ABC**, and R is the circumradius.

The equation $\sin \mathbf{A_1Q} = 2N$ remains valid when C is obtuse. But then (if A and B are still acute) the excircle of $\mathbf{A_1B_1C_1}$ that has center **A** is the one beyond $\mathbf{C_1A_1}$, so the tangent $\mathbf{A_1Q}$ is not s_1 but $s_1 - c_1$, and the amount of rotation is

$$2\mathbf{A_1Q} = 2(s_1 - c_1) = a_1 + b_1 - c_1.$$

The following alternative proof of Theorem 4.1 is possibly of some interest. Beginning with the acute-angled triangle **ABC**, let us reflect in the side **BC** to obtain **A′BC**, then reflect the latter in its side **CA′** to obtain **A′B′C**, and finally reflect **A′B′C** in **A′B′** to obtain **A′B′C′**, as in Fig. 4. Let the respective pedal triangles be $\mathbf{A_1B_1C_1}$, $\mathbf{A_1B_2C_2}$, $\mathbf{A_2B_2C_3}$, $\mathbf{A_3B_3C_3}$. Since **BC** is the external bisector of $\angle \mathbf{B_1A_1C_1}$, the great circle $\mathbf{C_1A_1}$ contains $\mathbf{B_2}$; similarly it also contains $\mathbf{C_3}$ and $\mathbf{A_3}$. The rotatory reflection *CBA*, which transforms the triangles **ABC** and $\mathbf{A_1B_1C_1}$ into **A′B′C′** and $\mathbf{A_3B_3C_3}$, is thus clearly exhibited as the reflection in the great circle $\mathbf{C_1A_1}$ combined with a rotation *along* that great circle, of amount

$$\mathbf{C_1C_3} = \mathbf{A_1A_3} = \mathbf{A_1B_2} + \mathbf{B_2C_3} + \mathbf{C_3A_3} = c_1 + a_1 + b_1 = 2s_1.$$

On the other hand, when C is obtuse (while A and B are acute) the point $\mathbf{B_2}$ is situated between $\mathbf{C_1}$ and $\mathbf{A_1}$, so we have

$$\mathbf{C_1C_3} = \mathbf{A_1A_3} = -\mathbf{B_2A_1} + \mathbf{B_2C_3} + \mathbf{C_3A_3} = -c_1 + a_1 + b_1 = 2(s_1 - c_1).$$

5. The principle of transformation. Let S denote the sphere in any particular position. Let E and F be two congruent transformations which change S into S^E and S^F (without moving the center). Then F changes S and S^E into S^F and S^{EF}. Since $S^{EF} = (S^F)^{F^{-1}EF}$, this means that F *transforms* the operation E into $F^{-1}EF$. Whatever kind of operation E may be, $F^{-1}EF$ is the same kind; e.g., if E is a rotation through a certain angle about an axis l, $F^{-1}EF$ will be a rotation through the same angle about the transformed axis l^F.

Now, since the reflection A transforms the rotatory reflection ABC into $A^{-1} \cdot ABC \cdot A = BCA$, it follows that A reflects the line of action $\mathbf{A_1C_1}$ of the former into the line of action $\mathbf{B_1A_1}$ of the latter; so we have an alternative proof that **BC** is the external bisector of the angle $\mathbf{B_1A_1C_1}$.

The same principle would have enabled us to foresee that the amount of rotation involved in ABC is the same as in BCA or CAB. (The remaining products CBA, ACB, BAC obviously involve the same amount of rotation, because they are the inverse operations.)

6. The case of a right triangle. When two of the mirrors are perpendicular, the pedal triangle collapses.

---

[3] For this use of the letters N and S, see Todhunter, *Spherical trigonometry*, London, 1914, pp. 29, 33. 92, 109; or McClelland and Preston, *A treatise on spherical trigonometry*, London, 1886, Part I, p. 55, and Part II, p. 11.

If only one right angle occurs, one line of action is the altitude to the hypotenuse; to be precise, if C is a right angle (so that $\mathbf{A}_1$ and $\mathbf{B}_1$ coincide with $\mathbf{C}$, and $AB=BA$), then $\mathbf{CC}_1$ is the line of action of $ABC=BAC$ (or, in the opposite sense, of $CBA=CAB$). By the principle of transformation, the only other line of action (viz., that of ACB and its inverse BCA) is the image of $\mathbf{CC}_1$ by reflection in either of the two perpendicular mirrors. The amount of rotation is equal to the perimeter of the collapsed pedal triangle, viz., $2h_c$.

If two right angles occur, there are only two inverse rotatory reflections, and the unique line of action is provided by that mirror which is perpendicular to both the others. But if all three angles are right angles, the product is the central inversion, and the line of action is indeterminate.

To sum up: the number of distinct lines of action, regardless of sense, is equal to the number of oblique angles.

7. Comparison with the work of Synge and Tuckerman. Synge represents the three mirrors by respectively perpendicular unit vectors $\mathbf{N}_1$, $\mathbf{N}_2$, $\mathbf{N}_3$, and thence by points (having the same names) on the unit sphere. He shows that the product of the three reflections is a *rotatory inversion*, i.e., a rotation about a certain axis combined with the central inversion (p. 168). The amount of the rotation, denoted by θ, is a certain function of the vectors $\mathbf{N}_1$, $\mathbf{N}_2$, $\mathbf{N}_3$. The six possible permutations of the three mirrors lead to rotations through $\pm\theta$ about three axes, each combined with the central inversion. These three "optic axes" are represented by unit vectors $\mathbf{A}_1$, $\mathbf{A}_2$, $\mathbf{A}_3$; and he shows very elegantly that the points $\mathbf{N}_1$, $\mathbf{N}_2$, $\mathbf{N}_3$ are the midpoints of the sides of the spherical triangle $\mathbf{A}_1\mathbf{A}_2\mathbf{A}_3$ (p. 170) and that $\pi+\theta$ is equal to the spherical excess of that triangle (p. 172).

Since the central inversion may be regarded as a rotatory reflection involving rotation through π, a rotatory inversion involving rotation through θ is the same as a rotatory reflection involving rotation through $\pi+\theta$ (or through $\pi-\theta$ in the opposite sense). The axis of the rotatory inversion joins the poles of the line of action of the rotatory reflection.

Thus Synge's $\mathbf{N}_1\mathbf{N}_2\mathbf{N}_3$ and $\mathbf{A}_1\mathbf{A}_2\mathbf{A}_3$ are the *polar triangles* of our $\mathbf{ABC}$ and $\mathbf{A}_1\mathbf{B}_1\mathbf{C}_1$. His statement that $\mathbf{N}_1$, $\mathbf{N}_2$, $\mathbf{N}_3$ are the midpoints of the sides of $\mathbf{A}_1\mathbf{A}_2\mathbf{A}_3$ is simply the dual of our statement that each side of triangle $\mathbf{ABC}$ makes equal angles with the two non-corresponding sides of triangle $\mathbf{A}_1\mathbf{B}_1\mathbf{C}_1$. (Theorem 3.2.) Similarly, dualizing the statement that $\mathbf{AB}$ is perpendicular to $\mathbf{CC}_1$, we find[4] that $\mathbf{N}_3$ is distant $\pi/2$ from the point of intersection $(\mathbf{N}_1\mathbf{N}_2\cdot\mathbf{A}_1\mathbf{A}_2)$.

Since the angles of Synge's triangle $\mathbf{A}_1\mathbf{A}_2\mathbf{A}_3$ are supplementary to the sides of its polar triangle (our $\mathbf{A}_1\mathbf{B}_1\mathbf{C}_1$), the spherical excess of the former is equal to

$$(\pi - a_1) + (\pi - b_1) + (\pi - c_1) - \pi = 2\pi - (a_1 + b_1 + c_1) = 2\pi - 2s_1.$$

Thus $\pi-\theta=2s$, in agreement with our Theorem 4.1.

Tuckerman obtains the same results again, representing the vectors by pure quaternions. His method shows very simply that $\pm\cos\theta/2$ is equal to the scalar triple product of the vectors $\mathbf{N}_1$, $\mathbf{N}_2$, $\mathbf{N}_3$ (which Synge denotes by P). Consequently

$$\cos\theta = 2P^2 - 1 = 8\sin\sigma\sin(\sigma-\alpha_1)\sin(\sigma-\alpha_2)\sin(\sigma-\alpha_3) - 1,$$

[4] Todhunter, *op. cit.*, p. 114.

where α_1, α_2, α_3, σ are the sides and semiperimeter of the spherical triangle $\mathbf{N_1N_2N_3}$. Comparing Synge's (3.10) with Tuckerman's analogous Eqs. (13), we see that

$$\sin^2 \theta/2 = k^{-2} = \cos^2 \alpha_1 + \cos^2 \alpha_2 + \cos^2 \alpha_3 - 2 \cos \alpha_1 \cos \alpha_2 \cos \alpha_3.$$

In terms of the mirror triangle **ABC** (with $2s_1 = \pi - \theta$), this takes the form

$$\cos^2 s_1 = \cos^2 A + \cos^2 B + \cos^2 C + 2 \cos A \cos B \cos C. \qquad (7.1)$$

Thus $\sin s_1 = P = 2N$, in agreement with (4.2).

8. Three mirrors forming a prism. When the common point of the three mirrors recedes to infinity, so that the mirrors are all perpendicular to one plane, we have essentially a two-dimensional problem: the product of reflections in the three sides of a plane triangle **ABC**. Work analogous to §2 gives $ABC = A'B''C'$, where A' is the reflection in a line $\mathbf{a}'$ perpendicular to both $\mathbf{b}''$ and $\mathbf{c}'$. We now have a glide-reflection: the product of the reflection A' and the translation $B''C'$ along the "line of action" $\mathbf{a}'$. Theorems 2.1 and 4.1 remain valid with the word "rotation" changed to "translation." The plane version of Theorem 3.1 is closely connected with the fact that the pedal triangle has angles $\pi - 2A$, $\pi - 2B$, $\pi - 2C$. Finally, (4.2) reduces to the well known formula

$$s_1 = \Delta/R$$

for the semiperimeter of the pedal triangle of a plane triangle.

9. The product of m reflections in m dimensions. Since the product of two reflections is a rotation, the product of m is equivalent to $[m/2]$ rotations (with an extra reflection if m is odd), and it is possible to arrange for the planes of the rotations to be all completely orthogonal, so that the rotations (and the extra reflection when it occurs) are commutative. Let the amounts of the rotations be $2s_1, 2s_2, \cdots, 2s_{[m/2]}$. We wish to express them in terms of the angles between pairs of mirrors. Let c_{jk} denote the cosine of the internal angle between the jth and kth mirrors. Then[6] $e^{\pm 2s_1 i}, e^{\pm 2s_2 i}, \cdots$ (and -1 if m is odd) are the roots of the equation

$$\begin{vmatrix} x+1 & -2c_{12}x & -2c_{13}x \cdots & -2c_{1m}x \\ -2c_{21} & x+1 & -2c_{23}x \cdots & -2c_{2m}x \\ \cdots & \cdots & \cdots & \cdots \\ -2c_{m1} & -2c_{m2} & -2c_{m3} \cdots & x+1 \end{vmatrix} = 0.$$

When $m = 3$, this reduces to

$$(x+1)^3 - 4(c_{23}^2 + c_{31}^2 + c_{12}^2 + 2c_{23}c_{31}c_{12})x(x+1) = 0;$$

so we have

$$(2 \cos s_1)^2 = (x^{1/2} + x^{-1/2})^2 = 4(c_{23}^2 + c_{31}^2 + c_{12}^2 + 2c_{23}c_{31}c_{12}),$$

in agreement with (7.1).

[6] For a proof, see Coxeter, *Lösung der Aufgabe* 245, Jahresbericht der Deutschen Mathematiker-Vereinigung, **49**, *4–6* (1939).

AVERAGES OVER NORMAL MODES OF COUPLED OSCILLATORS WITH APPLICATION TO THEORY OF SPECIFIC HEATS*

By ELLIOTT W. MONTROLL (*University of Pittsburgh*)

1. Introduction. It is well known that the vibrational contribution to the specific heat at constant volume of a crystalline solid or of a gas composed of complex molecules can be calculated from the Einstein equation[1]

$$C_v = k\sum_i (h\nu_i/2kT)^2/\sinh^2(h\nu_i/2kT), \tag{1}$$

where

h = Planck's constant
k = Boltzmann's constant
T = Temperature in degrees absolute.
$\{\nu_i\}$ = set of frequencies of normal modes of vibration.

The summation is to be extended over all frequencies. Eq. (1) can also be written as the Stieltjes integral

$$C_v = k\int_0^{\nu_L} (h\nu/2kT)^2 dN(\nu)/\sinh^2(h\nu/2kT), \tag{2}$$

where $N(\nu)$ is the number of normal modes with frequencies less than ν; and ν_L is the largest frequency of a normal mode.

To apply Eqs. (1) or (2) one must either know all the frequencies of normal modes or their distribution function. In the case of complex molecules and crystalline solids composed of N ($N=O(10^{23})$ in the latter case) particles, the procurement of this knowledge becomes equivalent to the determination of the $(3N-6)$ normal modes of N coupled oscillators (6 being the number of translational and rotational degrees of freedom). Mathematically this means finding the zeroes of a characteristic determinant of order $(3N-6)$ or the roots of a $(3N-6)$th degree equation. In highly symmetrical molecules and crystal lattices this characteristic determinant is factorable into several smaller ones; but to date $N(\nu)$ has never been derived exactly for any molecular model of a real crystal. Numerical approximations have been obtained for $N(\nu)$ but without any estimate of their errors.[2]

By taking traces of powers of the matrix of the determinant mentioned above one can obtain the moments of the distribution function $dN(\nu)$. It is the purpose of this note to show how, without a knowledge of $N(\nu)$ or the frequencies of the individual normal modes, one can obtain by the method of mechanical quadratures averages over the normal modes

---

* Received Dec. 4, 1946.

[1] R. H. Fowler, *Statistical mechanics*, Comb. Univ. Press, 1936, pp. 86–103.

[2] E. W. Kellermann, Phil. Trans. Roy. Soc. **238**, 513 (1940); M. Blackman, Proc. Roy. Soc. (A) **148**, 365–384 (1935); (A) **159**, 417–431 (1937); P. C. Fine, Phys. Rev. **56**, 355–359 (1939); M. Iona, Phys. Rev. **60**, 822 (1941); E. Montroll, J. Chem. Phys., **10**, 218–229 (1942); **11**, 481–495 (1943); E. Montroll and D. Peaslee, J. Chem. Phys., **12**, 98–106 (1944).

$$\bar{f} = \Sigma f(\nu_i) = \int_0^{\nu_L} f(\nu) dN(\nu), \tag{3}$$

(of which (1) is a special case) from the traces of powers of the matrix of the characteristic determinant. An expression will be given for the upper bound of the error in the calculation of (3) from a finite number of moments of $N(\nu)$.

2. Résumé of theory of mechanical quadratures. In this section we shall quote without proof some theorems on mechanical quadratures that will be useful in our work. A detailed exposition of these theorems has been given by G. Szegö.[3]

Let $\alpha(x)$ be a non decreasing function with infinitely many points of increase in the interval (a, b) and suppose the moments

$$\mu_n = \int_a^b x^n d\alpha(x), \qquad n = 0, 1, 2, \cdots \tag{4}$$

exist.

If we orthogonalize the set of non negative powers of x, viz. $1, x, x^2, \cdots, x^n$ with respect to the function $\alpha(x)$ we obtain the set of polynomials $p_0(z)$, $p_1(x)$, $\cdots$, $p_n(x)$, $\cdots$ uniquely determined by the conditions

a) $p_n(x)$ is a polynomial of precise degree n in which the coefficient of x^n is positive

b) the system $\{p_n(x)\}$ is orthonormal

$$\int_a^b p_n(x) p_m(x) d\alpha(x) = \delta_{mn} \qquad m, n = 0, 1, 2, \cdots. \tag{5}$$

Further, for $n \geqq 1$

$$p_n(x) = (D_{n-1}D_n)^{-1/2} \begin{vmatrix} \mu_0 & \mu_1 & \mu_2 & \cdots & \mu_n \\ \mu_1 & \mu_2 & \mu_3 & \cdots & \mu_{n+1} \\ \cdots & \cdots & \cdots & \cdots & \cdots \\ \mu_{n-1} & \mu_n & \mu_{n+1} & \cdots & \mu_{2n-1} \\ 1 & x & x^2 & \cdots & x^n \end{vmatrix}, \tag{6}$$

$$D_n = \begin{vmatrix} \mu_0 & \mu_1 & \cdots & \mu_n \\ \cdots & \cdots & \cdots & \cdots \\ \mu_n & \mu_{n+1} & \cdots & \mu_{2n} \end{vmatrix}. \tag{7}$$

When $\alpha(x)$ has only a finite number, say m, of points of increase there exist only m linearly independent orthonormal polynomials.[4]

Let $x_1 < x_2 < x_3 < \cdots < x_n$ denote the zeros of $p_n(x)$. There exist numbers $\lambda_1, \lambda_2, \cdots, \lambda_n$ such that by the Gauss-Jacobi mechanical quadrature formula

$$\int_a^b F(x) d\alpha(x) = \lambda_1 F(x_1) + \lambda_2 F(x_2) + \cdots + \lambda_n F(x_n), \tag{8}$$

where $F(x)$ is an arbitrary polynomial of degree $2n-1$. The values of the numbers λ

[3] Szegö, *Orthogonal polynomials*, Am. Math. Soc. Colloquium Ser., **23**, Chapt. 2–3 (1939).

[4] G. Szegö, *loc. cit.*, 25–27.

of course depend on n. They are often called Christoffel numbers and are given by fhe following equivalent expressions

$$\lambda_\nu = \int_a^b \left[\frac{p_n(x)}{p_n'(x)(x-x_\nu)}\right]^2 d\alpha(x), \tag{9a}$$

$$\lambda_\nu = \frac{k_{n+1}}{k_n}\,\frac{(-1)}{p_{n+1}(x_\nu)p_n'(x_\nu)}, \tag{9b}$$

$$\lambda_\nu^{-1} = \{p_0(x_\nu)\}^2 + \{p_1(x_\nu)\}^2 + \cdots + \{p_n(x_\nu)\}^2. \tag{9c}$$

Here k_n is the coefficient of highest power of x in $p_n(x)$ and from (6

$$k_n = (D_{n-1}/D_n)^{1/2}. \tag{10}$$

Furthermore, all numbers λ_ν are positive, and

$$\lambda_1 + \lambda_2 + \cdots + \lambda_n = \alpha(b) - \alpha(a).$$

It has been shown by Markoff[5] that when $F(x)$ is a continuous function with a continuous derivative of order $2n+1$, (8) can be generalized to

$$\int_a^b F(x)d\alpha(x) = \lambda_1 F(x_1) + \cdots + \lambda_n F(x_n) + F^{(2n)}(\xi)/(2n)!k_n^2, \tag{11}$$

where $a \leqq \xi \leqq b$. Clearly, if (11) is approximated by (8) an upper bound to the error can be determined by finding the value of ξ for which $F^{(2n)}(\xi)$ is a maximum and evaluating $F^{(2n)}(\xi)/(2n)!k_n^2$.

We shall now show that the moments μ_n can be found in a vibration problem if $\alpha(x)$ is interpreted as the number of normal modes with frequencies less than $\nu = x\nu_L$ and therefore that (11) can be employed to find averages over all the nomal modes of vibration of the system.

3. Theory of vibrations. When the kinetic and potential energies of a system of coupled elements are given by

$$T = \tfrac{1}{2}(a_{11}\dot{q}_1^2 + \cdots + a_{nn}\dot{q}_n^2), \tag{12}$$

$$V = \tfrac{1}{2}(b_{11}q_1^2 + \cdots + b_{nn}q_n^2 + 2b_{12}q_1q_2 + 2b_{13}q_1q_3 + \cdots + 2b_{n-1,n}q_{n-1}q_n), \tag{13}$$

the frequencies ν of normal modes are given by the roots of the characteristic equation[6]

$$\begin{vmatrix} (b_{11}/4\pi^2a_1^2) - \nu^2 & b_{12}/4\pi^2(a_1a_2)^{1/2} & \cdots & b_{1n}/4\pi^2(a_1a_n)^{1/2} \\ b_{21}/4\pi^2(a_2a_1)^{1/2} & (b_{22}/4\pi^2a_2^2) - \nu^2 & \cdots & b_{2n}/4\pi^2(a_2a_n)^{1/2} \\ \cdots & \cdots & \cdots & \cdots \\ b_{n1}/4\pi^2(a_na_1)^{1/2} & b_{n2}/4\pi^2(a_na_2)^{1/2} & \cdots & (b_{nn}/4\pi^2a_n^2) - \nu^2 \end{vmatrix} = 0. \tag{14}$$

If we let B be the matrix whose elements are $b_{ij}/4\pi^2(a_ia_j)^{1/2}$, and $\pm\nu_1, \pm\nu_2, \cdots, \pm\nu_n$ be the $2n$ roots of (14), and if $\Sigma\nu^m$ represents the sum of the mth powers of the roots, then we have

[5] A. A. Markoff, *Differenzenrechnung*, Leipzig, 1896, p. 29.

[6] E. T. Whittaker, *Analytical dynamics*, Camb. Univ. Press, 1927, p. 179.

$$\Sigma\nu^0 = 2n, \qquad \Sigma\nu^{2m+1} = 0, \qquad \Sigma\nu^{2m} = 2 \text{ trace } B^m. \tag{15}$$

Further, if we interpret x in (4) as the ratio ν/ν_L and $\alpha(x)$ as the number of values of ν/ν_L (where ν is a root of (14)) which are less than x, it is clear from (4) and (15) that

$$\mu_0 = \int_{-1}^{1} d\alpha(x) = \Sigma\nu^0 = 2n, \tag{16a}$$

$$\mu_{2m+1} = \int_{-1}^{1} x^{2m+1} d\alpha(x) = \Sigma(\nu/\nu_L)^{2m+1} = 0, \tag{16b}$$

$$\mu_{2m} = \int_{-1}^{1} x^{2m} d\alpha(x) = \Sigma(\nu/\nu_L)^{2m} = 2\nu_L^{-2m} \text{ trace } B^m. \tag{16c}$$

The averages of interest, (3), are $\bar{f} = \Sigma f(\nu_j)$, where the summation extends over all positive roots of the determinant (14). By defining a new function

$$F(\nu) = f(\nu), \qquad \text{if} \quad \nu \geqq 0 \tag{17a}$$

and

$$F(\nu) = f(-\nu), \quad \text{if} \quad \nu < 0, \tag{17b}$$

(3) can be written as

$$\bar{f} = \frac{1}{2}\int_{-1}^{1} F(x\nu_L) d\alpha(x), \tag{18}$$

which is of the form of (11). Since the moments μ_n can be determined from (16), $p_n(x)$ can be evaluated from (6) and $\bar{f}$ obtained by applying (11).

4. Numerical example. To demonstrate the manner of application of (18) let us consider the steps required in the determination of the specific heat of tungsten. It is to be emphasized that the purpose of this example is merely to review the details of a calculation—too few moments are employed to obtain results that could be expected to be in agreement with observed specific heats.

Tungsten forms a body centered cubic lattice. Its equations of motion have been determined by Fine, and Montroll and Peaslee[2] who used the assumption that the Cauchy condition on the elastic constants is satisfied. The traces of the characteristic determinant were found in the latter paper and the moments of the frequency distribution were determined. The moments, μ_n, there presented in table II differ somewhat from those defined by eq. 4. Those of table II (when $\tau = 2/3$), which we shall denote by μ_n' are related to the μ_n's of eq. 4, in a lattice of N atoms, by $\mu_n = 6N\mu_n'/\nu_L$, so that the moments $\mu_0 \cdots \mu_8$ are

$$\mu_0 = 6N, \qquad \mu_1 = \mu_3 = \mu_5 = \cdots = 0, \qquad \mu_2 = \tfrac{1}{2}(6N),$$
$$\mu_4 = (11/36)(6N), \qquad \mu_6 = (61/288)(6N), \qquad \mu_8 = (733/4608)(6N).$$

Substituting these moments into (7) we obtain

$$D_0 = 6N, \qquad D_1 = \tfrac{1}{2}(6N)^2, \qquad D_2 = (1/36)(6N)^3,$$
$$D_3 = [65/2(36)^3](6N)^4, \qquad D_4 = [(65)(31)/16(36)^5](6N)^5.$$

and from (6)

$$p_0(x) = 1/(6N)^{1/2}, \qquad p_1(x) = 2^{1/2}x/(6N)^{1/2}, \qquad p_2(x) = (3/2)2^{1/2}(2x^2 - 1)/(6N)^{1/2},$$
$$p_3(x) = 2(2/65)^{1/2}(18x^3 - 11x)/(6N)^{1/2},$$
$$p_4(x) = (1/4)(2/31)^{1/2}(288x^4 - 306x^2 + 65)/(6N)^{1/2}.$$

The roots of $p_4(x)$ are

$$x_1 = -.8769, \qquad x_2 = -.5418, \qquad x_3 = .5418, \qquad x_4 = .8769.$$

Thus, from (9c) we see that

$$\lambda_1 = \lambda_4 = (.2172)(6N), \qquad \lambda_2 = \lambda_3 = (.2828)(6N).$$

Thus, choosing the function $f(\nu)$ to be

$$f(\nu) = f(x\nu_L) = k(x\theta)^2/\sinh^2 \theta x,$$

where $\theta = h\nu_L/2kT$ we obtain from (1), (11), and (18

$$C_v \simeq 3Nk\{(.4344)(.8769\theta)^2/\sinh^2(.8769\theta) + (.5656)(.5418\theta)^2/\sinh^2(.5418\theta)\}.$$

Qualitatively our method is equivalent to replacing the entire frequency spectrum by a small number, say n, of specially chosen sharp frequencies. These frequencies and their weight factors are chosen so that the values obtained for all averages over polynomials of degree $(2n-1)$, or less, are exact. In conclusion, it might be mentioned that in general analogous methods can be used in evaluating averages over characteristic values of linear operators.

THE SUBSONIC FLOW ABOUT A BODY OF REVOLUTION*

By E. V. LAITONE (*Cornell Aeronautical Laboratory*)

In cylindrical coordinates the Laplace differential equation, which defines the irrotational incompressible fluid flow, becomes

$$\phi_{xx} + \phi_{rr} + \frac{1}{r}\phi_r + \frac{1}{r^2}\phi_{\theta\theta} = 0, \tag{1}$$

where the last term vanishes when the flow has axial symmetry about the x axis.

In this case a solution of Eq. (1) based on a source distribution $f(x)$ per unit length along the x axis from $x=0$ to $x=L$ is

$$\phi = u_\infty x - \frac{1}{4\pi}\int_0^L \frac{f(\xi)d\xi}{[(x-\xi)^2 + r^2]^{1/2}},$$
$$u = \phi_x = u_\infty + \frac{1}{4\pi}\int_0^L \frac{f(\xi)(x-\xi)d\xi}{[(x-\xi)^2 + r^2]^{3/2}}, \tag{2}$$
$$v = \phi_r = \frac{r}{4\pi}\int_0^L \frac{f(\xi)d\xi}{[(x-\xi)^2 + r^2]^{3/2}},$$

where $v/u = (dr/dx)_0$ satisfies the fixed boundary conditions given by the body shape.

* Received Dec. 9, 1946.

The linearized differential equation for the velocity potential of a compressible fluid flow with axial symmetry is given by

$$\beta^2\phi_{xx} + \phi_{rr} + \frac{1}{r}\phi_r = 0, \tag{3}$$

where for subsonic flow

$$\beta = \sqrt{1 - M^2} > 0.$$

The first method of Goldstein and Young[1] may be used to convert Eq. (2) into a linear perturbation solution of Eq. (3) in the following manner

$$\begin{aligned}
\Delta\phi &= -\frac{1}{4\pi\beta}\int_0^L \frac{f(\xi)d\xi}{[(x-\xi)^2 + (\beta r)^2]^{1/2}}, \\
\Delta u &= \frac{1}{4\pi\beta}\int_0^L \frac{f(\xi)(x-\xi)d\xi}{[(x-\xi)^2 + (\beta r)^2]^{3/2}}, \\
\Delta v &= \frac{\beta r}{4\pi}\int_0^L \frac{f(\xi)d\xi}{[(x-\xi)^2 + (\beta r)^2]^{3/2}}, \\
\left(\frac{\Delta v}{u_\infty}\right)_0 &= \left(\frac{dr}{dx}\right)_0\left[1 + \left(\frac{\Delta u}{u_\infty}\right)_0\right].
\end{aligned} \tag{4}$$

Equation (4) can then provide a solution for a fixed given body shape for all Mach numbers less than unity ($0 < \beta \leqq 1$) as shown in ref. 1.

If the substitution $\xi = x + \beta rz$ is introduced into Eq. (4) and the Taylor Expansion is written as

$$f(\xi) = f(x + \beta rz) = \sum_{n=0}^{\infty} \frac{(\beta rz)^n}{n!} f^{(n)}(x),$$

then Eq. (4) becomes

$$\begin{aligned}
\Delta u &= -\frac{1}{4\pi\beta}\sum_{n=0}^{\infty} \frac{(\beta r)^{n-1} f^{(n)}(x)}{n!} \int_{-x/\beta r}^{(L-x)/\beta r} \frac{z^{n+1}dz}{(1+z^2)^{3/2}}, \\
\Delta v &= \frac{1}{4\pi}\sum_{n=0}^{\infty} \frac{(\beta r)^{n-1} f^{(n)}(x)}{n!} \int_{-x/\beta r}^{(L-x)/\beta r} \frac{z^n dz}{(1+z^2)^{3/2}},
\end{aligned} \tag{5}$$

or, to the first order terms in βr,

$$\begin{aligned}
\Delta u = -\frac{1}{4\pi\beta}\Bigg\{ & \frac{f(x)}{x}\cdot\left(\frac{1 - 2x/L}{1 - x/L}\right) + f'(x)\left[\log (4x/L)(1 - x/L) - 2\log \beta r/L - 2\right] \\
& + f''(x)\cdot(L/2)(1 - 2x/L) + f'''(x)\cdot(L^2/12)\left[(1 - x/L)^2 + (x/L)^2\right] + \cdots \\
& + f^{(n)}(x)\cdot\left[\frac{(\beta r)^{n-1}}{n!}\int_{-x/\beta r}^{(L-x)/\beta r} \frac{z^{n+1}dz}{(1+z^2)^{3/2}}\right] + O(\beta r)\Bigg\},
\end{aligned} \tag{6}$$

---

[1] S. Goldstein and A. D. Young, *The linear perturbation theory of compressible flow, with applications to wind tunnel interference*, Brit., A.R.C., R. & M. 1909 (1943).

$$\Delta v = \frac{1}{4\pi}\{2f(x)/\beta r - f''(x)[\beta r \log(\beta r/L)] + O(\beta r)\}, \tag{7}$$

for $0<x<L$.

On the body surface to a first order approximation

$$(\Delta v/u_\infty)_0 = (dr/dx)_0 = f(x)/2\pi\beta r_0 u_\infty, \tag{8}$$

or

$$f(x) = 2\pi\beta u_\infty r_0 (dr/dx)_0 = \beta u_\infty S', \tag{9}$$

where

$$S = \pi r_0^2.$$

Then

$$2\left(\frac{\Delta u}{u_\infty}\right) = -\frac{1}{\pi}\left\{\frac{S'}{2x}\left(\frac{1-2x/L}{1-x/L}\right) - S''\left(1+\log\frac{\beta r}{L} - \log 2\sqrt{\frac{x}{L}\left(1-\frac{x}{L}\right)}\right)\right.$$
$$\left. + \frac{S^{(3)}}{4}L\left(1-\frac{2x}{L}\right) + \frac{S^{(4)}}{24}L^2\left(1-\frac{2x}{L}+\frac{2x^2}{L^2}\right) + \cdots\right\}, \tag{10}$$

for any x other than 0 or L.

Eqs. (8) and (10) provide the pressure distribution on (or along the streamlines $r\to 0$) a slender symmetrical body of revolution in either incompressible or subsonic potential flow. They also provide a first order Mach number correction for the subsonic potential flow on any body of revolution. For example, the surface pressure coefficient (C_p) at $x=L/2$ for a symmetrical body of revolution at any Mach number (M) less than unity would be given by

$$\left(\frac{C_p}{Cp_{M=0}}\right)_{\max} = 1 + \frac{\log\sqrt{1-M^2}}{1-(L^2S^{(4)}/48S'' + \cdots) + \log(r/L)}. \tag{11}$$

Eq. (11) agrees with the expression obtained by Lees[2] for a slender prolate spheroid ($S^{(n)}=0$ for $n>2$).

The flow about any body of revolution is given to the first order by Eqs. (4) and (9) as

$$2\left(\frac{\Delta u}{u_\infty}\right) = \frac{1}{2\pi}\int_0^L \frac{S'(\xi)(x-\xi)d\xi}{[(x-\xi)^2+(\beta r)^2]^{3/2}},$$
$$\left(\frac{\Delta v}{u_\infty}\right) = \frac{\beta^2 r}{4\pi}\int_0^L \frac{S'(\xi)d\xi}{[(x-\xi)^2+(\beta r)^2]^{3/2}}. \tag{12}$$

Eq. (12) shows that at large transverse distances from a body of revolution

$$\frac{\Delta u}{u_\infty} = \frac{1}{4\pi\beta^3 r^3}\int_0^L S'(\xi)\cdot(x-\xi)d\xi,$$

---

[2] Lester Lees, *A discussion of the application of the Prandtl-Glauert method to subsonic compressible flow over a slender body of revolution*, NACA, TN **1127** (1946).

so that the subsonic flow wind tunnel wall correction for a body of revolution would vary as $1/(1-M^2)^{3/2}$.

Eq. (7) may be written

$$f(x) = 2\pi\beta r r'(u_\infty + \Delta u) + \frac{(\beta r)^2}{2} f''(x) \log (\beta r/L) + O(\beta^2 r^2 f).$$

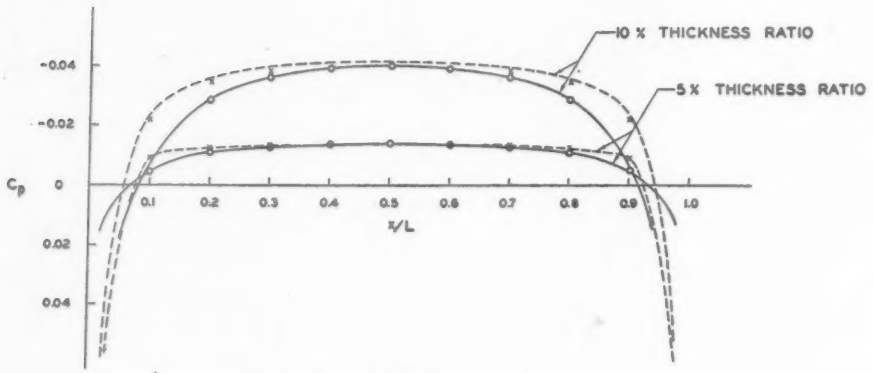

FIG. 1. Prolate spheroid.
—— Equation 12
○ Equation 10
- - - Exact Potential Flow Solution
× Equation 14, [Equation 10—$(dr/dx)^2$]

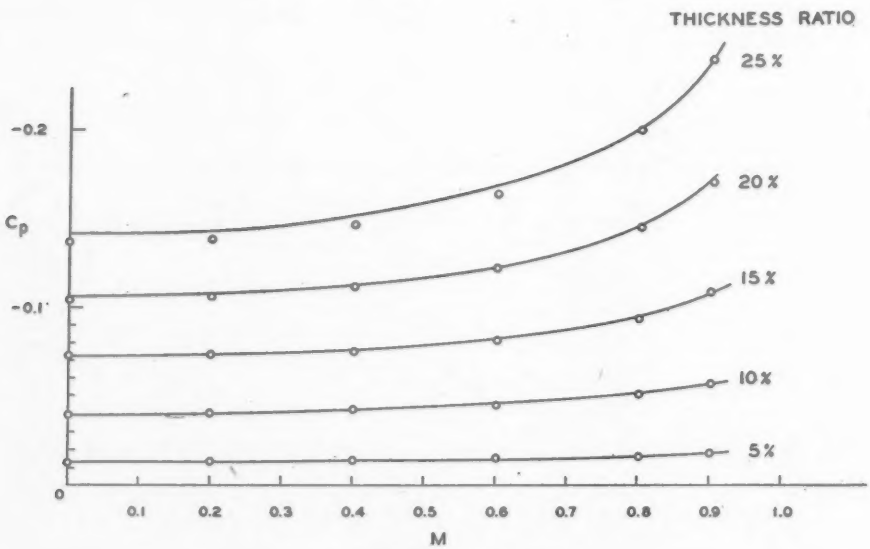

FIG. 2. Prolate spheroid, $x = L/2$.
—— Equation 12
○ Equation 10

Therefore, for $0<x<L$,

$$f(x) = 2\pi u_\infty \beta r r'[1 + (\log \beta r/L)(3\beta^2 r r''/2 + \beta^2 r^2 r^{(3)}/2r' + r r'' + r'^2) + O(r^2)]$$
$$= \beta u_\infty S'(x) + O(r^4 \log r), \quad \text{for} \quad \beta > 0. \tag{13}$$

Eq. (13) shows that at least for incompressible flow ($\beta=1$) Eq. (12) will provide the surface velocities accurate to the order $r^4 \log r = 0$. A corresponding statement cannot be made for subsonic flow however since the compressibility effects of the flow have been considered only to the first order in Eq. (3).

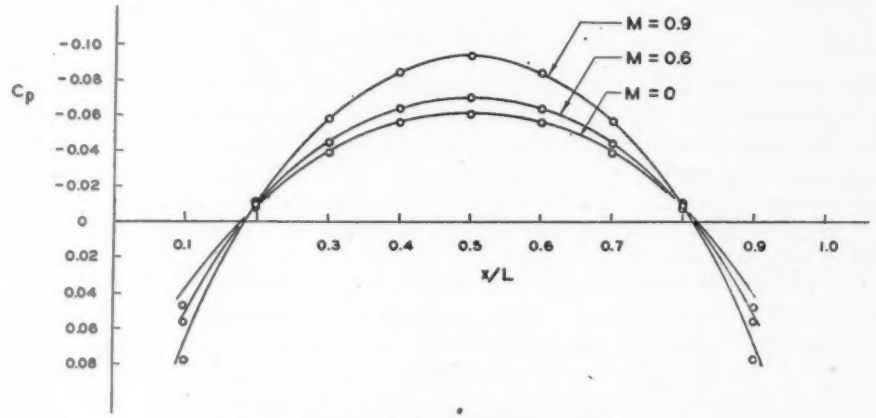

FIG. 3. 10% parabolic arc body of revolution
—— Equation 12—$(dr/dx)^2$
○ Equation 10—$(dr/dx)^2$

The pressure coefficient for compressible flow is given to the second order by

$$C_p = -2(\Delta u/u_\infty) - (\Delta v/u_\infty)^2 - (\Delta u/u_\infty)^2(1 - M^2) + O(\phi_x^3, \phi_r^4),$$

which in view of Eqs. (8) and (10) becomes

$$C_p = -2(\Delta u/u_\infty) - (r')^2 + O(r^4 \log r). \tag{14}$$

Figure 1 shows a comparison of the exact incompressible potential flow pressure distribution on a prolate spheroid (ellipsoid of revolution) with that obtained from Eqs. (10), (12) and (14). Figure 2 shows the effect of Mach number on the maximum C_p of various thickness ratio prolate spheroids as computed from Eqs. (10) and (12). Figure 3 shows the effect of Mach number on the pressure distribution of a parabolic arc body of revolution as obtained from Eq. (14) in conjunction with Eqs. (10) and (12).

A CRITERION FOR STABLE CHARACTERISTIC EXPONENTS*

By AUREL WINTNER (*The Johns Hopkins University*)

1. Let $f(t)$ be a real-valued, continuous, periodic function and let the unit of length on the t-axis be so chosen that the period of $f(t)$ becomes 1. Then the linear differential equation

$$x'' + f(t)x = 0 \tag{1}$$

has two solutions of the form

$$x = e^{\lambda t}g(t), \qquad x = e^{-\lambda t}h(t), \tag{2}$$

where $g(t)$ and $h(t)$ have the period, 1, of $f(t)$ and do not vanish identically. The numbers $\pm\lambda$ occurring in (2), the characteristic exponents of (1), are determined mod $2\pi i$ only. If λ is not a multiple of πi, it is clear that the two solutions (2) are linearly independent. If λ is a multiple of πi, it depends on the elementary divisors of certain linear substitutions whether (1) does or does not possess two linearly independent solutions of the form (2) (in the second case, the general solution of (1) contains a secular term, that is, a term containing the factor t).

Let the differential equation (1) be called of stable type if every solution, $x(t)$, remains bounded as $t \to \pm\infty$, and let the characteristic exponents $\pm\lambda$ of (1) be called of stable type if they are purely imaginary (including 0). Then it is clear that (1) cannot be of stable type unless the characteristic exponents are, and that (1) must be of stable type if the characteristic exponents are of stable type and distinct. Needless to say, the two characteristic exponents, λ and $-\lambda$, are considered as distinct if and only if they are distinct mod $2\pi i$ (that is, if λ is not a multiple of πi).

2. The usual way of calculating λ is supplied by Hill's method of infinite determinants (the zeros of the resulting transcendental equation being all possible values,

$$\pm\lambda, \qquad \pm\lambda \pm 2\pi i, \qquad \pm\lambda \pm 4\pi i, \cdots,$$

of the characteristic exponent). For certain purposes, a less elaborate procedure is more convenient. Quite a direct procedure happens to be contained in the classical proof (Cauchy-Fuchs-Floquet) for the mere *existence* of solutions of the form (2). In fact, this existence proof is based on the consideration of the linear substitutions of the "monodromy group." These are binary substitutions of determinant 1, have a common pair of latent roots, and the logarithms of these roots are precisely the characteristic exponents. In other words, $e^{\pm\lambda}$ is the root of a reciprocal quadratic equation, say

$$e^{\pm 2\lambda} - 2\alpha e^{\pm\lambda} + 1 = 0, \tag{3}$$

where α is a constant uniquely determined by the periodic coefficient function of (1).

Accordingly, the calculation of λ can be reduced to the calculation of α. But α can be calculated from $f(t)$, by applying the method of successive approximations to those two solutions of (1) which are determined by the initial conditions

* Received March 12, 1947.

$$x(0) = 1, \quad x'(0) = 0 \quad \text{and} \quad x(0) = 0, \quad x'(0) = 1.$$

This procedure, which seems to go back to Liapounoff (cf. pp. 425–431 of vol. IV, part III (1902) of Forsyth's *Theory of Differential Equations*), leads to the following representation of α:

Put

$$F(t) = \int_0^t f(t_0)dt_0 \tag{4}$$

and

$$F_n = \{F(1) - F(t_1) + F(t_n)\} \prod_{k=1}^{n-1} \{F(t_k) - F(t_{k+1})\}, \tag{5}$$

where $n = 1, 2, \cdots$ (with the understanding that

$$\prod_{k=1}^{n-1} = 1 \quad \text{if} \quad n = 1,$$

that is, if the product is vacuous); so that

$$F_n = F_n(t_1, \cdots, t_n).$$

Then, if the constants $\alpha_1, \alpha_2, \cdots$ are defined by

$$\alpha_n = \frac{1}{2} \int_0^1 dt_1 \int_0^{t_1} dt_2 \cdots \int_0^{t_{n-1}} F_n(t_1, \cdots, t_n)dt_n \tag{6}$$

(that is, if the integral of (5) over the n-dimensional polytope

$$0 \leqq t_n \leqq t_{n-1} \leqq \cdots \leqq t_1 \leqq 1 \tag{7}$$

is denoted by $2\alpha_n$), the series

$$\alpha = 1 - \alpha_1 + \alpha_2 - \cdots + (-1)^k\alpha_k + \cdots \tag{8}$$

is convergent and represents the coefficient in (3). This is the substance of the verifications which will be found loc. cit.

This method does not seem to be generally known among applied mathematicians; it is not mentioned in Strutt's usually quite complete monograph.

3. Since (6), hence (8), is real-valued, and since the roots of the quadratic equation (3) are

$$e^{\pm\lambda} = \alpha \pm (\alpha^2 - 1)^{1/2},$$

it is clear that the characteristic exponents $\pm\lambda$ are of stable type (that is, purely imaginary, including 0) if and only if

$$-1 \leqq \alpha \leqq 1,$$

and that they are of stable type and distinct (mod $2\pi i$) if and only if

$$-1 < \alpha < 1. \tag{9}$$

Hence, the stability of (1) depends on whether the sum of the numerical series (8) does or does not satisfy these conditions.

Liapounoff has used this method in order to show that, if $f(t)=f(t+1)$ is positive throughout, the characteristic exponents of (1) must be of stable type whenever the average value of $f(t)$, that is, the constant term in the Fourier expansion of $f(t)$, is sufficiently small; namely, less than 4 (cf. loc. cit.). Liapounoff's proof can be interpreted as amounting to an application of the second mean-value theorem in integral calculus. By using the first mean-value theorem instead of the second, two stability criteria of quite another type will be deduced in the sequel. Neither of them will assume that $f(t) \geqq 0$. The first of them is as follows:

(i) *Let $f(t)$ be a real-valued, continuous function of period* 1. *Suppose that its average*

$$\mu = \int_0^1 f(t)dt \tag{10}$$

and its absolute maximum

$$M = \max |f(t)| \tag{11}$$

satisfy the inequalities

$$\sum_{n=2}^{\infty} M^n/(2n-1)! < \mu \leqq 1 \tag{12}$$

(*which are compatible with* $\min f(t) < 0$); *for instance, that*

$$M^2 e^M < 6\mu \leqq 6. \tag{13}$$

Then the characteristic exponents of (1) *are of stable type and distinct.*

That (13) is sufficient for (12), is seen by comparing coefficients.

As to the possibility mentioned parenthetically after (12), it is sufficient to observe that, while (11) and (12) imply that

$$\mu > 0, \tag{14}$$

(14) and (10) do not imply that $f(t)$ is non-negative throughout.

4. According to (4), the first factor on the right of (5) is identical with the difference

$$\int_0^1 f(t)dt - \int_{t_n}^{t_1} f(t)dt,$$

where $0 \leqq t_n \leqq t_1 \leqq 1$. It follows therefore from (11) and (5) that

$$|F_n| \leqq M \prod_{k=1}^{n-1} |F(t_k) - F(t_{k+1})|.$$

On the other hand, from (4) and (11),

$$|F(t_k) - F(t_{k+1})| \leqq M(t_k - t_{k+1}),$$

where $t_{k+1} \leqq t_k$, by (7). Hence, the inequality

$$|F_n| \leqq M^n D_n \tag{15}$$

holds at every point of the polytype (7), if $D_n = D_n(t_1, \cdots, t_n)$ is an abbreviation for the product

$$D_n = \prod_{k=1}^{n-1} (t_k - t_{k+1}), \tag{16}$$

the (non-negative) square-root of the discriminant of the polynomial $\prod_{k=1}^{n}(z-t_k)$.

The integral of the product (16) over the polytope (7) is known to have the value $1/(2n-1)!$. It follows therefore from (6) and (15) that

$$|\alpha_n| \leqq \tfrac{1}{2}M^n/(2n-1)!. \tag{17}$$

Hence, by the first of the inequalities (12),

$$\sum_{n=2}^{\infty} |\alpha_n| < \tfrac{1}{2}\mu. \tag{18}$$

According to (5) and the parenthetical remark which follows (5), the function F_1 is identical with the constant $F(1)$. It follows therefore from (6) that $\alpha_1 = \frac{1}{2}F(1)$. In view of (4) and (10), this means that

$$\alpha_1 = \tfrac{1}{2}\mu. \tag{19}$$

Consequently, from (8) and (18),

$$|\alpha - (1 - \tfrac{1}{2}\mu)| < \tfrac{1}{2}\mu.$$

In view of the second of the inequalities (12), the last formula line implies that

$$0 < \alpha < 1. \tag{20}$$

Since this, in turn, implies that (9) is satisfied, the proof is complete.

The first of the assumptions (12) can be improved somewhat. In fact, it is clear from the proof of (15) that (15) can be refined to

$$|F_n| \leqq M^n D_n - M^n(t_1 - t_n)D_n, \tag{21}$$

where $(t_1 - t_n)D_n$ is positive (within the polytope).

5. Since only (9) was needed but (20) was deduced, it is natural to ask after a condition which, in contrast to (12), leads to the α-range complementary to (21), that is, to the range

$$-1 < \alpha \leqq 0. \tag{22}$$

Such a condition is contained in the following dual of (i):

(ii) *The pair of assumptions*, (12), *of* (i) *can be replaced by*

$$\sum_{n=2}^{\infty} M^n/(2n-1)! < 4 - \mu \leqq 2; \tag{23}$$

for instance, (13) *can be replaced by*

$$M^2 e^M < 24 - 6\mu \leqq 12. \tag{24}$$

In fact, (17) and (19) were obtained without any hypothesis and are therefore applicable whether (12) is assumed or not. But (17), (19) and (8) imply that

$$|\alpha| \leqq |1 - \tfrac{1}{2}\mu| + \tfrac{1}{2}\sum_{n=2}^{\infty} M^n/(2n-1)!.$$

Hence, by the first of the inequalities (23),

$$|\alpha| < |1 - \tfrac{1}{2}\mu| + 2 - \tfrac{1}{2}\mu.$$

On the other hand, the second of the inequalities (23) can be written in the form $\mu \geqq 2$, which means that

$$|1 - \tfrac{1}{2}\mu| = \tfrac{1}{2}\mu - 1.$$

This completes the proof, since the last two formula lines imply the inequality $|\alpha| < 1$, which is (9).

Conclusion. If μ, M are defined by (10), (11), then either (12) or (23) [and so, in particular, either (13) or (24)] is sufficient for stability.

As an illustration, let

$$f(t) = (a + b\cos 2\pi t)^{-1}, \quad \text{where} \quad 0 < b < a;$$

so that (1) becomes the equation known from the problem of frequency modulation. In this case, (10) and (11) reduce to

$$\mu = (a^2 - b^2)^{-1/2} \quad \text{and} \quad M = (a - b)^{-1},$$

and so the above inequalities supply explicit conditions for pairs (a, b) which are sure to be of stable type. Needless to say, the resulting inequalities for a and b are just sufficient for stability. Incidentally, since $f(t)$ is now positive, Liapounoff's criterion, $\mu < 4$, also is applicable.

LOWER BUCKLING LOAD IN THE NON-LINEAR BUCKLING THEORY FOR THIN SHELLS*

By HSUE-SHEN TSIEN (*Massachusetts Institute of Technology*)

For thin shells the relation between the load P and the deflection ϵ beyond the classical buckling load is very often non-linear. For instance, when a uniform thin circular cylinder is loaded in the axial direction, the load P when plotted against the end-shortening ϵ has the characteristic shown in Fig. 1. If the strain energy S and the total potential $\varphi = S - P\epsilon$ are calculated, their behavior can be represented by the curves shown in Figs. 2 and 3. It can be demonstrated that the branches OC and AB corresponds to stable equilibrium configurations and the branch BC to unstable equilibrium configurations. The point B is then the point of transition from stable to unstable equilibrium configurations.

It was proposed by the author in a previous paper[1] that the point A was the critical point for buckling of the structure under external disturbances, using the S, ϵ curve for "testing machine" loading and the φ, P curve for "deadweight" loading. The load P for the unbuckled configuration of the shell corresponding to the point A was called

* Received April 2, 1947.

[1] H. S. Tsien, *A theory for the buckling of thin shells*, J. Aero. Sciences 9, 373–384 (1942).

the lower buckling load of the shell. The energy represented by the vertical distance from the point A to the curve BC is then the minimum external excitation required to cause the buckling at point A.

However, if the external excitation is large, there is no reason why buckling cannot occur at the point B' directly under the point B. The minimum external excitation required is then given by the energy represented by the distance $B'B$. This amount of energy is actually absorbed by the structure during buckling. Since the curve BA represents the final state of the structure after buckling, for buckling to happen between B' and A, energy is absorbed, and for buckling to happen between A and C, energy is released. But in any event, the lower limit of buckling load is definitely

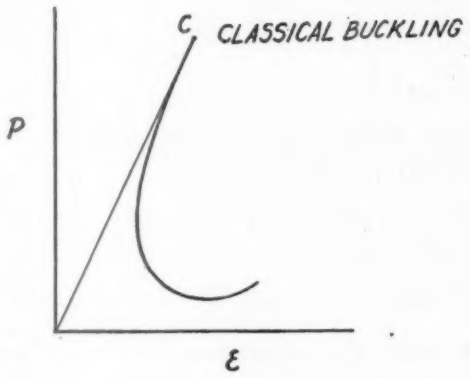

FIG. 1.

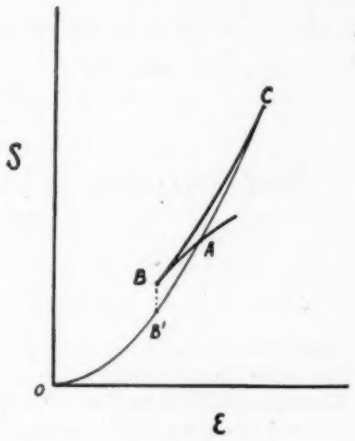

FIG. 2.

given by the point B', not the point A. Therefore the lower buckling load should be the load P corresponding to the point B'.

By referring to Figs. 11 and 13 of the aforementioned paper, and assuming a square wave pattern, we find the lower buckling stress σ of thin uniform cylindrical shells under axial load to be given by

$$\sigma = 0.42Et/R$$

for testing machine loading and

$$\sigma = 0.19Et/R$$

for deadweight loading. The corresponding values under the previously proposed criteria are $\sigma = 0.46Et/R$ and $\sigma = 0.298Et/R$ for the two cases.

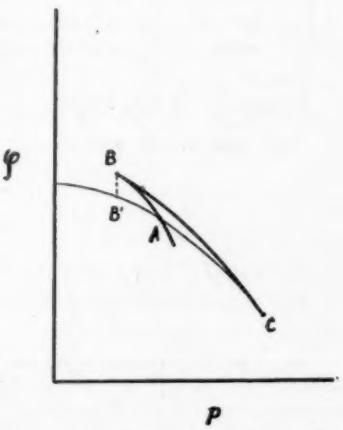

FIG. 3.

CORRECTIONS TO MY PAPER

ON AN EXTENSION OF THE VON KÁRMÁN-TSIEN METHOD TO TWO-DIMENSIONAL SUBSONIC FLOW WITH CIRCULATION AROUND CLOSED PROFILES*

QUARTERLY OF APPLIED MATHEMATICS, **4**, 291–297 (1946)

BY C. C. LIN (*Brown University*)

Page 292, line 3: for "*is now an a parallel footing*" read "*is now on a parallel footing.*"

Page 293, line 8: for "*in the region exterior to*" read "*in the region R_0 exterior to.*"

Page 293, line 9: for "*such that R_0*" read "*such that.*"

* Received Jan. 20, 1947.

CORRECTIONS TO MY PAPER

THE ANALOGY BETWEEN MULTIPLY-CONNECTED SLICES AND SLABS*

QUARTERLY OF APPLIED MATHEMATICS, **3**, 279–290 (1946)

BY RAYMOND D. MINDLIN (*Columbia University*)

Equations (2.4), (2.6), (6.2), (6.3): replace $(1+\nu_1)$ by E_1 in the coefficient of $\nabla^2 T$.

Equation (2.6): replace α by α_1.

Equation (6.2) is obtained from (6.1) and (2.4) and not from (6.1) and (2.6).

The reference to Biot's analogies at the end of Sec. 4 should read "analogies . . . between gravity loading and boundary pressures and dislocations and between thermal loading and dislocations."

The integration by parts following Eq. (4.6) is incomplete with the result that the following corrections should be made:

Equations (4.9), (4.10), (7.5), (7.15): multiply the last integral by 2.

Equations (7.13), (7.20): replace $[(1-\nu_1)(1-\nu_2)-1]$ by $[(1-\nu_1)(1-\nu_2)-2]$.

* Received April 22, 1947.

BOOK REVIEWS

Mathematical Theory of Elasticity. By I. S. Sokolnikoff with the collaboration of R. D. Specht. McGraw-Hill Book Co., New York and London, 1946. xi+373 pp. $4.50.

There are five chapters in this book, three of them dealing with the fundamentals of the theory of elasticity, one dealing with the torsion and flexure of homogeneous beams, and the last chapter dealing with variational methods in elasticity.

In the chapter on analysis of strain we find a careful discussion of the properties of infinitesimal strain including Cesaro's proof for the *sufficiency* of the six equations of compatibility. A brief section is added on finite strain, showing the difference between the Eulerian and Lagrangian approach and giving selected references to contempory work. To this reader it seems regrettable that no mention is made

of the early work by Kirchhoff, Boussinesq and the Cosserats on this subject and no indication given with regard to the nature of the progress which has been made since then.

There follows a chapter on analysis of stress, containing all the essential facts on this subject. The third chapter is devoted to the subject of stress-strain relations. Among the topics discussed are the generalized Hooke's law together with a description of types of elastic symmetry; various forms of the complete system of differential equations of the linear theory for the isotropic body; the strain energy function including thermodynamic considerations often not included in elasticity texts; Kirchhoff's uniqueness proof for the solutions of the linear theory; and finally Saint Venant's principle.

In the foregoing three chapters the author uses his own distinctive symbols for stresses and strains, and tensor notation to the extent of writing for instance the three differential equations for the stresses in the form $\tau_{ij,j}+F_i=0$. No use is made of results of the theory of tensors and in order to study specific problems the author restates the fundamental equations of the theory in the notation which is customary in the American literature.

Nearly one-half of the book is devoted to the theory of torsion and flexure, mainly on the basis of Saint Venant's theory. The classical solutions of the torsion problem for the ellipse, rectangle, equilateral and isosceles right triangle are derived in the usual way. About twenty pages are devoted to an introduction of complex-variable theory, as a preparation to Mushelisvili's method for the boundary problem for the two-dimensional Laplace equation. As applications of this method one finds solutions of the torsion problem for the cardioid, for a loop of the lemniscate, for the section bounded by two circular arcs and for the inverse of an ellipse. There follows a discussion of the membrane analogy, a section giving references to experimental work, and a section on the torsion problem for multiply connected cross sections, with the example of Bredt's formula for the thin walled section without partitions.

In order to treat the Michell theory of torsion of shafts with variable circular cross section there is included a section on orthogonal curvilinear coordinates (without the use of tensor notation). As an example the solution for the conical shaft is given.

After this there is presented the Bessel-function solution for the torsion of the circular cylinder twisted by load distributions other than that of the Saint Venant theory, and also the relation between the torsion problem for the nonisotropic beam and for the isotropic beam.

There follows a treatment of the flexure problem with emphasis on the importance of leaving arbitrary the coordinate system in the cross section instead of choosing the system of principal axes through the centroid of the section. The *center of flexure* is defined as the load point giving zero mean local twist. Here one misses mention of the possibility of alternate definitions of this point and of some of the recent literature on the subject. A discussion of the center of *twist* would have been welcome also.

Explicit solutions of the flexure problem are presented for beams which have as cross sections an ellipse, a rectangle, an equilateral triangle, the section bounded by two concentric circles, and the cardioid.

It is somewhat of an anticlimax to have the work of this chapter conclude with a treatment of the elementary ("technical") theory of bending of beams with straight axis, including the solution of some very simple examples.

In the last section we find references to special extensions of the theory of torsion and flexure. Some topics are omitted such as the work on torsion with variable twist of thin walled sections, or of the problem of the effective width of I, T and box beam flanges, or of the effect of transverse shear deformation on the bending of beams.

The last chapter of the book is devoted to a study of variational methods. Following the example of Trefftz in the "Handbuch der Physik" there are given careful statements of the theorem of minimum potential energy (assuming infinitesimal strains and Hooke's law), and of the corresponding minimum theorem for the stresses. In somewhat unusual order the principle of virtual work is derived from the principle of minimum potential energy and stated (without qualification!) to be equivalent to the latter. There follows a proof of the reciprocity theorem; an introduction to the direct methods of the calculus of variations with the example of the twisted bar of rectangular cross-section; and a study of error estimates for the direct methods.

The final section of the chapter on variational methods describes the method of finite differences, including some recent developments, as applied to the two-dimensional Laplace equation.

Within the limits which the authors have set themselves—limits which to the reviewer appear to be somewhat narrower than the title of the book indicates—their work can be said to represent an interesting addition to the literature on the theory of elasticity.

E. REISSNER

An index of mathematical tables. By A. Fletcher, J. C. P. Miller and L. Rosenhead, McGraw-Hill Book Company Inc., New York and Scientific Computing Service Ltd., London, 1946. viii+450 pp. $16.00.

The need of an extensive index of available mathematical tables has long been felt by workers in applied mathematics. The usefulness of such an index is felt, not only in making possible the numerical solution of a mathematical problem by the use of existing tables but also in influencing the choice between various mathematical formulations of a problem to take advantage of such existing tables. Moreover, as pointed out in the preface, the index will be useful also to makers of mathematical tables, in showing what has been done, thus avoiding duplication and stimulating work in the direction of filling the main gaps.

The work is divided into two parts. Part I contains an index according to functions. Part II is a bibliography listed alphabetically by authors. An alphabetic index to Part I is also included. While Part I is the cardinal feature of the book, Part II gives a concise reference list of books and papers containing tables or dealing with such things as errors, in particular tables or the bibliography of tables.

Part I indicates references, cross-references, scope of these references, and eventual errors on such material as—arithmetical tables, mathematical constants, tables of algebraic and elementary functions, tables of the higher functions, tables of integrals, tables of solution of transcendental equations, tables for numerical computations by differences, etc.

In appraising the task undertaken by the authors, one should consider the widely scattered character of the information collected, the enormous quantity of material accumulated, its duplication and its eventual reliability and finally, the fact that the authors did not confine themselves to mere indexing but have indicated in a great many cases the errors involved and accomplished a selection by discarding material of mere historical value.

The preface states—"I hope that this index will be a useful servant to the many scientists the world over who are working to build up a better civilization. To them this work is respectfully dedicated." The international character of the accomplishment will not escape those scientific workers who have tried to obtain copies of material which is scarce or available only in a geographically remote location.

It is essential to continue work along the lines of this index in keeping it up-to-date and also perhaps to facilitate speedy access to the material which might be urgently needed by the reader and might otherwise be difficult to obtain. Encouragement and help in accomplishing these further aims seem to fall particularly well within the responsibility of the newly created United Nations Educational Scientific and Cultural Organization.

M. A. Biot

Contributions to the study of oscillatory times series. By M. G. Kendall. Cambridge, at the University Press; New York, The Macmillan Company, 1946. 67 pp. $1.75.

This work is an outline of the application of certain common schemes of statistical analysis to a few sequences of the type encountered in studies of economic time series. The viewpoint is that of the statistician.

The book is divided into seven chapters. The first is concerned with the qualitative discussion of methods to be employed, and with the construction of three time series from random sampling numbers according to linear autoregression equations of the second order. Chapters two through six are concerned with the analysis of these series by the correlogram, the periodogram and the variate difference schemes. Chapter seven contains the author's summary, in which he concludes, as one might suspect, that schemes of analysis not based on considerations of the generating processes give rise to meaningless results. An appendix contains tables for harmonic analysis.

As an account of inadequacies of the methods discussed, the paper will interest statisticians, but mathematicians and physicists who have been interested in the general time series problem in the broader sense will notice the lack of reference to a large body of the work done in this field.

J. Krumhansl

[illegible]PORTANT DOVER PUBLICATIONS

[illegible] KNOWLEDGE AND [illegible] NEBULAE by Martin Johnson [illegible] by Professor E. A. Milne. 5½ x 8½. 190 pages. $2.75

[illegible] is the first publication of a [illegible] study of the meanings of Time in [illegible] Astronomy, and Philosophy [illegible] the Relativities of Einstein and of [illegible] the first modern attempt to [illegible] out the meanings of various [illegible] of Time, inspired by Milne's new Relativity, which suggests that many [illegible] in [illegible] physics, particularly in the fields of atomic physics [illegible] harmony might be [illegible] by the use of more than one concept of Time. [illegible] commend it to the reader [illegible] —E. A. Milne

[illegible] sections provide [illegible] material on atomic and astronomical [illegible] sufficient to permit non-specialists to read the main sections of the [illegible]

PARTIAL TABLE OF CONTENTS

[illegible] and Time in [illegible] Relativity as Problem in the [illegible] of Natural Laws. Analysis [illegible] Interlocking of Time- and [illegible] Variation [illegible] Time. Analysis of Milne's Reconstruction [illegible] Experimental Consequences [illegible] Milne's [illegible] of Time-Scales. Criticue of [illegible] Time in Physical and [illegible] Sciences [illegible] Theory of Scientific Knowledge.

[illegible] OF FUNCTIONS, PART II: Applications and Further Development of the General Theory, by Konrad Knopp. Translated by Frederick Bagemihl. x + 150 pages. 4¼ x 6¾. Index. Bibliography. [illegible]50

[illegible] publication of PART II, [illegible] the previous publication of PART I: [illegible] the General Theory of Analytic Functions, students of mathematical [illegible] now have available the complete text of an outstanding introduction [illegible] of functions which the American Mathematical Monthly reviews [illegible] "The two parts of Knopp's Funktionentheorie have long been recognized [illegible] summaries of the principal results of the theory of analytic [illegible]

[illegible] OF FUNCTIONS, PART I: Elements of the General Theory of Analytic Functions, by Konrad Knopp. Translated by Frederick Bagemihl. vi + 146 pages. 4¼ x 6¾. Index. Bibliography. $1.50

NEW, 1947 CATALOG OF DOVER SCIENTIFIC BOOKS

[illegible] now available for your permanent reference use as a buying guide for outstanding books on various phases of mathematics, physics, and chemistry. Because increasing production costs make it impossible to guarantee that all of the Dover Books listed in the catalog will remain in print at present low prices, we suggest that you secure the catalog immediately and check it against your book-buying plans.

DOVER PUBLICATIONS, INC. Department Q.A.
1780 Broadway, New York 19, New York

CONTENTS

Important McGraw-Hill Books

MECHANICAL VIBRATIONS. New third edition

By J. P. Den Hartog, Massachusetts Institute of Technology. 502 pages, $6.00
[illegible] the many applications of [illegible] and calculations to the practical vibration problems encountered by the practicing engineer. Advances made during the past six years have been [illegible].

DIFFERENTIAL AND INTEGRAL CALCULUS

By Harold M. Bacon, Stanford University. 771 pages, $4.00
Presents material so that the student can master it with a minimum of explanation by the instructor. Illustrative examples are worked out in great detail.

MATHEMATICAL THEORY OF ELASTICITY

By I. S. Sokolnikoff, University of California at Los Angeles. 373 pages, $4.50
Gives a thorough foundation in the mathematical theory of elasticity, followed by the application of the theory to problems on extension, torsion, and flexure of isotropic cylindrical bodies.

APPLIED MATHEMATICS FOR ENGINEERS AND PHYSICISTS

By Louis A. Pipes, Harvard University. 621 pages, $5.50
Covers the topics of higher mathematics related to the fields of electrical, mechanical, and civil engineering, as well as to classical physics.

Send for copies on approval

McGRAW-HILL BOOK COMPANY, Inc.

330 West 42nd Street New York 18, N.Y.